[redacted]

NASA TECHNICAL MEMORANDUM

UB
NASA TM X-1321

UB
NASA TM X-1321

[redacted]

EFFECTS OF VARIOUS CANOPIES ON THE AERODYNAMIC CHARACTERISTICS OF A MANNED LIFTING ENTRY VEHICLE AT MACH 0.06 TO 6.8

by Charles L. Ladson

Langley Research Center
Langley Station, Hampton, Va.

NATIONAL AERONAUTICS AND SPACE ADMINISTRATION • WASHINGTON, D. C. • DECEMBER 1966

[redacted]

[redacted] NASA TM X-1321

EFFECTS OF VARIOUS CANOPIES ON THE AERODYNAMIC CHARACTERISTICS OF A MANNED LIFTING ENTRY VEHICLE AT MACH 0.06 TO 6.8

By Charles L. Ladson

Langley Research Center
Langley Station, Hampton, Va.

[redacted]

[redacted]

[redacted]

[redacted]

NATIONAL AERONAUTICS AND SPACE ADMINISTRATION

[redacted]

U. S. Government Agencies and Contractors Only

CONFIDENTIAL

EFFECTS OF VARIOUS CANOPIES ON THE AERODYNAMIC CHARACTERISTICS OF A MANNED LIFTING ENTRY VEHICLE AT MACH 0.06 TO 6.8*

By Charles L. Ladson
Langley Research Center

SUMMARY

X67-10837

An investigation has been conducted at the Langley Research Center to determine the effects of different canopy shapes on the longitudinal performance and the longitudinal, directional, and lateral stability characteristics of the HL-10 vehicle with the current tip and center fins. Results of this investigation show that addition of a small "bubble type" canopy to the basic HL-10 vehicle ahead of the center of gravity causes only a small loss in subsonic maximum lift-drag ratio but can produce large unstable increments in directional and lateral stability throughout the Mach number range. At transonic speeds, the configuration with this canopy was directionally unstable. Addition of a full-length canopy with a large amount of taper at the aft end produced a reduction in trim angle of attack, which in turn caused a substantial loss in subsonic maximum lift-drag ratio. If a canopy is desired, the best compromise seems to be a full-length canopy with the ridge line parallel to the vehicle center line (designated canopy D). This canopy produces a moderate loss in subsonic lift-drag ratio with no large changes in the lateral stability characteristics.

At hypersonic speeds the full-length canopy had no appreciable effect on the maximum lift-drag ratio or on the longitudinal and lateral aerodynamic characteristics. Surface oil-flow studies, however, showed that at hypersonic speeds some areas of high shear exist on the canopy which could create heat-protection problems.

[redacted] Author

INTRODUCTION

An investigation of a manned lifting entry vehicle having a maximum hypersonic lift-drag ratio of about 1 has been underway at the Langley Research Center since early 1962. The objective of these studies has been to determine the aerodynamic characteristics, to expose problems, and to develop solutions to these problems. As a result of preliminary work, a configuration with negative camber, a flat bottom, a blunt leading

---

*Title, Unclassified.

CONFIDENTIAL

edge, and a delta planform designated HL-10, was selected for testing throughout the Mach number range. Results of this investigation, most of which are published in references 1 to 29, show that this body shape in combination with toed-in, rolled-out tip fins and a vertical center fin (designated I_4 and E_2, respectively) has static stability and is controllable throughout the Mach number range for values of lift coefficient up to about 0.5. A summary of the trimmed characteristics is presented in reference 16.

Several contractual studies have been made to determine the capability of the HL-10 and other lifting bodies for various earth-orbit missions and to determine the vehicle size, weight, and launch-vehicle compatability for these missions. (See refs. 30 to 33.) Results of these studies indicate that for some missions, the use of a canopy on the HL-10 vehicle could reduce the total vehicle weight by allowing the vehicle length to be reduced while retaining sufficient height for a manned vehicle. For example, at the 20 percent body station the total thickness of the HL-10 vehicle is 19 percent of the body length. If a pilot is placed at this position and if it is assumed that a total vehicle height (pilot plus structure plus clearance) of 5 feet (1.5 m) is necessary, the vehicle length would be 26.3 feet (8 m). By use of a small canopy at this same location, the vehicle thickness could be increased to about 25 percent of the vehicle length, which results in a total vehicle length of only 20 feet (6.1 m) for the same 5-foot (1.5-m) vertical thickness. The addition of a canopy would also improve the pilot's visibility since, for the same amount of transparent area, the pilot's eye level could be raised well above the vehicle center line. Extending a canopy to the vehicle trailing edge would provide an increase in the vehicle base thickness at the center line which would simplify attachment of the spacecraft to the launch vehicle and would also provide additional area for the crew access passage. This aft-end access has been shown in the studies to be desirable for logistic missions in that, for rear-end docking with an orbiting space station, it facilitates transfer of crew and cargo between the spacecraft and the space station.

The addition of a canopy to the basic HL-10 vehicle would not be without some disadvantages. A canopy may have adverse effects on the longitudinal and directional stability characteristics as well as on performance. At hypersonic speeds, the window area, whether located in the canopy or on the body, would probably have to be shielded from the flow, and serious heating problems could arise. Also, building a pressurized vehicle would be more difficult with a canopy than without.

The purpose of this report is to provide aerodynamic data showing the effect of different canopy shapes on the basic longitudinal performance and the longitudinal, directional, and lateral stability characteristics of the HL-10 vehicle. Preliminary data from tests of an early body-fin combination (refs. 5, 11, 17, 18, and unpublished data) are summarized herein. Although this early configuration without canopy was directionally unstable at some combinations of angle of attack and Mach number, the data have been presented herein to provide a more complete summary of canopy effects. Data have also been obtained with three canopy shapes on the current tip-fin center-fin configuration of the HL-10 vehicle and are presented for Mach numbers from 0.35 to 2.16 at angles of attack up to about 30°. The subsonic trimmed characteristics were obtained in the Langley 300-MPH 7- by 10-foot tunnel by Bernard Spencer, Jr. The transonic and low supersonic data were obtained in the Langley high-speed 7- by 10-foot tunnel and the Langley 8-foot transonic pressure tunnel by Linwood W. McKinney and Charles D. Harris, respectively. Data presented at supersonic speeds on these three canopy shapes are from reference 28. Some additional data for one canopy shape at a Mach number of 6.8 show the longitudinal aerodynamic characteristics as well as surface oil-flow patterns for various canopy lengths.

SYMBOLS

b span, in. (cm)

C_A axial-force coefficient, $\frac{\text{Axial force}}{qS}$

C_D drag coefficient, $\frac{\text{Drag}}{qS}$

C_L lift coefficient, $\frac{\text{Lift}}{qS}$

C_N normal-force coefficient, $\frac{\text{Normal force}}{qS}$

C_l rolling-moment coefficient, $\frac{\text{Rolling moment}}{qSb}$

$C_{l_\beta} = \partial C_l/\partial\beta$ per degree (for $M = 6.8$)

$= \Delta C_l/\Delta\beta$ per degree (for all other values of M)

C_m pitching-moment coefficient, $\frac{\text{Pitching moment}}{qSl}$

$C_{m_\alpha} = \partial C_m/\partial\alpha$ per degree

C_n yawing-moment coefficient, $\frac{\text{Yawing moment}}{qSb}$

$C_{n_\beta} = \partial C_n/\partial\beta$ per degree (for $M = 6.8$)

$= \Delta C_n/\Delta\beta$ per degree (for all other values of M)

C_Y side-force coefficient, $\frac{\text{Side force}}{qS}$

$C_{Y_\beta} = \partial C_Y/\partial\beta$ per degree (for M = 6.8)

$= \Delta C_Y/\Delta\beta$ per degree (for all other values of M)

L/D	lift-drag ratio
l	body length, in. (cm)
M	free-stream Mach number
q	free-stream dynamic pressure, lbf/ft^2 $\left(\text{N/m}^2\right)$
R	Reynolds number based on body length l
r	radius, in. (cm)
S	reference area equal to projected planform area with elevons, in^2 $\left(\text{cm}^2\right)$
x	distance along longitudinal axis of body, in. (cm)
α	angle of attack, deg
β	angle of sideslip, deg
γ	flight-path angle, deg
δ_e	elevon deflection angle; angle between elevon surface and model surface ahead of elevon measured in plane normal to elevon hinge line; positive when trailing edge is down
δ_{ef}	elevon-flap deflection angle; angle between elevon flap and body upper surface in region of elevon; positive when trailing edge is above body surface at $\delta_e = 0^\circ$
δ_{if}	deflection angle of inner flap on tip fin; angle between flap and tip-fin inner surface measured normal to hinge line; positive when trailing edge moves toward body center line, deg
δ_{of}	deflection angle of outer flap on tip fin; angle between flap and tip-fin outer surface measured normal to hinge line; positive when trailing edge moves toward body center line, deg

θ model pitch angle; angle between model center line and horizontal

ϕ radial angle from model center line; 0° defined as forward

ψ rudder included angle; positive for converging trailing edge, deg

MODELS AND DESIGNATIONS

Three-view drawings showing the details of the HL-10 configuration with fins D and E are presented in figure 1(a) and with fins I_4 and E_2 in figure 1(b). The latter configuration, as described in reference 16, incorporates tip-fin flaps, an elevon flap, and a converging rudder to improve both the subsonic maximum trimmed lift-drag ratio and the transonic longitudinal stability characteristics of the vehicle. Since these flaps have different deflection angles for the various operational speed ranges, the following table is presented to define the combination used in each speed range:

Mode	δ_{ef}, deg	δ_{if}, deg	δ_{of}, deg	ψ, deg
Subsonic	-8	0	40	12
Transonic	20	30	0	-12
Hypersonic	0	0	0	-12

Cross sections of the model with tip fins I_4 and center fin off are presented in figure 1(c).

Details of the canopies studied previously and those of the present investigation are given in figure 2. Photographs of the models with and without canopy are presented in figure 3. All tip-fin, center-fin, and canopy designations used herein are consistent with those established for the HL-10 program in references 1 to 29. Tip fins D, D-1, and D-2 have essentially the same geometry.

Three models were used in the present investigation: an 8-inch (20.32-cm) model constructed of stainless steel, a 16-inch (40.64-cm) model constructed of aluminum, and a 30.54-inch (77.57-cm) model constructed of wood. The photographs in figure 3 are of the 16-inch (40.64-cm) model. Details and photographs of the 8-inch (20.32-cm) model are presented in reference 15.

All coefficients are based on the total projected planform area, the span, and the length of the model. The moment center for all models is located at 53 percent of the body length behind the nose and at 1.25 percent of the body length below the reference center line. The reference areas and lengths are as follows:

S		b		l	
ft^2	m^2	in.	cm	in.	cm
0.1585	0.0147	5.155	13.094	8.00	20.32
.634	.0589	10.30	26.188	16.00	40.64
2.31	.2145	19.68	50.00	30.54	77.57

APPARATUS, TESTS, AND PROCEDURE

The data contained herein were obtained in several different facilities in order to cover the Mach number range of interest. The facilities, Mach numbers, Reynolds numbers, dynamic pressures, model lengths, and angles of attack and sideslip are listed in table I.

Descriptions of most of these facilities are presented in reference 34. Six-component electrical strain-gage balances were used to obtain the force and moment data. No corrections to the data have been made for base pressure.

All longitudinal performance data are referred to the stability-axis system, whereas the stability results are referred to the body-axis system. All directional and lateral stability data up to $M = 2.16$ were obtained from tests at two sideslip angles. At $M = 6.86$, the directional and lateral stability data were obtained at five sideslip angles between 0° and 8°. Insomuch as the data were linear with β, only the slopes have been presented.

To give an indication of the accuracy of the data, the static-calibration accuracy of the balances in terms of the aerodynamic coefficients is presented in table II. The accuracy for the angles of attack and sideslip was within $\pm 0.2^{\circ}$.

PRESENTATION OF RESULTS

The results of this investigation are presented in four sections, and an index to the figures in each section follows.

DISCUSSION

Summary of Previous Data

During the course of HL-10 tests at Langley Research Center, some data were obtained on the vehicle with various canopies at several Mach numbers. Some of these results have been published, but no summary was made. These data are presented herein to provide a more complete compilation of all available canopy tests on the vehicle.

Results of subsonic and supersonic tests of a small center-line bubble-type canopy, designated canopy A, are reported in references 7 and 18. This canopy, with its origin at $0.09l$, increased the thickness of the body by about $0.03l$. (See fig. 2(a).) The incremental changes in subsonic ($M = 0.06$) directional and lateral stability due to this canopy at various longitudinal locations on the vehicle are presented in figure 4. In general, the canopy caused an unstable increment in both directional stability (as would be expected from adding area ahead of the vehicle center of gravity) and lateral stability. An exception is noted at the high angle of attack (45°) for the more rearward locations of the canopy. This stabilizing increment is probably the result of a vortex flow at this high angle of attack which results in higher pressures on the lee side of the canopy. At supersonic speeds and low angles of attack, the addition of the canopy with origin at $0.09l$ results in losses in both directional and lateral stability (fig. 5).

Tests of the full-length center-line canopy, D, at Mach numbers below 2.8 are reported in reference 6. With this canopy, the center fin was tested in two vertical positions: (1) mounted on the top of the canopy (fin E) and (2) partially embedded in the canopy (fin O). (See fig. 2(a).) A summary of the Mach number effects on the longitudinal trim characteristics with $\delta_e = 0^{\circ}$ for this canopy is presented as figure 6. In general, the canopy produces a nose-down increment in pitching moment which is reflected in figure 6 as a lower trim angle of attack and higher longitudinal stability. The effect on trim angle of attack is most noticeable at transonic speeds. The lower trim angles of attack for the vehicle with canopy naturally decrease the trimmed lift coefficient and lift-drag ratio. The effects of changing the position of the center fin are small. Addition of this same canopy (with windshield cover shown in fig. 2(a)) at $M = 6.8$ produces a small loss in lift-drag ratio with essentially no change in stability (see fig. 7).

The directional and lateral stability characteristics of the configuration with canopy D and various combinations of tip fin and center fin are presented in figure 8 for several Mach numbers and are summarized as a function of Mach number in figure 9. A detailed study of figure 8 shows that at subsonic and supersonic speeds the increment in stability due to the addition of the canopy is a function of the fin configuration. Thus a strong upper-surface flow interaction must exist between canopy and fins. At hypersonic speeds (fig. 8(k)) the canopy has no appreciable effects on the stability characteristics in the angle-of-attack range of the tests since the canopy is essentially shielded from the flow. The Mach number summary of the effects of this canopy on directional and lateral stability (fig. 9) shows that, in general, addition of the canopy so that the center fin is partially shielded (center fin O) results in a loss of stability, whereas addition of the canopy with the center-fin area held constant (center fin E) results in a gain in stability. This gain is the result of moving the center fin farther away from the vehicle center line, and thus placing it in a higher energy flow field.

Results of Present Tests

Two full-length center-line canopies, D and E, and a large bubble-type canopy, F were tested with tip fins I_4 and center fin E_2 (see fig. 2(b)) at Mach numbers from 0.35 to 2.16. With this fin combination, the vehicle without canopy is stable throughout the test range of Mach number and angle of attack.

Tests at $M = 0.35$ were made with the tip-fin flap, elevon flap, and rudder in the subsonic mode for elevon deflection angles from 0° to -15°. Canopies D and F, in general, caused a slight loss in lift with little change in pitching moment for all elevon deflection angles investigated (fig. 10). Canopy E, however, has a large amount of taper or camber in its side view (see fig. 2(b)) and produces a positive increment in lift and a reduction in pitching moment and trim angle of attack. Although the positive increment in lift due to addition of canopy E tends to offset the lower trim angle of attack, this canopy still exhibits the lowest trimmed lift and lift-drag ratio of the canopies tested (see fig. 11). Canopy F, the bubble-type canopy, causes the least reduction in trimmed maximum lift-drag ratio at subsonic speeds.

The longitudinal characteristics at $M = 0.40$ to $M = 2.16$ with the tip-fin flap, rudder, and elevon flap in the transonic mode and $\delta_e = 0^{\circ}$ were essentially the same as those observed at $M = 0.35$ with flaps in the subsonic mode (see fig. 12). The vehicle with canopy E always trims at a lower angle of attack because of the positive increment in lift produced over the aft part of the configuration. This effect diminishes at the higher angles of attack at supersonic speeds as the canopy becomes shielded from the flow. The summary of the longitudinal results shows that addition of canopies D and F affects the trim conditions at $\delta_e = 0^{\circ}$ less than addition of canopy E. (See fig. 13(a).) Comparison of the effects of the three canopies at a constant lift coefficient of 0.20 (fig. 13(b)) or a constant angle of attack of 24° (fig. 13(c)) shows that for these cases, only small changes in performance result from addition of the canopies.

Detail directional and lateral stability characteristics of the vehicle with and without the three canopies are presented in figure 14 at various Mach numbers for $\delta_e = 0^{\circ}$. The overall results of these tests are shown in the summary plots, figure 15. For trim conditions at $\delta_e = 0^{\circ}$ (fig. 15(a)), the canopies reduce the level of directional and lateral stability for Mach numbers below about 1.0. At higher Mach numbers canopies D and E generally increase stability. This increase in stability is the result of the vertical tail being placed farther from the vehicle center line in a higher energy flow region. Canopy F, because of its destabilizing increment, produces a directionally unstable configuration at the higher transonic speeds; this canopy also shows the largest incremental loss in stability throughout the Mach number range. Canopy D also produces a directionally unstable configuration at $M = 0.95$. This is due to the very high trim angle of attack at this Mach number (about 26°; see fig. 13(a)) and may not be a problem unless trimmed lift coefficients on the order of 0.5 are required at this Mach number. These general trends are also observed when the various canopies are compared at a lift coefficient of 0.20 (fig. 15(b)) or at an angle of attack of 24° (fig. 15(c)) except that canopy D does not cause a directionally unstable region at these lower angles of attack.

Variation of Canopy D Length

Tests were made at a Mach number of 6.8 with the tip-fin flap, elevon flap, and rudder in the hypersonic mode to determine the effects of canopy D and shortened versions of canopy D (all with windshield cover) on the longitudinal characteristics of the HL-10 vehicle with tip fin I_4 and center fin E_2. The results, presented in figure 16, were the same with and without the canopies. Previous results (fig. 7) with tip fin D and center fin E show the same level of lift-drag ratio for the vehicle with canopy, but a slight increase in lift-drag ratio for the vehicle without canopy.

Schlieren flow photographs of the vehicle with canopy D and the two shortened versions at angles of attack of 20° and 30° are presented as figure 17. At 20° angle of attack the shock wave off the canopy is evident, but at an angle of attack of 30° it is not visible. Surface oil-flow studies were also made at an angle of attack of 30° (the approximate angle for maximum lift-drag ratio at hypersonic speeds) and the results are presented in figure 18. For all three canopy lengths a region of high shear is noted along the ridge line of the windshield cover. On the models with the two shortened canopies the flow over the body upper surface has separated ahead of the canopy windshield but evidently reattaches on the canopy to form the high shear area. Another region of high shear is noted along the sides of the canopy, slightly below the ridge line. This may be caused by the leading-edge vortex striking the upper surface of the vehicle. These regions of high shear could be problem areas for heat protection of a canopy at hypersonic speeds.

Canopy Visibility Study

A mockup of the forward portion of a 28-foot-long (8.5 m) HL-10 vehicle was constructed for use in visibility studies. The results of some of these studies with canopy D installed are presented in figure 19. The lowest visual angle permitted by model geometry is presented as a function of radial angle ϕ for model attitudes of 0°, 10°, 20°, and 30° with respect to the horizontal. These measurements were made for the pilot's eye located at 20 percent of the body length behind the vehicle nose and 10 percent of the body length above the horizontal reference line. With this location of the pilot, the distance from the eye level to the upper surface of the canopy is 2.5 percent of the vehicle length, or slightly more than 8 inches (20.3 cm) on the 28-foot (8.5 m) mockup. Thus these visual angles may be optimistic, especially on smaller length vehicles, since the pilot would probably have to be lower in the vehicle to provide the proper clearance.

To provide an indication of the visibility of 300-foot-wide (91.4 m) runway markers during the landing approach, the visual angles of figure 19 have been used for various vehicle altitudes to obtain the results presented in figure 20. For an altitude of 50 feet (15.2 m) at the end of the flare, the side runway markers are visible for radial angles greater than about 40° off the vehicle center line or about 225 feet (68.6 m) ahead of the vehicle. As the altitude decreases to 25 feet (7.6 m), the runway markers are visible for about 350 feet (106.7 m) ahead of the vehicle. Although some subsonic aircraft have routinely landed with limited or no forward visibility, these curves are presented for design information only and are not intended to be indicative of the visibility requirements for landing of a lifting entry vehicle.

CONCLUDING REMARKS

An investigation has been conducted at the Langley Research Center to show the effects of different canopy shapes on the longitudinal performance and the longitudinal, directional, and lateral stability characteristics of the HL-10 vehicle with the current tip fins and center fins. Results of this investigation show that addition of a small bubble-type canopy to the basic HL-10 vehicle ahead of the vehicle center of gravity produces only a small loss in subsonic maximum lift-drag ratio but can produce large unstable increments in directional and lateral stability throughout the Mach number range. At transonic speeds, the configuration with this canopy was directionally unstable. Addition of a full-length canopy which incorporates a large amount of taper at the aft end produces a reduction in trim angle of attack, which in turn causes a substantial loss in subsonic maximum lift-drag ratio. If a canopy is desired, the best compromise seems to be a full-length canopy with the ridge line parallel to the vehicle center line (designated canopy D in the text). This canopy produces a moderate loss in subsonic lift-drag ratio with no large changes in the lateral stability characteristics.

Addition of the full-length canopy at hypersonic speeds has no appreciable effect on the maximum lift-drag ratio or on the longitudinal or lateral aerodynamic characteristics. Surface oil-flow studies, however, show that at hypersonic speeds some areas of high shear exist on the canopy which could be problem areas from a heat-protection standpoint.

Langley Research Center,
National Aeronautics and Space Administration,
Langley Station, Hampton, Va., August 16, 1966,
124-07-02-56-23.

[redacted]

REFERENCES

1. Rainey, Robert W.; and Ladson, Charles L.: Preliminary Aerodynamic Characteristics of a Manned Lifting Entry Vehicle at a Mach Number of 6.8. NASA TM X-844, 1963.

2. Ware, George M.: Aerodynamic Characteristics of Models of Two Thick 74° Delta Manned Lifting Entry Vehicles at Low-Subsonic Speeds. NASA TM X-914, 1964.

3. Ladson, Charles L.: Aerodynamic Characteristics of a Manned Lifting Entry Vehicle at a Mach Number of 6.8. NASA TM X-915, 1964.

4. Dunavant, James C.; and Everhart, Philip E.: Investigation of the Heat Transfer to the HL-10 Manned Lifting Entry Vehicle at a Mach Number of 8. NASA TM X-998, 1964.

5. Rainey, Robert W.; and Ladson, Charles L.: Aerodynamic Characteristics of a Manned Lifting Entry Vehicle at Mach Numbers From 0.2 to 1.2. NASA TM X-1015, 1964.

6. McShera, John T., Jr.; and Campbell, James F.: Stability and Control Characteristics of a Manned Lifting Entry Vehicle at Mach Numbers From 2.29 to 4.63. NASA TM X-1019, 1964.

7. Ware, George M.: Effect of Fin Arrangements on Aerodynamic Characteristics of a Thick 74° Delta Manned Lifting Entry Vehicle at Low-Subsonic Speeds. NASA TM X-1020, 1965.

8. Harris, Julius E.: Longitudinal Aerodynamic Characteristics of a Manned Lifting Entry Vehicle at a Mach Number of 19.7. NASA TM X-1080, 1965.

9. Everhart, Philip E.; and Hamilton, H. Harris: Investigation of Roughness-Induced Turbulent Heating to the HL-10 Manned Lifting Entry Vehicle at a Mach Number of 8. NASA TM X-1101, 1965.

10. Campbell, James F.; and McShera, John T., Jr.: Stability and Control Characteristics From Mach Numbers 1.50 to 2.86 of a Model of a Manned Lifting Entry Vehicle. NASA TM X-1117, 1965.

11. McShera, John T., Jr.; and Campbell, James F.: Aerodynamic Characteristics From Mach 1.50 to 2.86 of a Lifting Entry Vehicle Alone, With Adapter Sections, and With a Saturn Launch Vehicle. NASA TM X-1125, 1965.

12. Harvey, William D.: Pressure Distribution on HL-10 Manned Lifting Entry Vehicle at a Mach Number of 19.5. NASA TM X-1135, 1965.

13. Johnston, Patrick J.: Stability Characteristics of a Manned Lifting Entry Vehicle at a Mach Number of 20.3 in Helium. NASA TM X-1156, 1965.

[redacted]

14. Spencer, Bernard, Jr.: An Investigation of Methods of Improving Subsonic Performance of a Manned Lifting Entry Vehicle. NASA TM X-1157, 1965.

15. Ladson, Charles L.: Aerodynamic Characteristics of a Manned Lifting Entry Vehicle With Modified Tip Fins at Mach 6.8. NASA TM X-1158, 1965.

16. Rainey, Robert W.: Summary of an Advanced Manned Lifting Entry Vehicle Study. NASA TM X-1159, 1965.

17. Ware, George M.: Full-Scale Wind-Tunnel Investigation of the Aerodynamic Characteristics of the HL-10 Manned Lifting Entry Vehicle. NASA TM X-1160, 1965.

18. Silvers, H. Norman; and Campbell, James F.: Stability Characteristics of a Manned Lifting Entry Vehicle With Various Fins at Mach Numbers From 1.50 to 2.86. NASA TM X-1161, 1965.

19. Moul, Martin T.; and Brown, Lawrence W.: Some Effects of Directional Instability on Lateral Handling Qualities of an Early Version of a Manned Lifting Entry Vehicle. NASA TM X-1162, 1965.

20. Campbell, James F.: Effects of Tip-Fin Geometry on Stability Characteristics of a Manned Lifting Entry Vehicle From Mach 1.50 to 2.86. NASA TM X-1176, 1965.

21. Harris, Charles D.: Effect of Elevon Deflection and of Model Components on Aerodynamic Characteristics of a Manned Lifting Entry Vehicle at Mach Numbers of 0.20 to 1.20. NASA TM X-1226, 1966.

22. Spencer, Bernard, Jr.; and Fox, Charles H., Jr.: Subsonic Longitudinal Control Characteristics of Several Elevon Configurations for a Manned Lifting Entry Vehicle. NASA TM X-1227, 1966.

23. Harris, Charles D.: Control-Surface Hinge-Moment and Elevon Normal-Force Characteristics at Transonic Speeds on a Manned Lifting Entry Vehicle. NASA TM X-1241, 1966.

24. Harris, Charles D.: Transonic Aerodynamic Characteristics of a Manned Lifting Entry Vehicle With and Without Tip Fins. NASA TM X-1248, 1966.

25. Harvey, William D.: Experimental Investigation of Laminar Heat-Transfer Characteristics of a Manned Lifting Entry Vehicle at a Mach Number of 20. NASA TM X-1306, 1966.

26. Stubbs, Sandy M.: Landing Characteristics of a Dynamic Model of the HL-10 Manned Lifting Entry Vehicle. NASA TN D-3570, 1966.

27. Campbell, James F.; and Watson, Carolyn B.: Stability and Control, Hinge-Moment, and Pressure-Coefficient Data for the HL-10 Manned Lifting Entry Vehicle at Mach Numbers From 1.41 to 2.16. NASA TM X-1300, 1966.

28. Campbell, James F.; and Grow, Josephine W.: Stability and Control Characteristics of a Manned Lifting Entry Vehicle at Mach Numbers From 1.50 to 2.16 Including Hinge Moment and Pressure Distribution Data. NASA TM X-1314, 1966.

29. Campbell, James F.; and Jernell, Lloyd S.: Effects of Various Center-Fin and Tip-Fin Arrangements on Aerodynamic Characteristics of a Manned Lifting Entry Vehicle From Mach Numbers 1.50 to 2.86. NASA TM X-1299, 1966.

30. Anon.: A Lifting Re-Entry, Horizontal-Landing-Type Logistic Spacecraft. D2-22921 (Contract NAS 9-1689), The Boeing Co., Feb. 3, 1964.

31. Anon.: Mission Requirements of Lifting Systems – Operational Aspects. D2-82531 (Contract NAS 9-3522), The Boeing Co., Aug. 1965.

32. Anon.: Mission Requirements of Lifting Systems – Engineering Aspects. Rept. No. B831 (Contract No. NAS 9-3562), McDonnell Aircraft Corp., Aug. 27, 1965.

33. Kuhlman, W. H.: Parametric Study of Logistics-Type Entry Vehicles. Repts. SM-48783 to SM-48787 (Contract No. NAS 2-2461), Missile & Space Systems Div., Douglas Aircraft Co., Inc., Sept. 1965.

34. Schaefer, William T., Jr.: Characteristics of Major Active Wind Tunnels at the Langley Research Center. NASA TM X-1130, 1965.

TABLE I.- TEST PARAMETERS

Langley facility	Model length, l		Dynamic pressure, q		M	R	α, deg	β, deg
	in.	cm	lb/ft^2	kN/m^2				
300-MPH 7- by 10-foot tunnel	30.54	77.57	170	8.1	0.35	5.3×10^6	-4 to 21	0
High-speed 7- by 10-foot tunnel	16.00	40.64	210	10.1	0.40	3.2×10^6	0 to 28	-5, 0, +5
			415	19.9	.60	4.4		
			525	25.1	.70	4.9		
			625	29.9	.80	5.2		
			675	32.3	.86	5.4		
			725	34.7	.92	5.5		
8-foot transonic pressure tunnel	16.00	40.64	280	13.4	0.95	2.7×10^6	0 to 24	0, 5
			295	14.1	1.00	2.1		
			280	13.4	1.20	1.8		
Unitary plan wind tunnel	16.00	40.64	380	18.2	1.50	1.6×10^6	-4 to 40	0, 3
			385	18.4	1.80	1.6		
			370	17.7	2.16	1.6		
11-inch hypersonic tunnel	8.00	20.32	380	18.2	6.86	1.7×10^6	0 to 40	0 to 8

TABLE II.- BALANCE ACCURACY

M	C_N	C_A	C_m	C_l	C_n	C_Y
0.35	0.0064	0.0078	0.0013	0.0006	0.0013	0.0013
.40	.0160	.0038	.0014	.0003	.0007	.0038
.60	.0078	.0019	.0007	.0001	.0004	.0019
.70	.0064	.0015	.0006	.0001	.0003	.0015
.80	.0054	.0013	.0005	.0001	.0002	.0013
.86	.0050	.0012	.0004	.0001	.0002	.0012
.92	.0046	.0011	.0004	.0001	.0002	.0011
.95	.0120	.0028	.0011	.0002	.0005	.0028
1.00	.0114	.0027	.0010	.0002	.0005	.0027
1.20	.0120	.0028	.0011	.0002	.0005	.0028
1.50	.0088	.0021	.0008	.0002	.0004	.0021
1.80	.0087	.0020	.0008	.0001	.0004	.0020
2.16	.0091	.0021	.0008	.0002	.0004	.0021
6.86	.0026	.0012	.0003	.0001	.0002	.0008

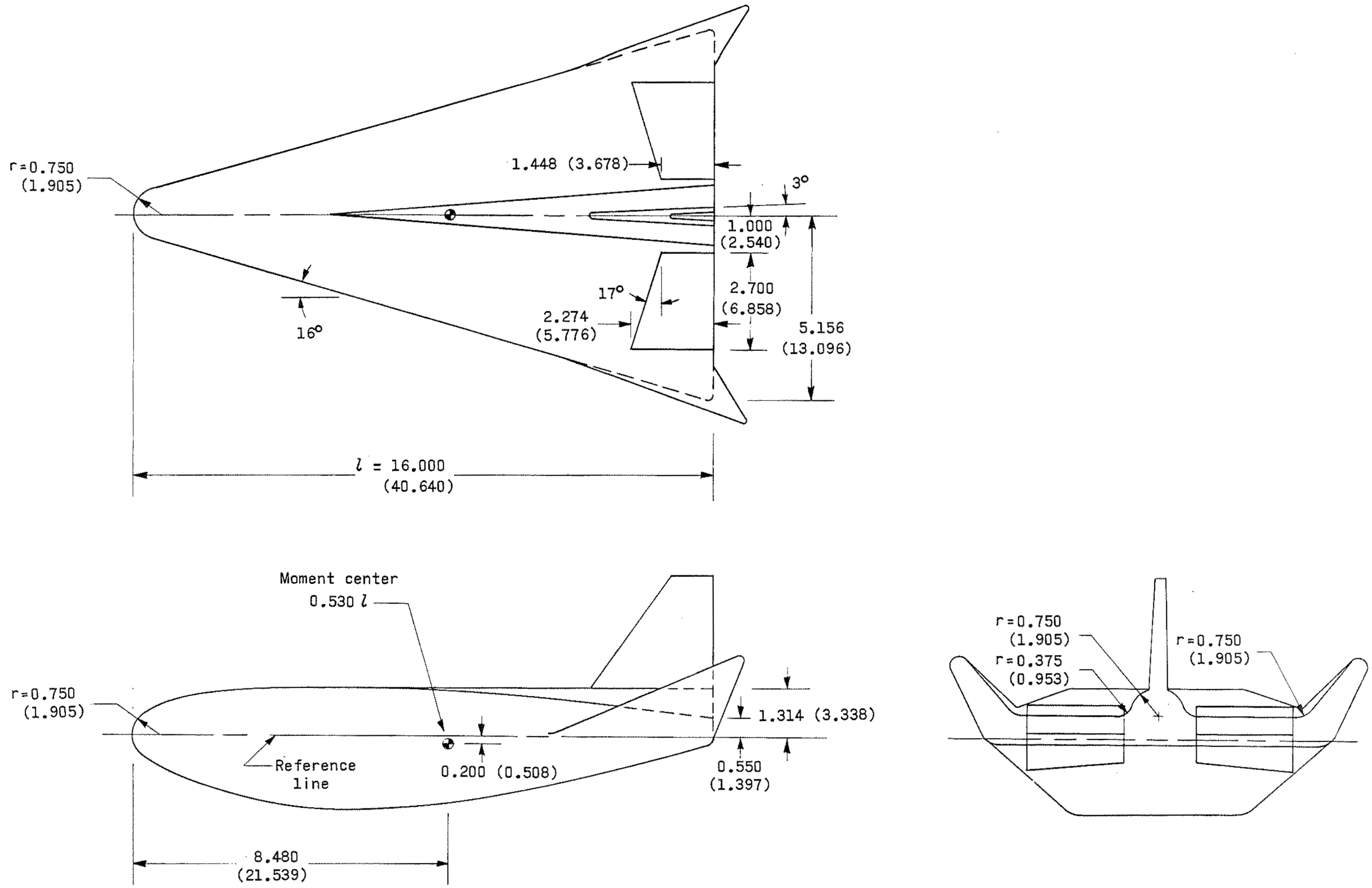

(a) Tip fin D; center fin E.

Figure 1.- Model drawings. (All dimensions are in inches unless otherwise noted; parenthetical dimensions are in centimeters.)

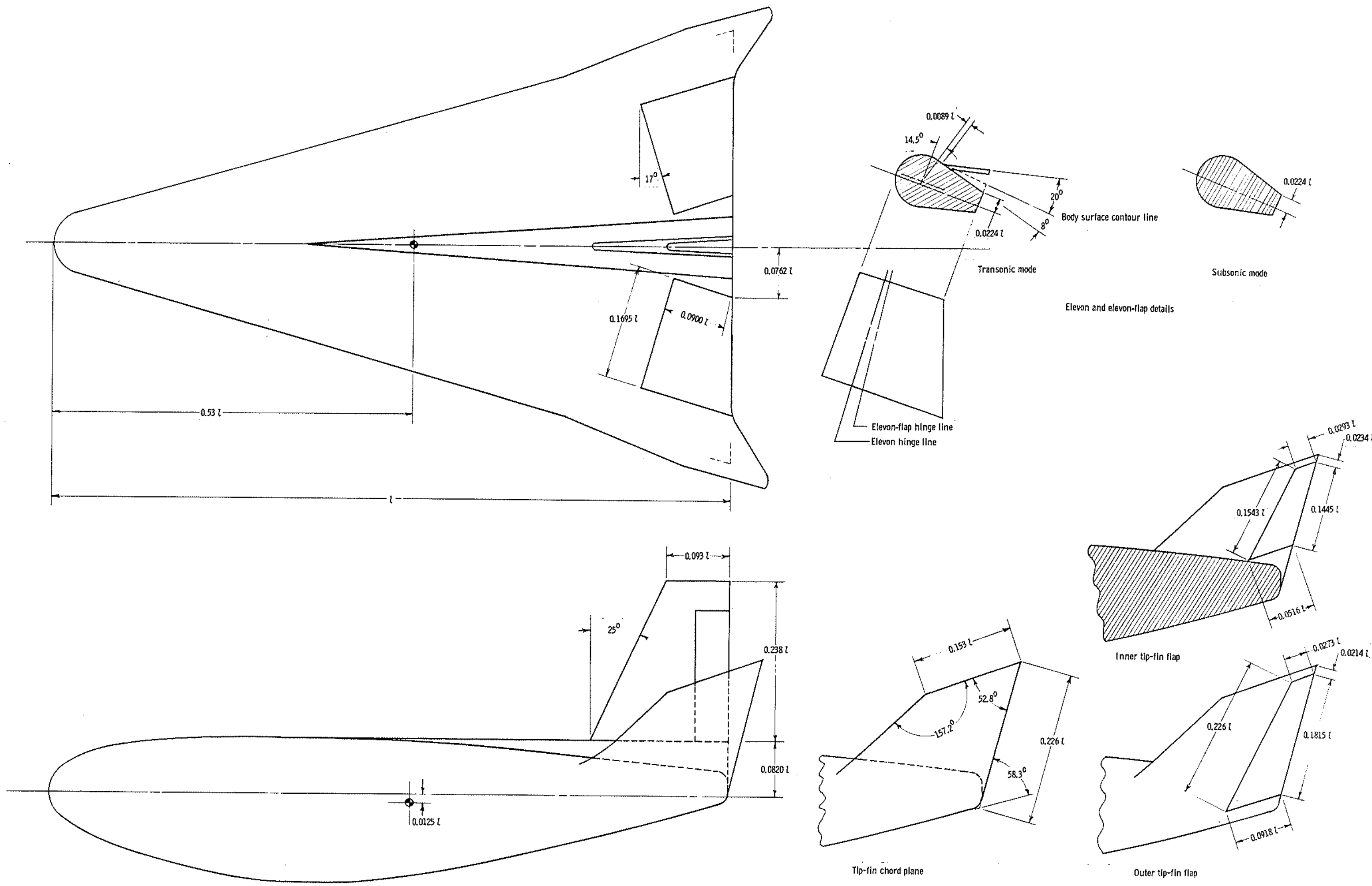

(b) Tip fin I_4; center fin E_2; tip-fin flap and elevon-flap details.

Figure 1.- Continued.

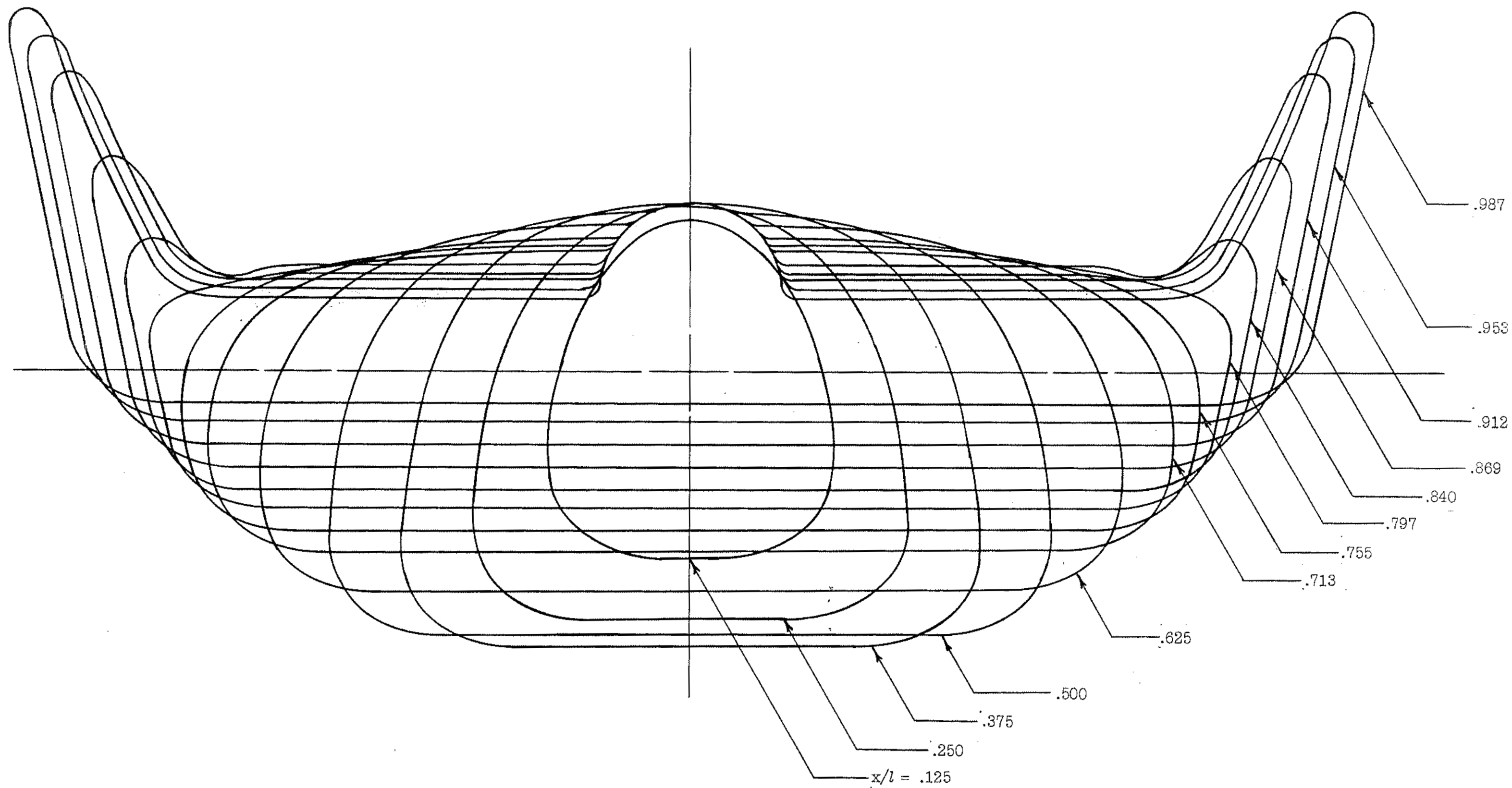

(c) Cross sections of model with tip fin I4 and center fin off.

Figure 1.- Concluded.

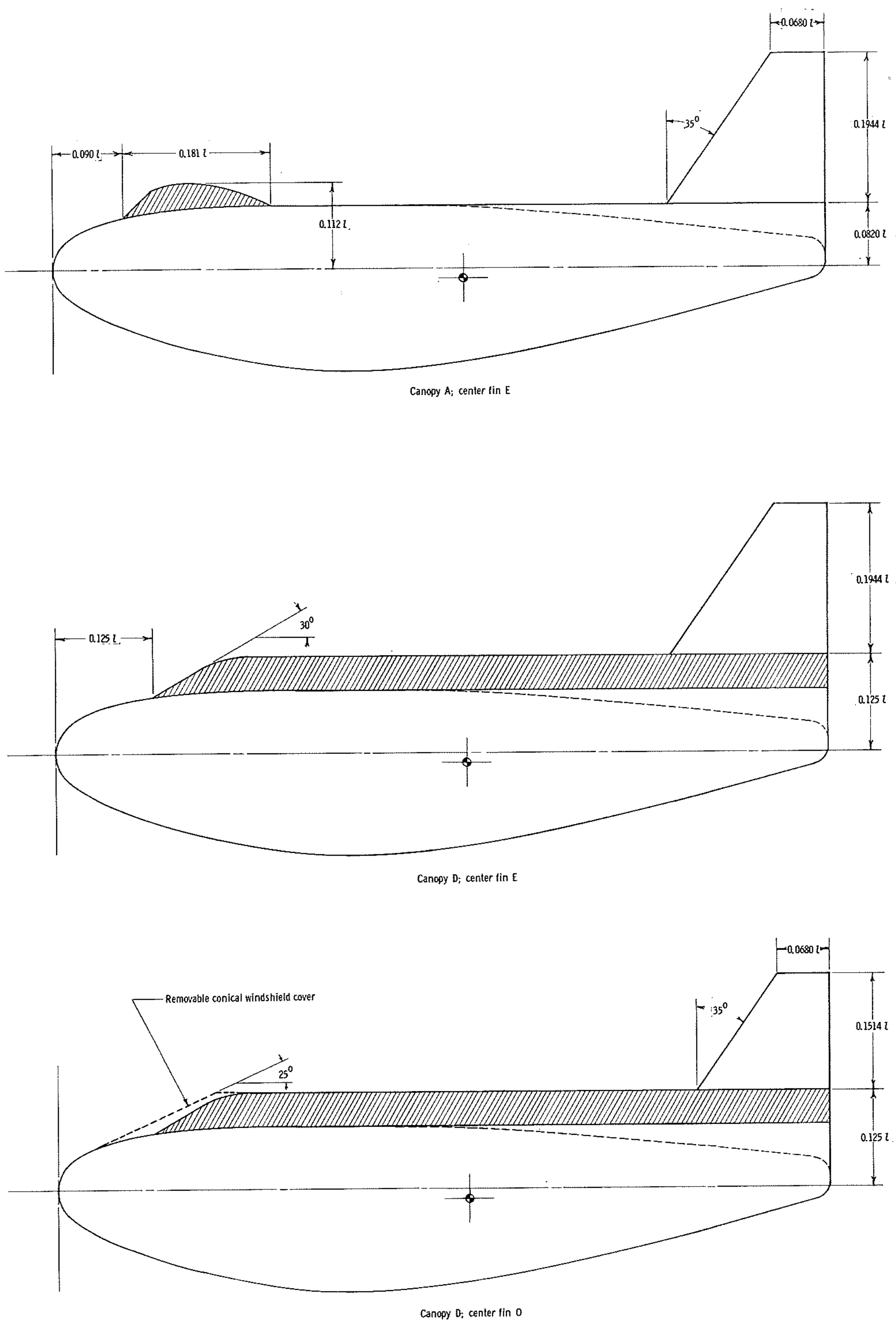

(a) Canopies previously tested with tip fin D.

Figure 2.- Longitudinal sections of canopies.

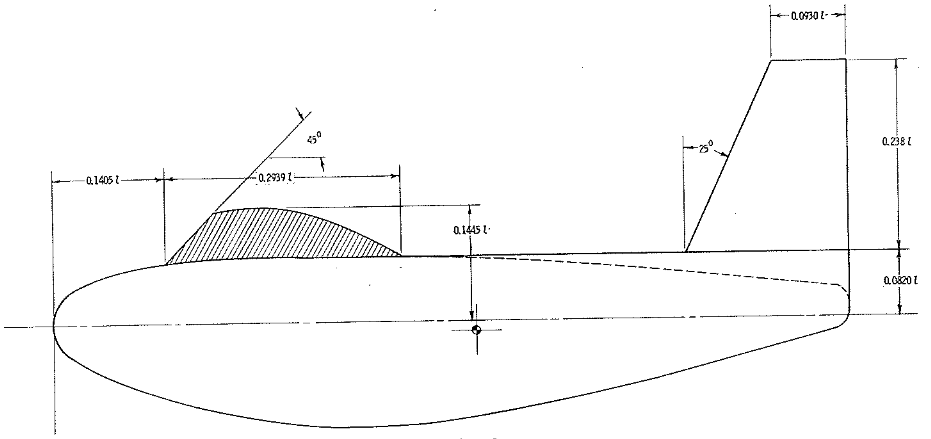

Canopy F

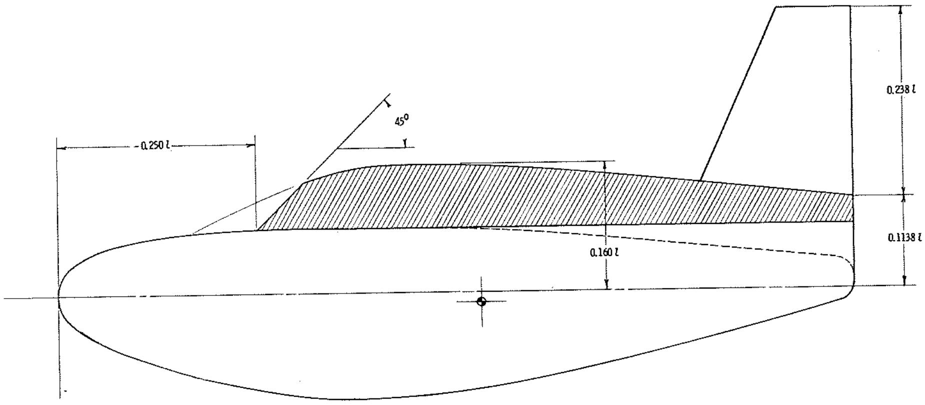

Canopy E

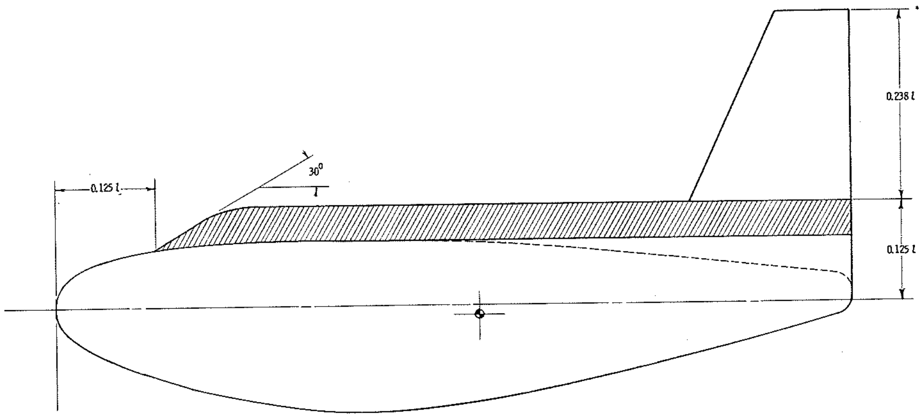

Canopy D

(b) Canopies tested in present program with tip fin I_4 and center fin E_2.

Figure 2.- Continued.

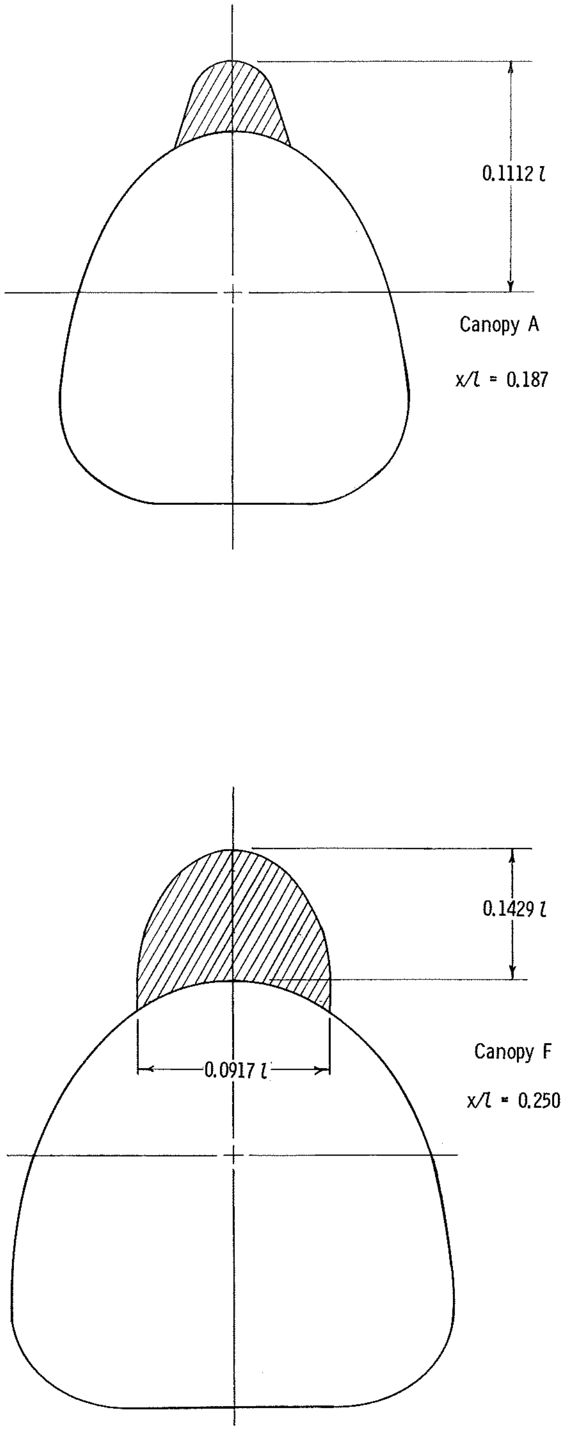

(c) Cross sections of canopies A and F.

Figure 2.- Continued.

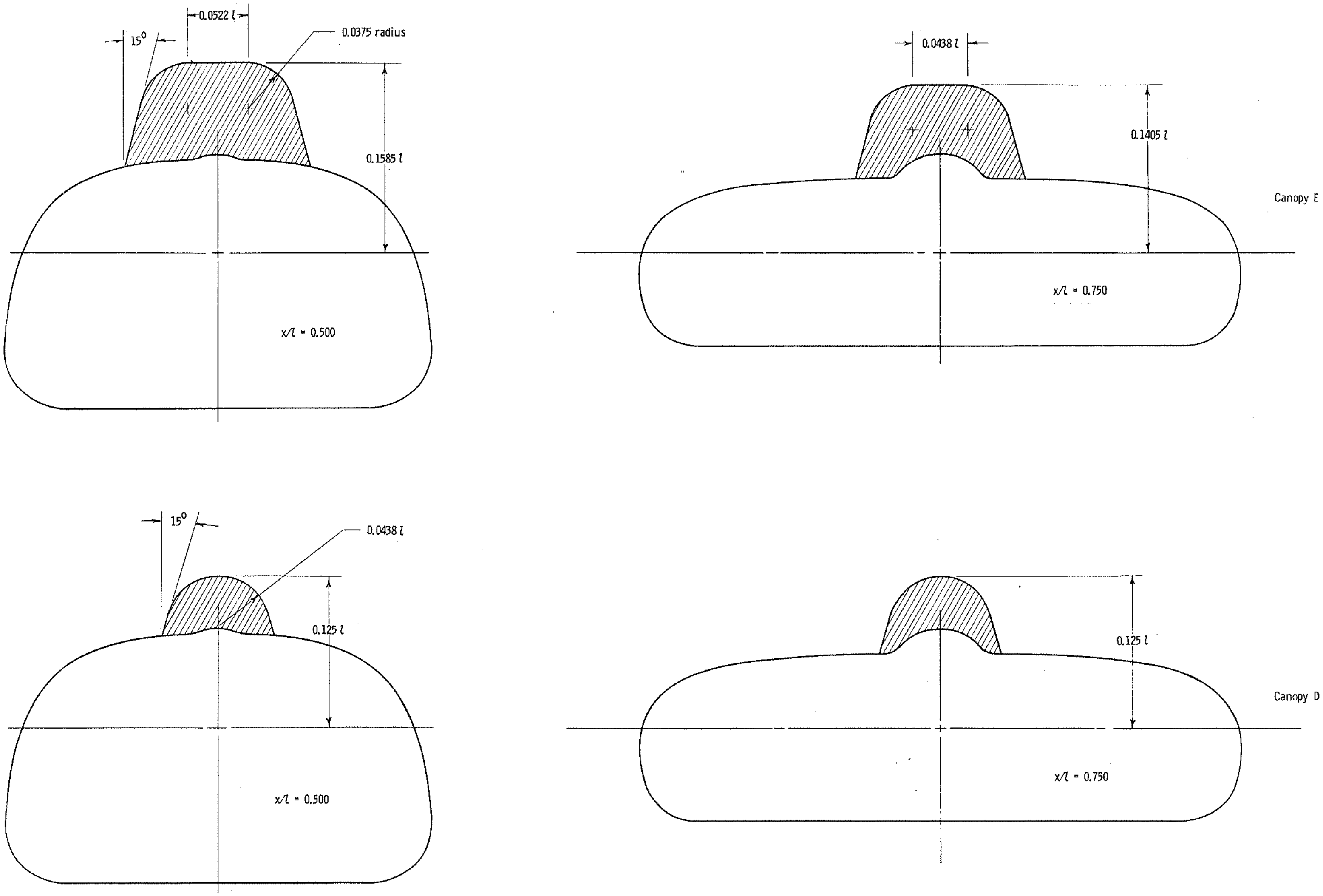

(d) Cross sections of canopies D and E.

Figure 2.- Concluded.

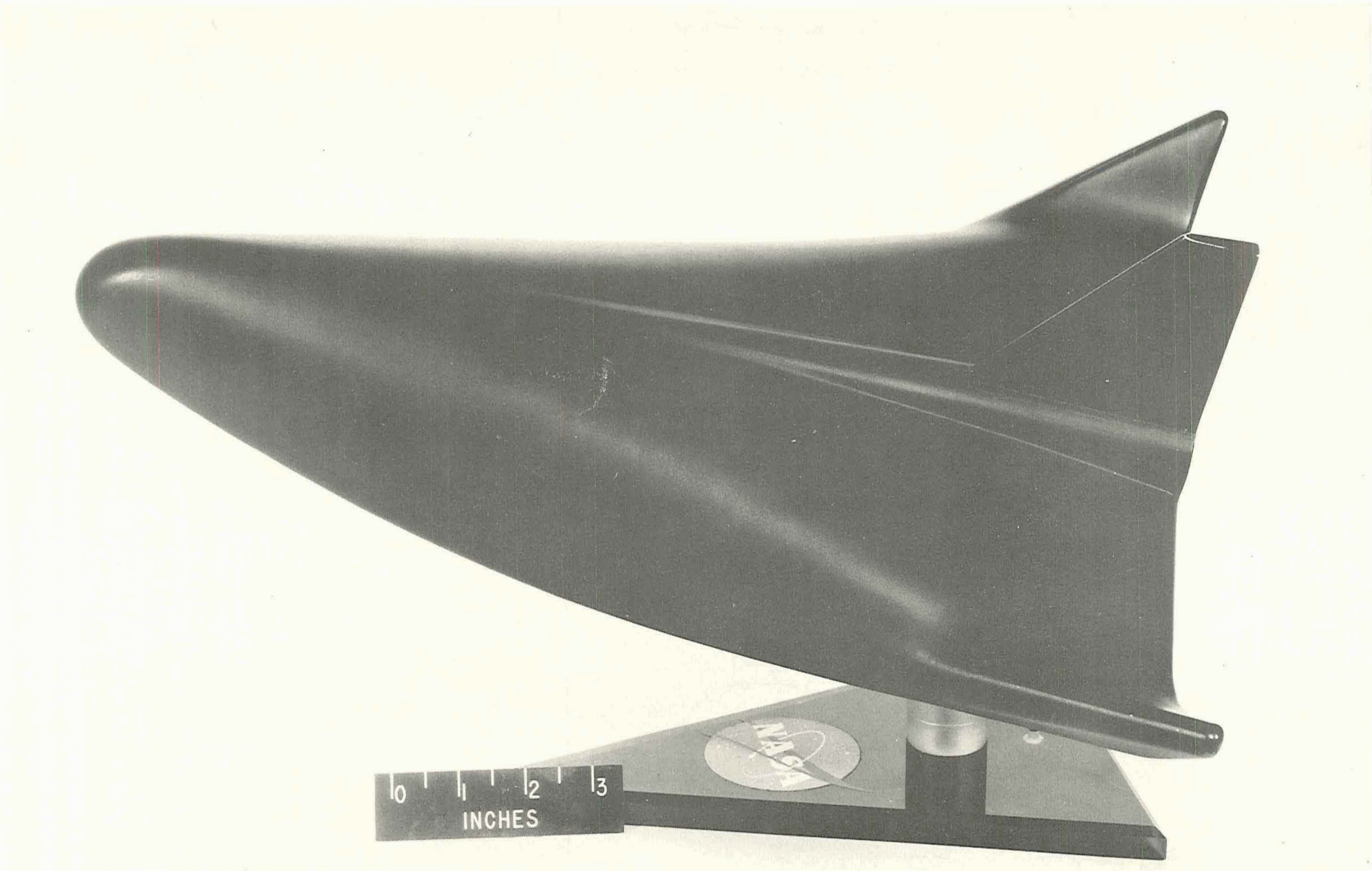

(a) Tip fin D; center fin E; canopy off.

L-65-6469

Figure 3.- Photographs of the HL-10 vehicle with various canopies and tip fins tested.

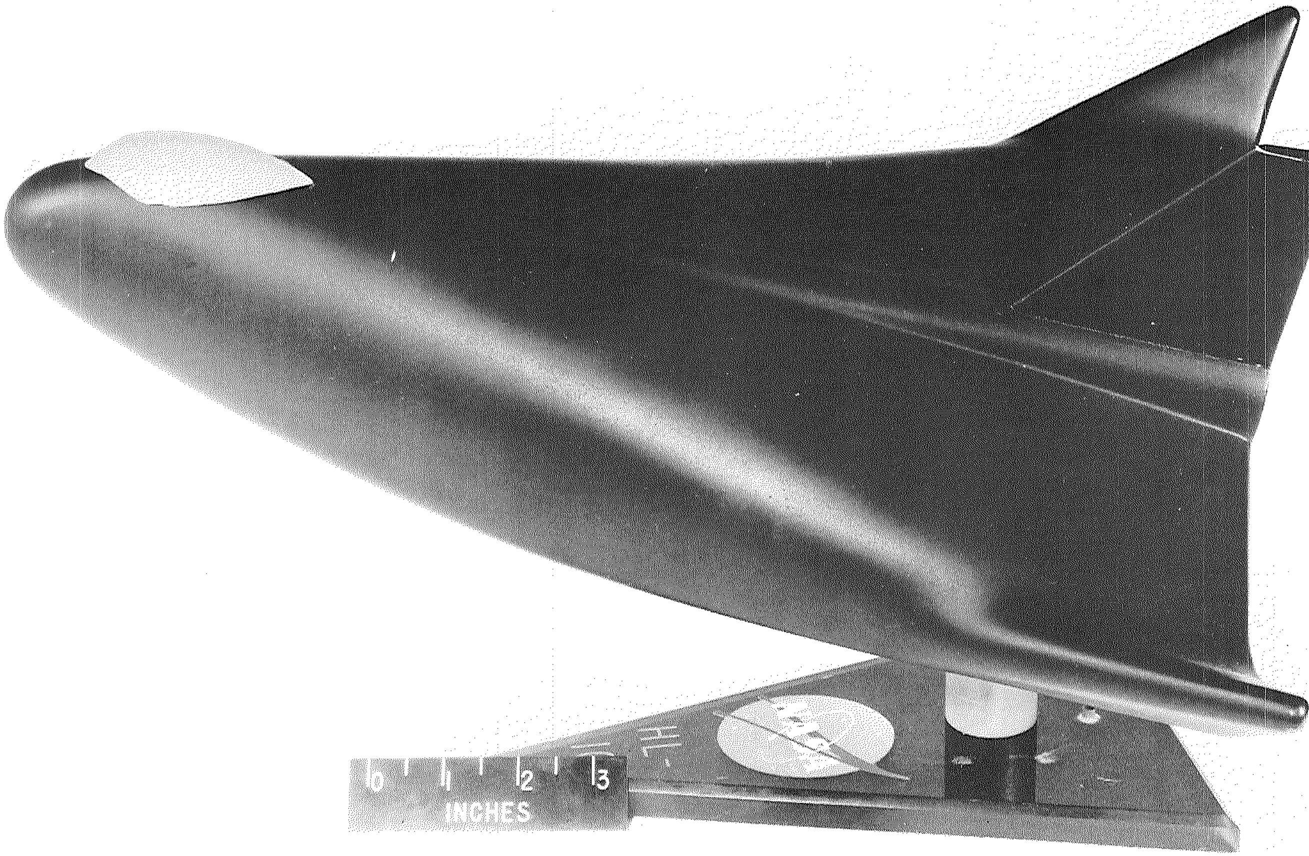

(b) Tip fin D; center fin E; canopy A. L-65-6471

Figure 3.- Continued.

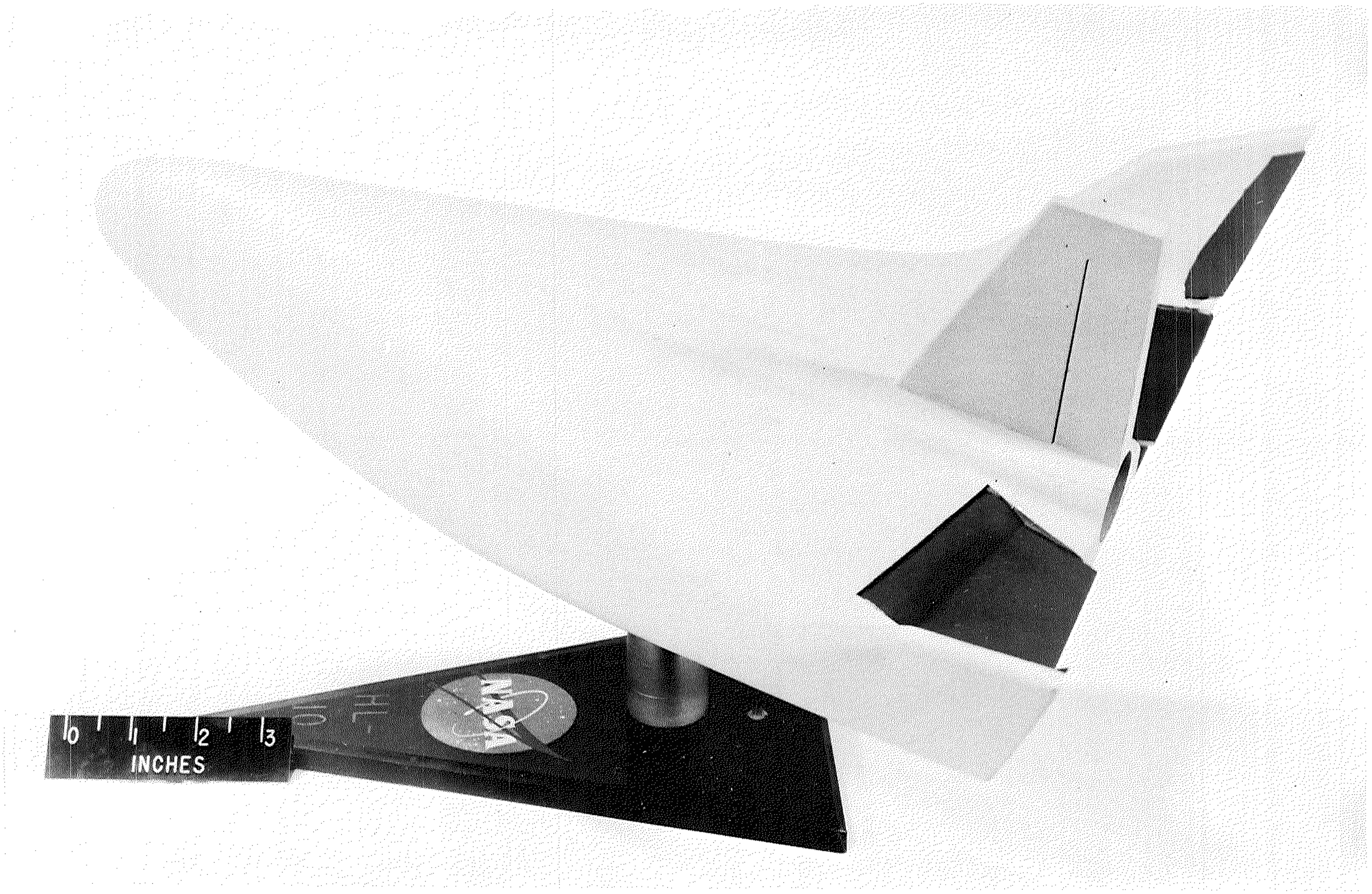

(c) Tip fin I_4; center fin E_2; canopy off.

L-65-6470

Figure 3.- Continued.

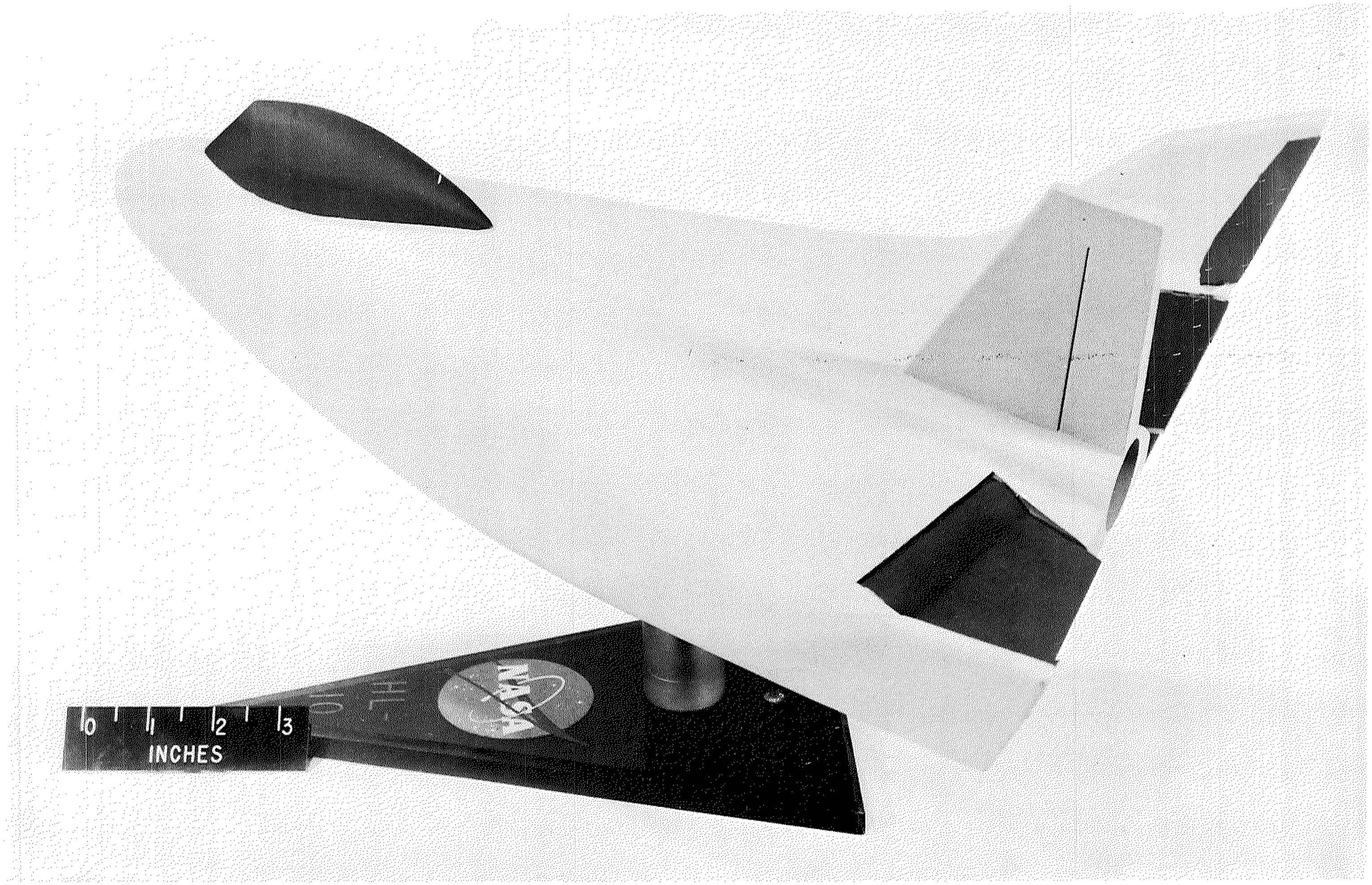

(d) Tip fin I_4; center fin E_2; canopy F. L-65-6468

Figure 3.- Continued.

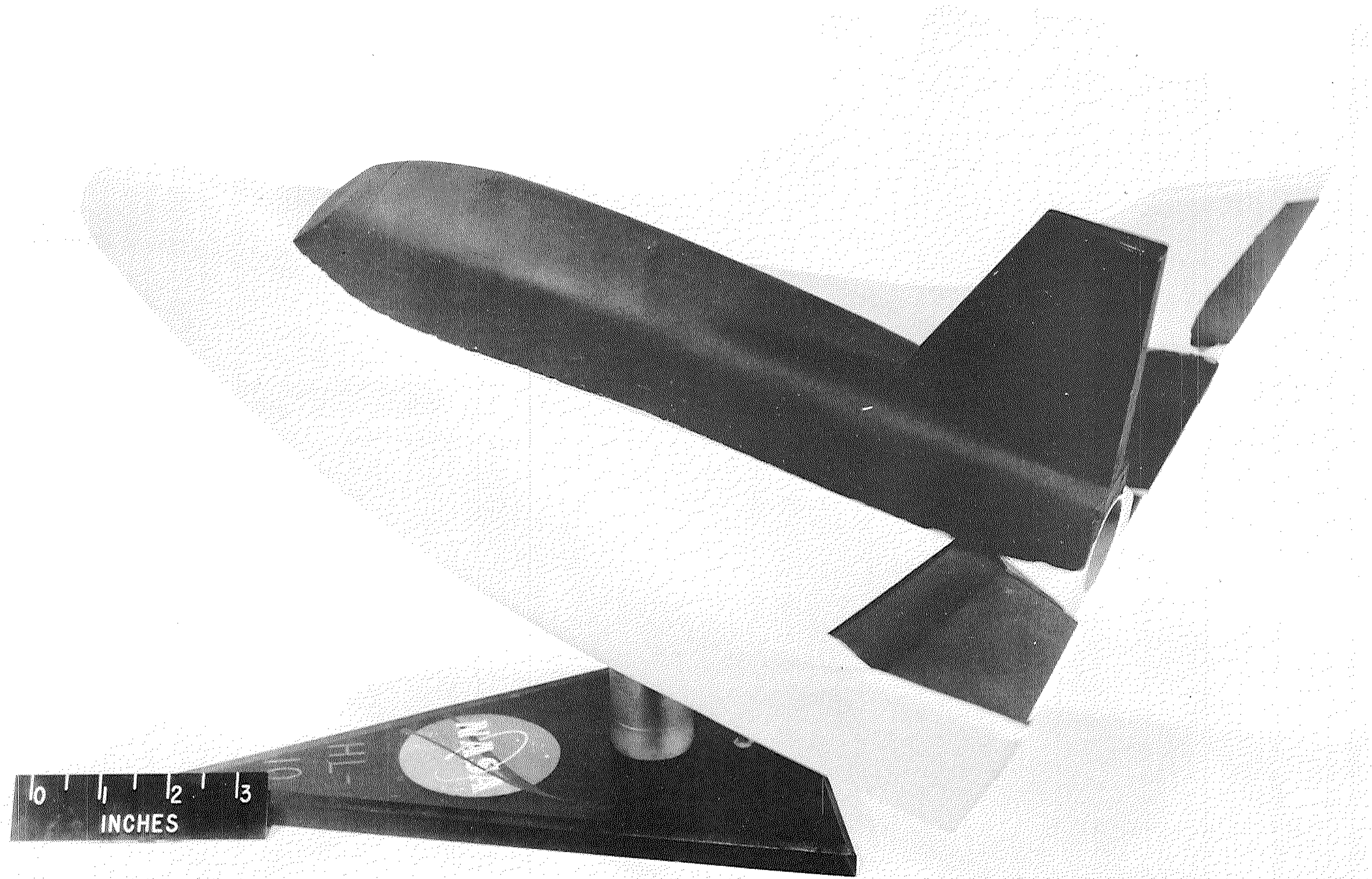

(e) Tip fin I_4; center fin E_2; canopy E.

L-65-6473

Figure 3.- Continued.

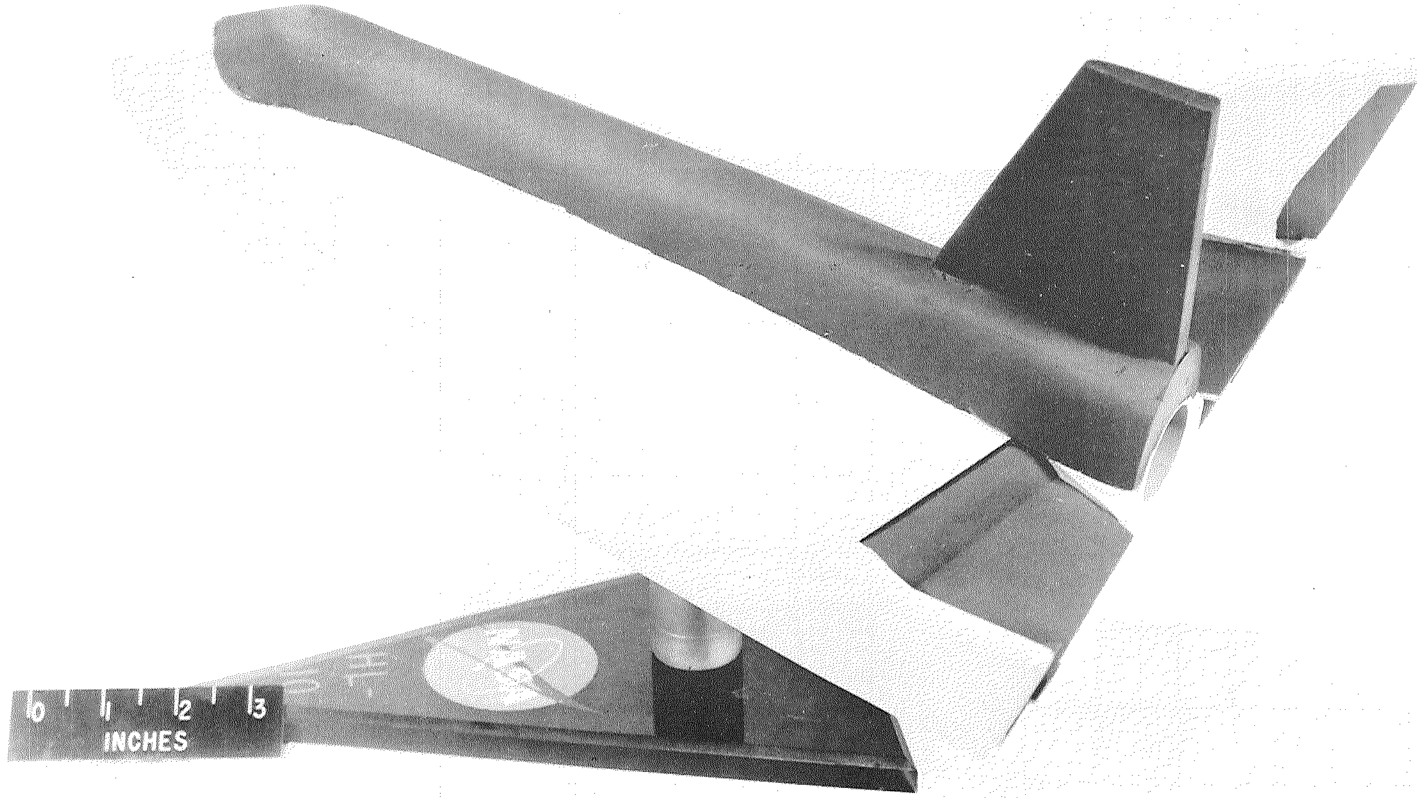

(f) Tip fin I_4; center fin E_2; canopy D.

L-65-6472

Figure 3.- Concluded.

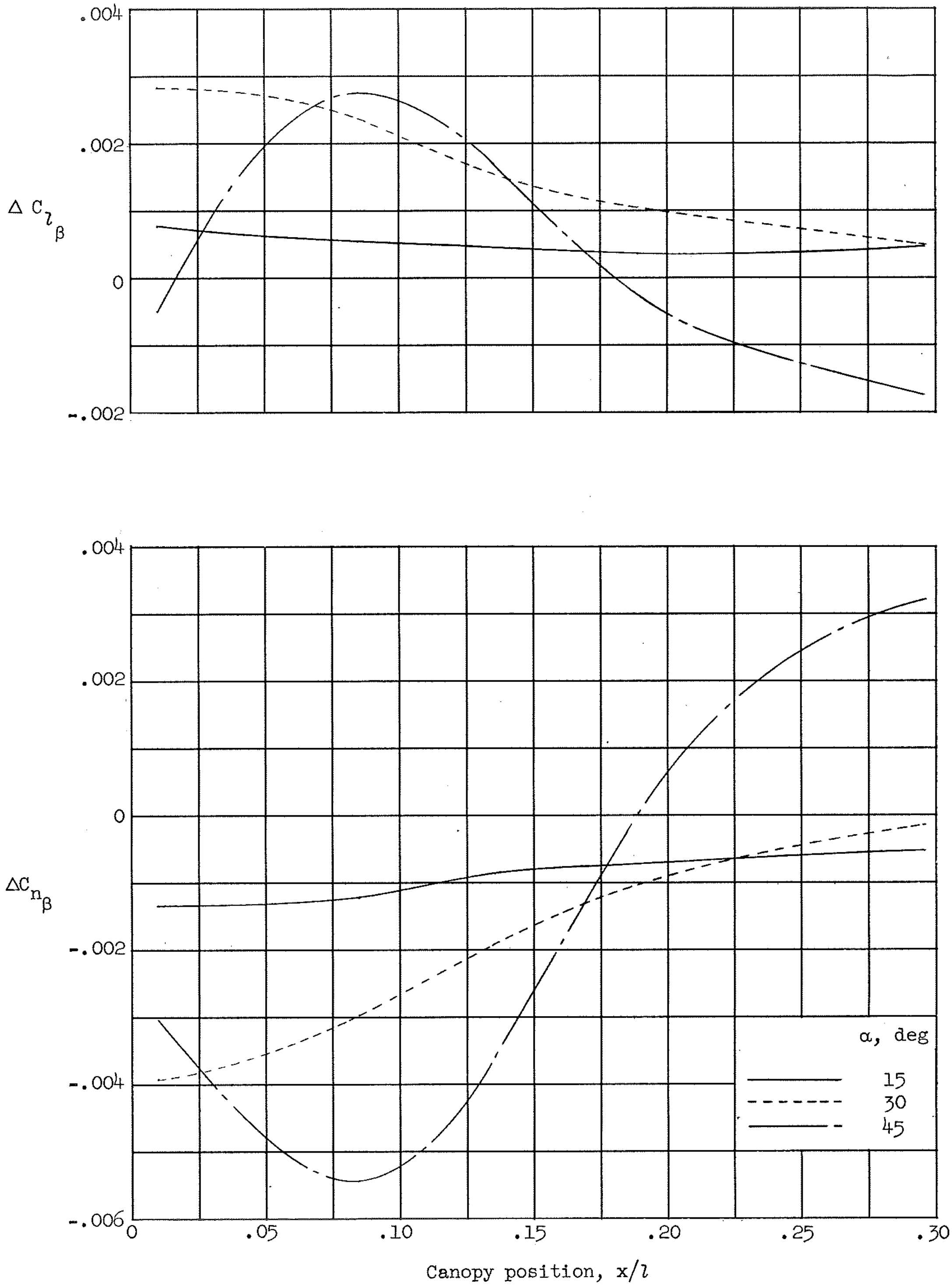

Figure 4.- Incremental effects on directional and lateral stability due to adding canopy A at various longitudinal locations. Tip fins off; center fin E; M = 0.06. Data from reference 7.

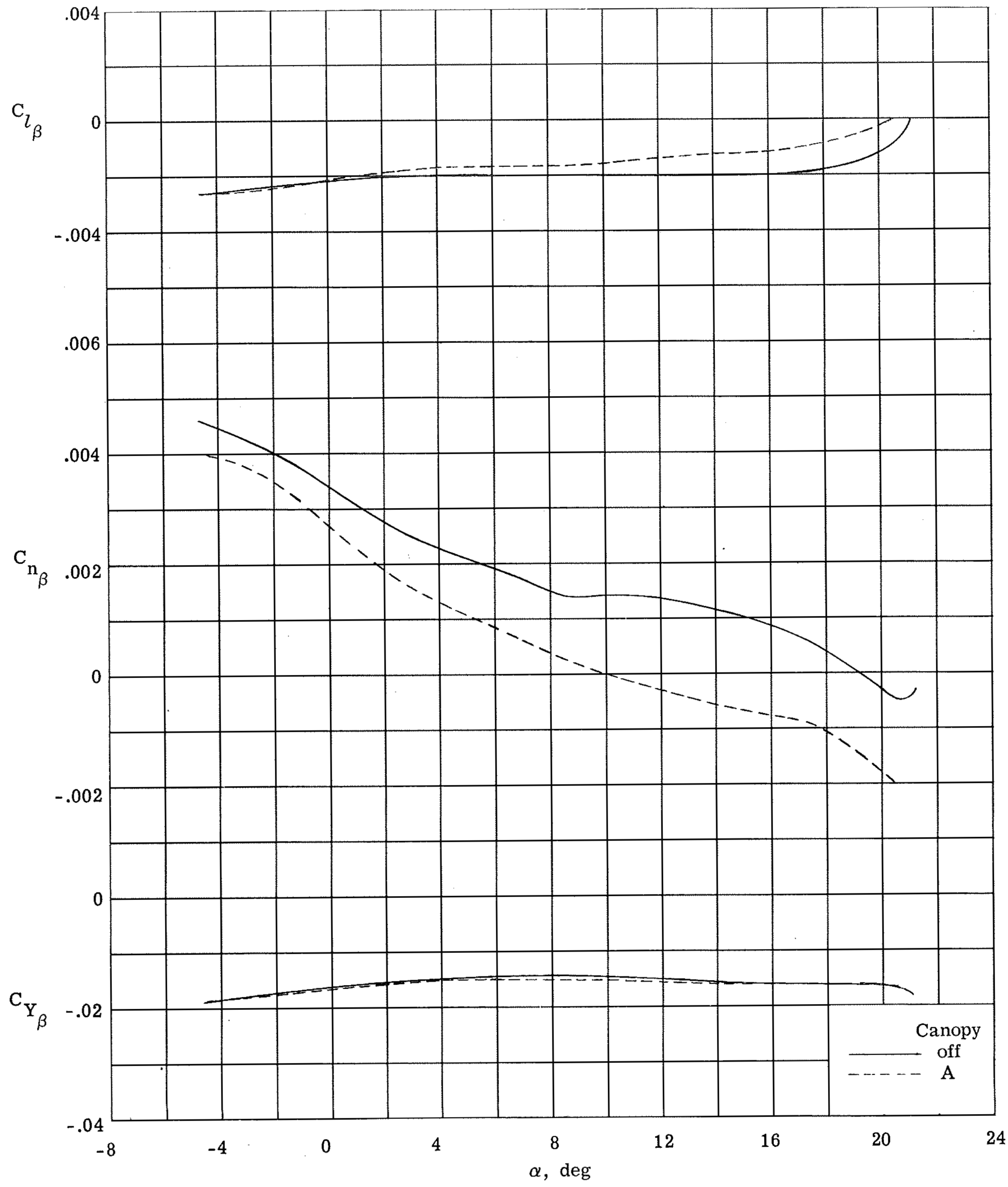

(a) M = 1.50.

Figure 5.- Effects of canopy A on the directional and lateral stability characteristics at supersonic speeds. Canopy origin at 0.09l; tip fin J; center fin E. Data from reference 18.

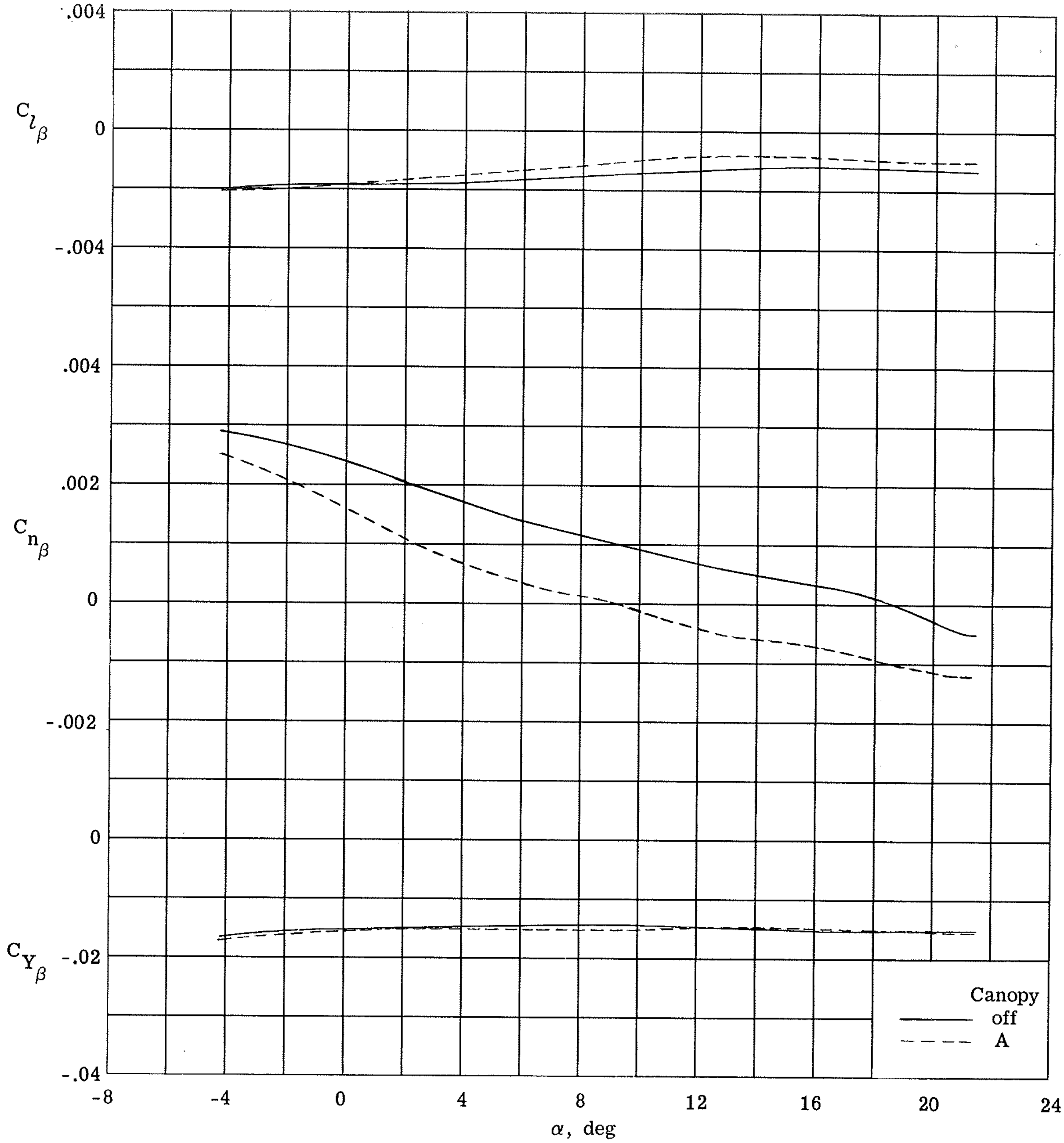

(b) M = 1.80.

Figure 5.- Continued.

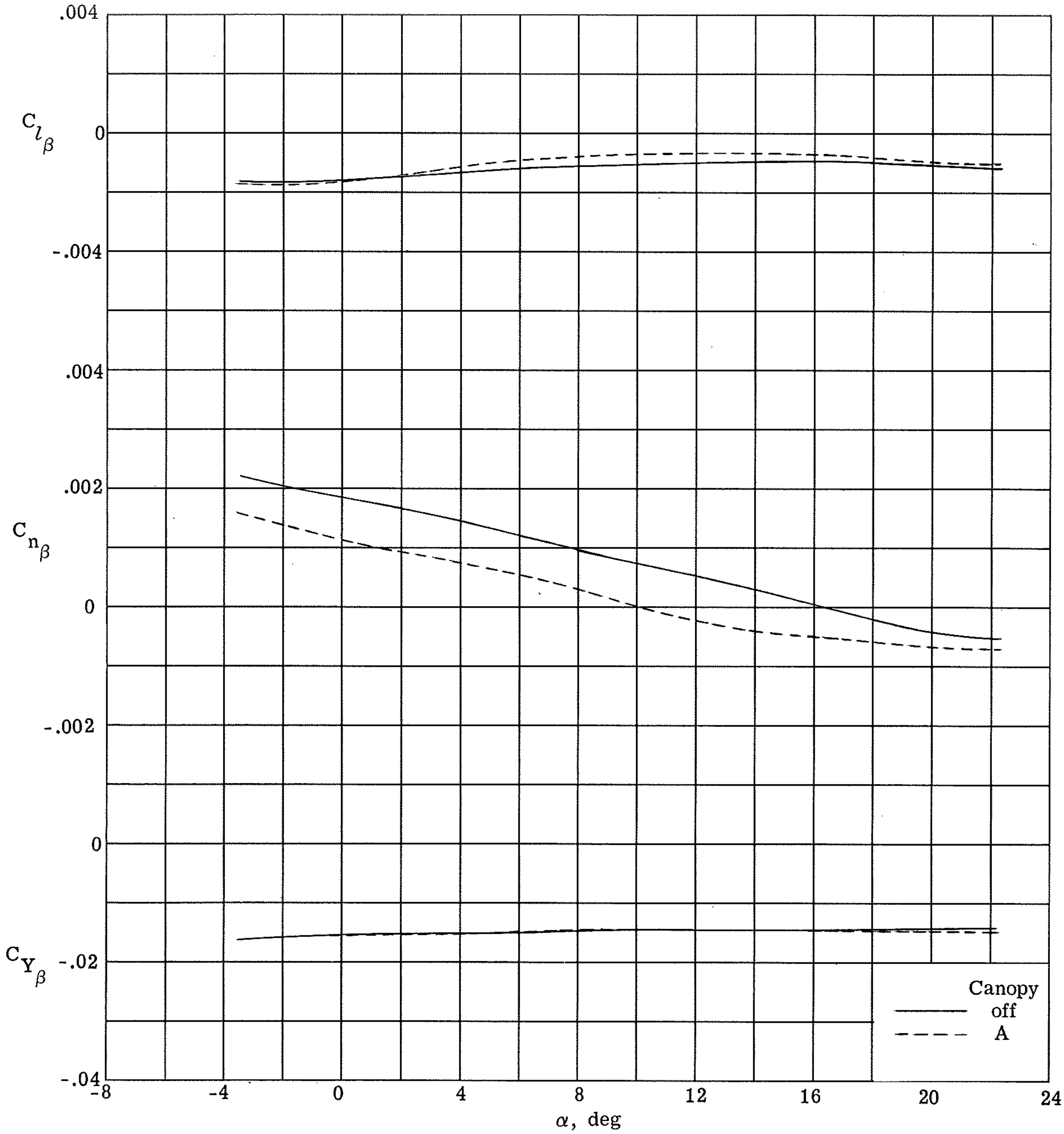

(c) M = 2.16.

Figure 5.- Concluded.

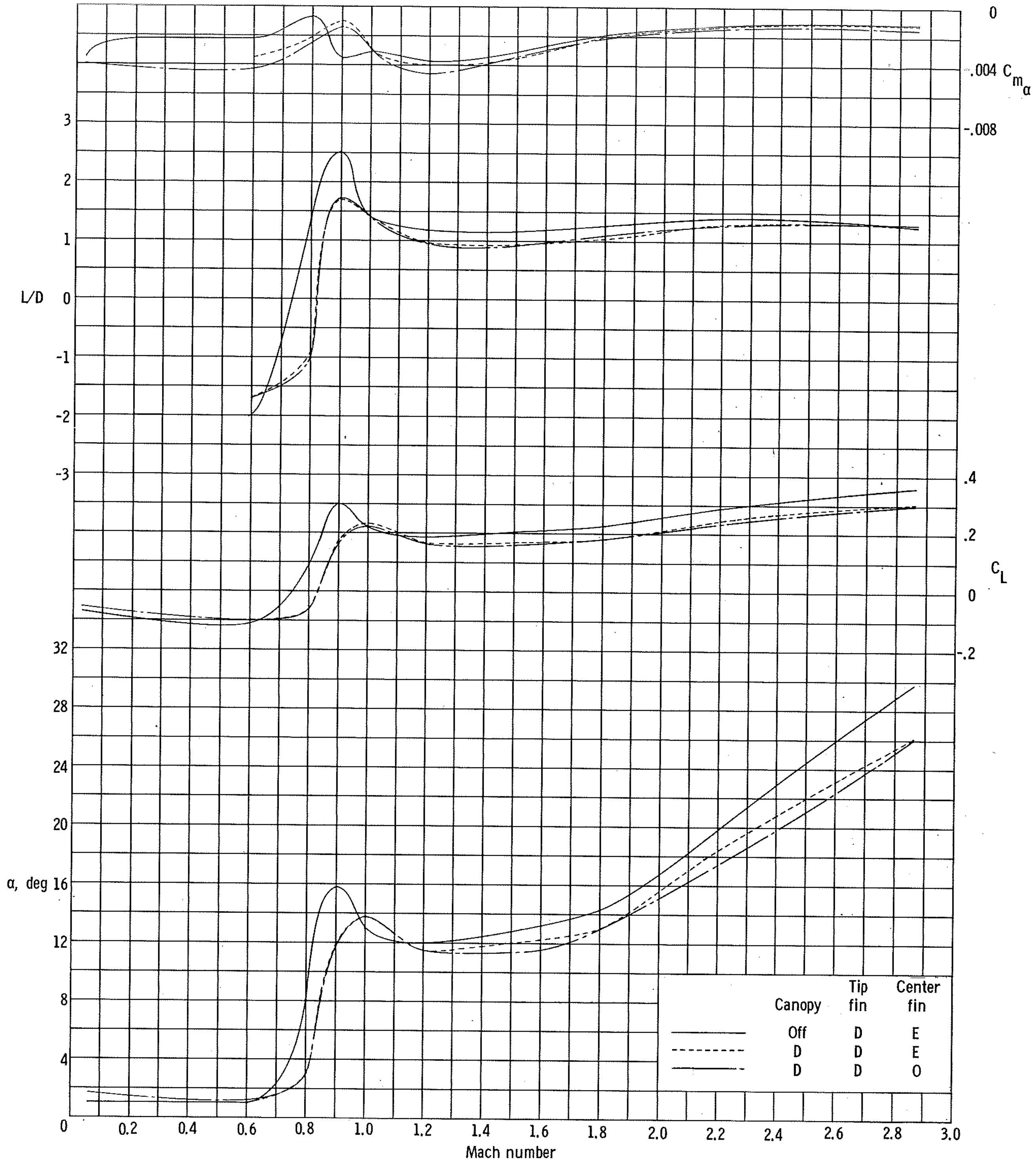

Figure 6.- Effects of canopy D on the longitudinal characteristics at trim with $\delta_e = 0^o$. Data from references 5, 7, 10, and 11, and unpublished results at $M = 0.06$.

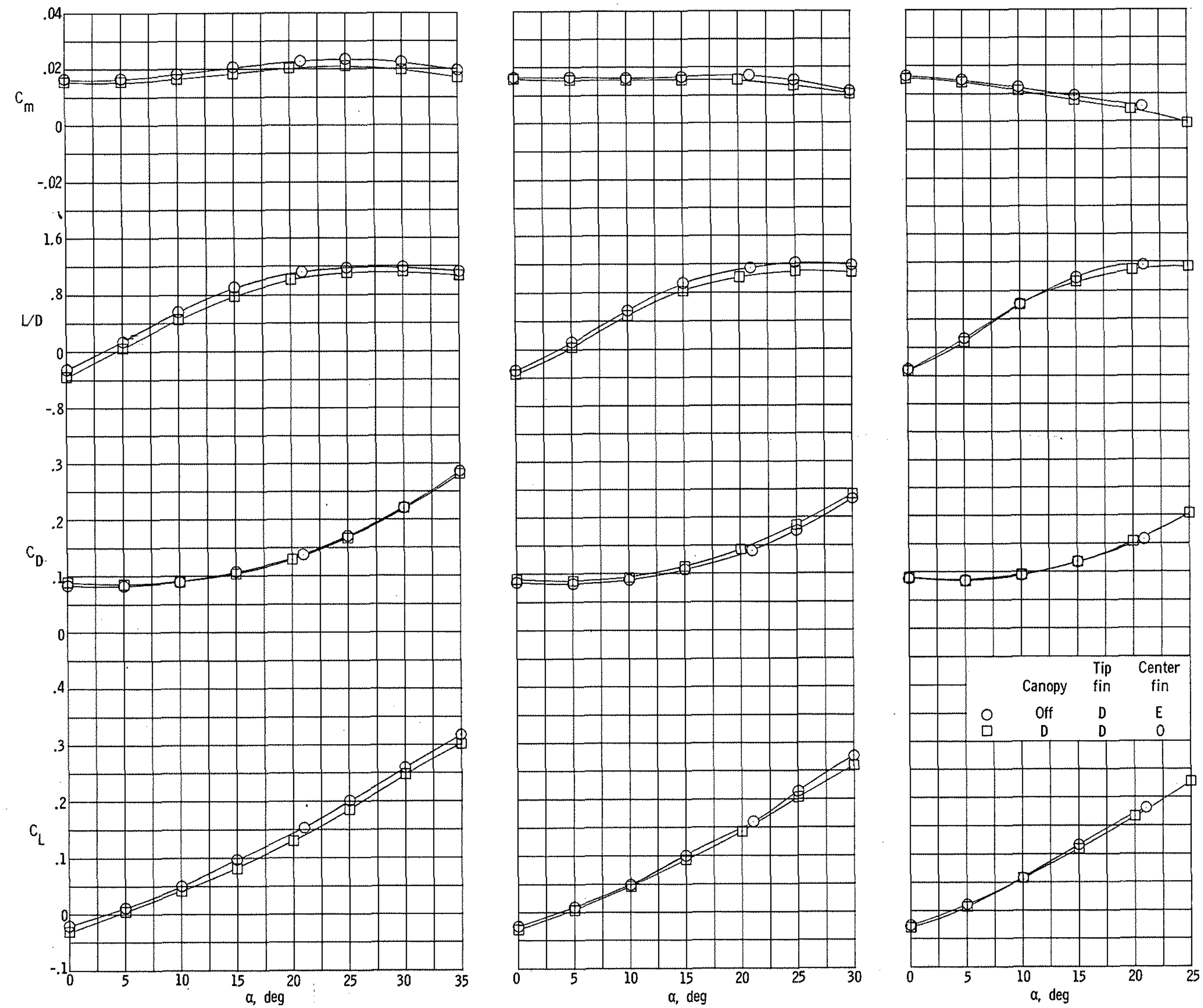

(a) $\delta_e = 0^{\circ}$.

(b) $\delta_e = 15^{\circ}$.

(c) $\delta_e = 30^{\circ}$.

Figure 7.- Effects of canopy D on the longitudinal characteristics at $M = 6.8$ for several elevon deflection angles. Canopy-off data from reference 3.

CONFIDENTIAL

CONFIDENTIAL

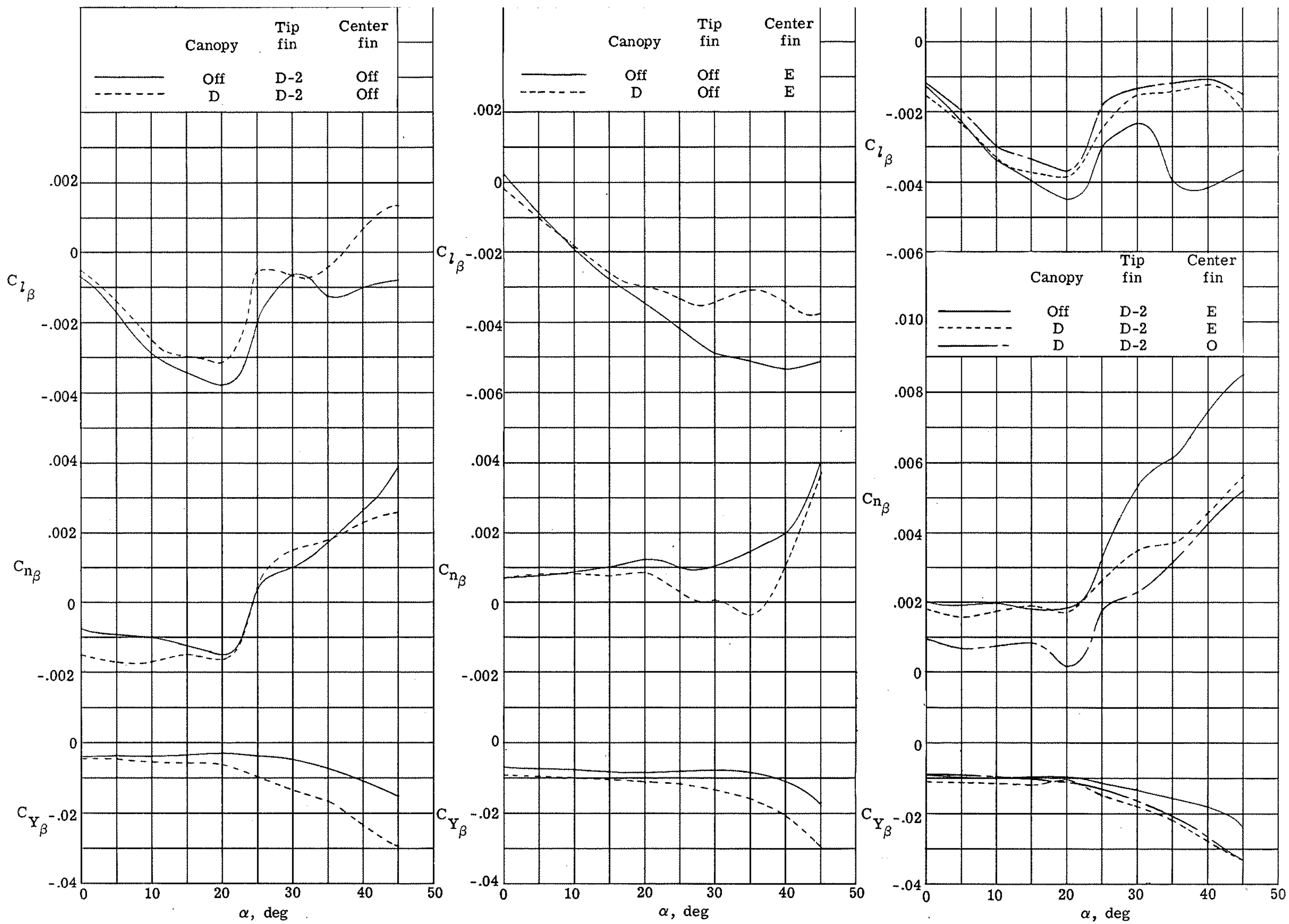

(a) M = 0.06; data from reference 7 and unpublished results.

Figure 8.- Effects of canopy D on the directional and lateral stability characteristics at various Mach numbers for $\delta_e = 0^0$.

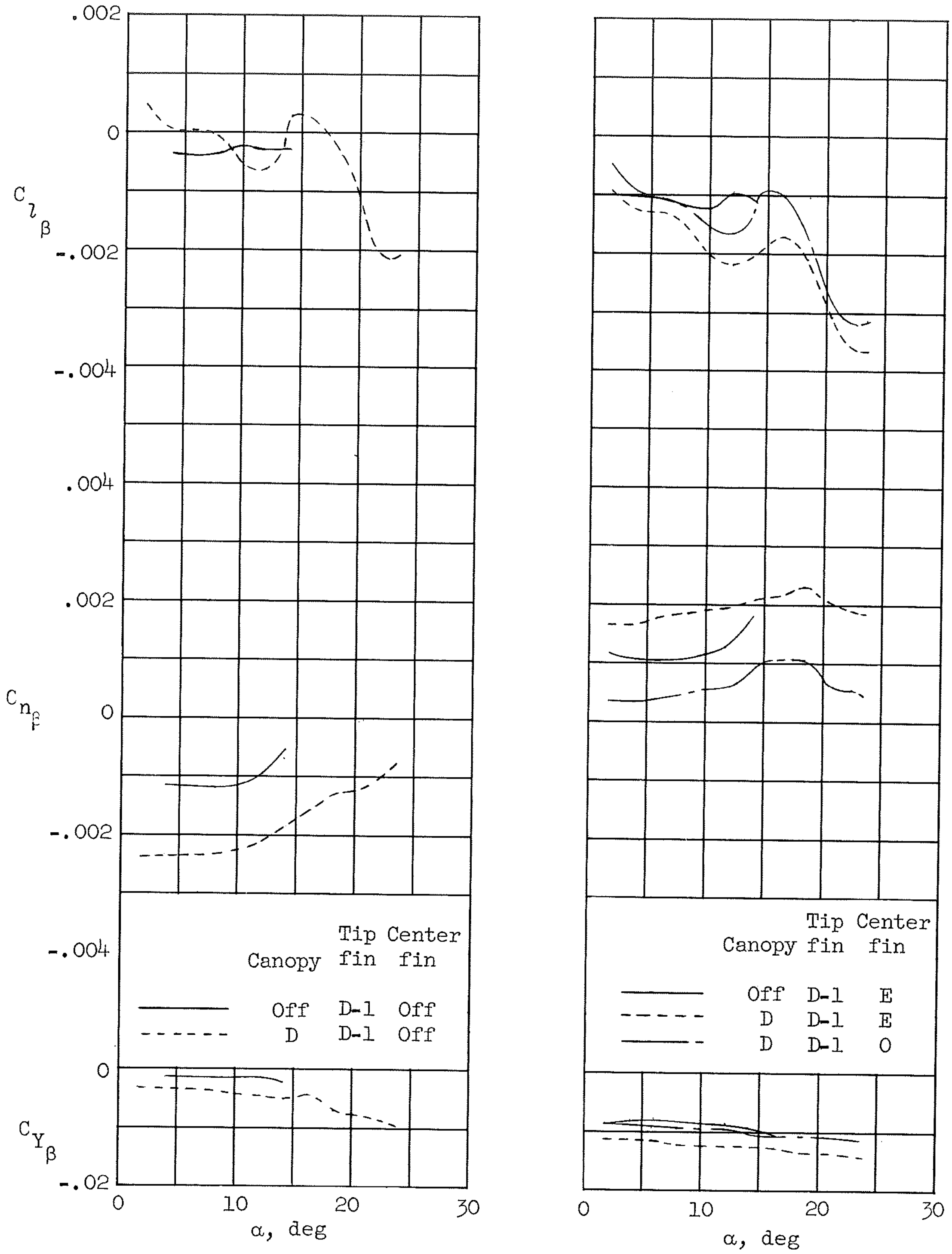

(b) M = 0.60; data from reference 5.

Figure 8.- Continued.

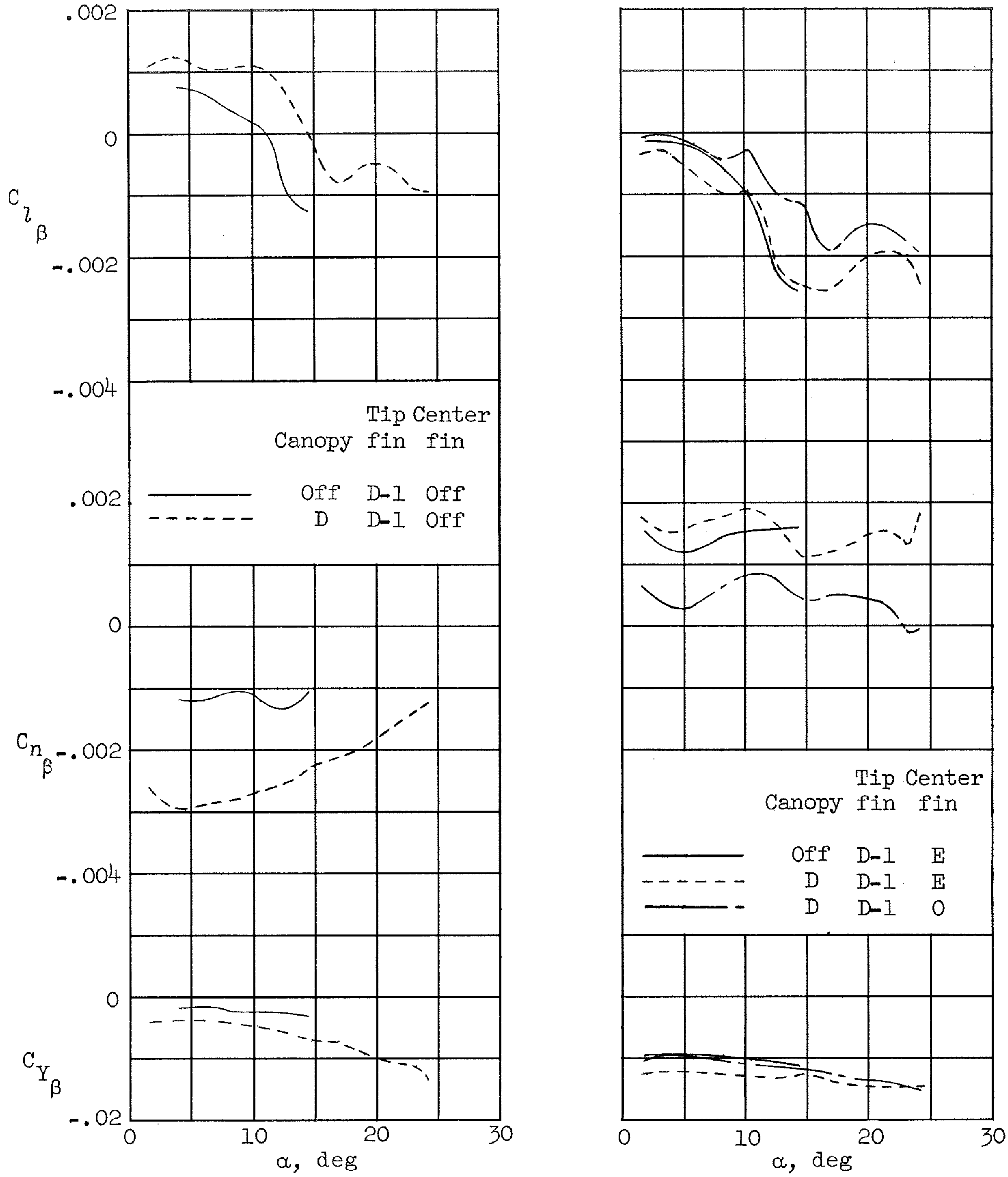

(c) M = 0.80; data from reference 5.

Figure 8.- Continued.

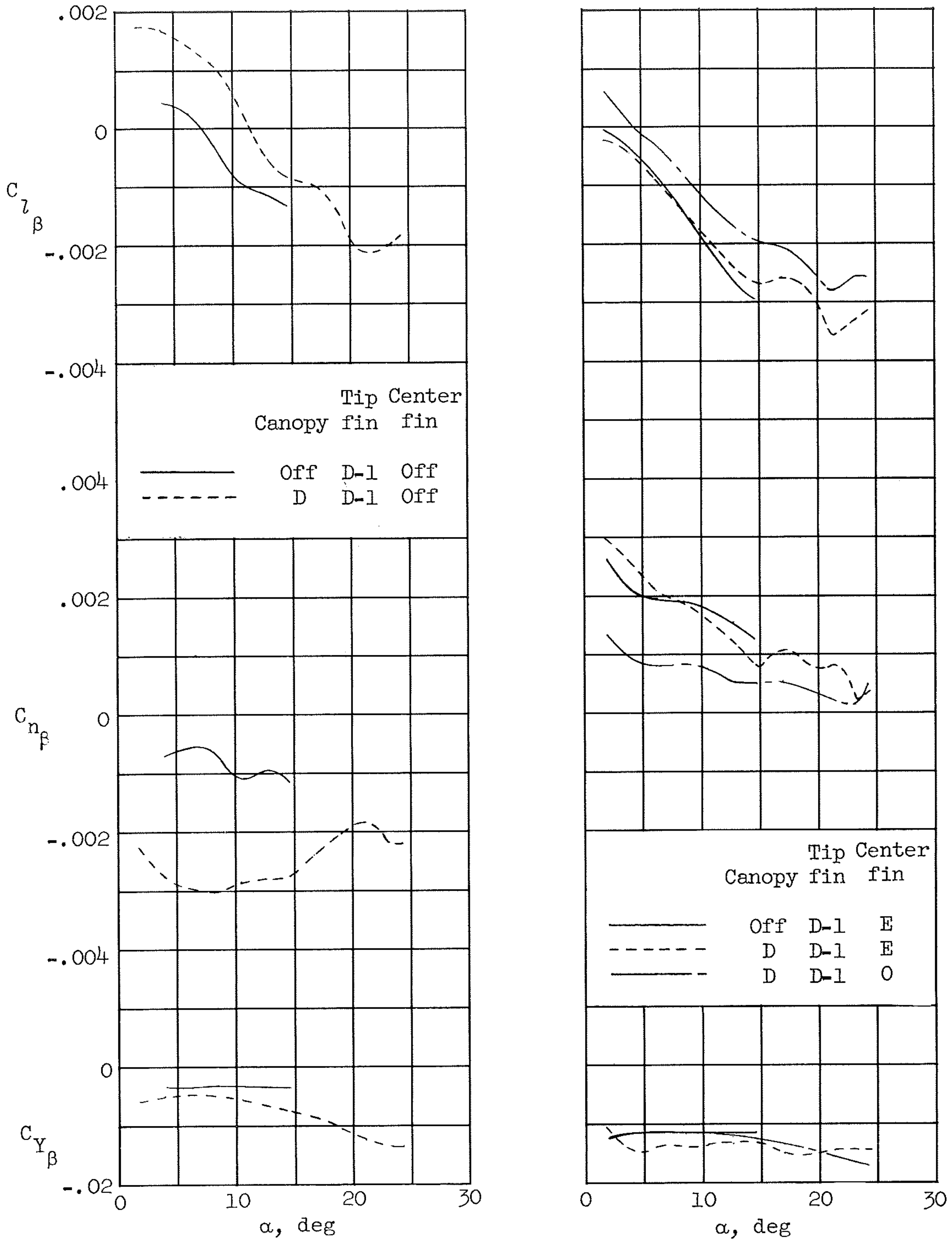

(d) M = 0.90; data from reference 5.

Figure 8.- Continued.

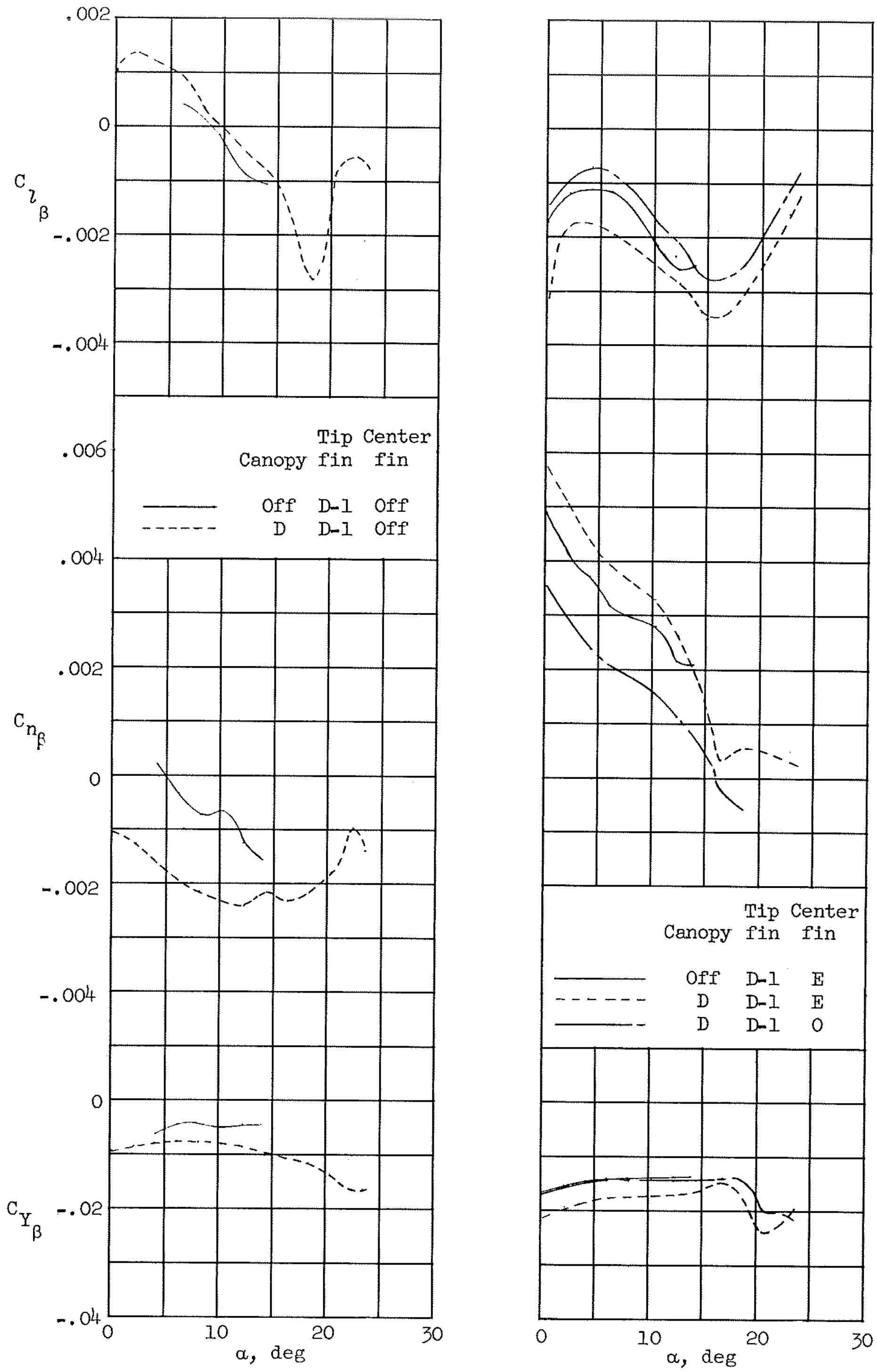

(e) M = 1.00; data from reference 5.

Figure 8.- Continued.

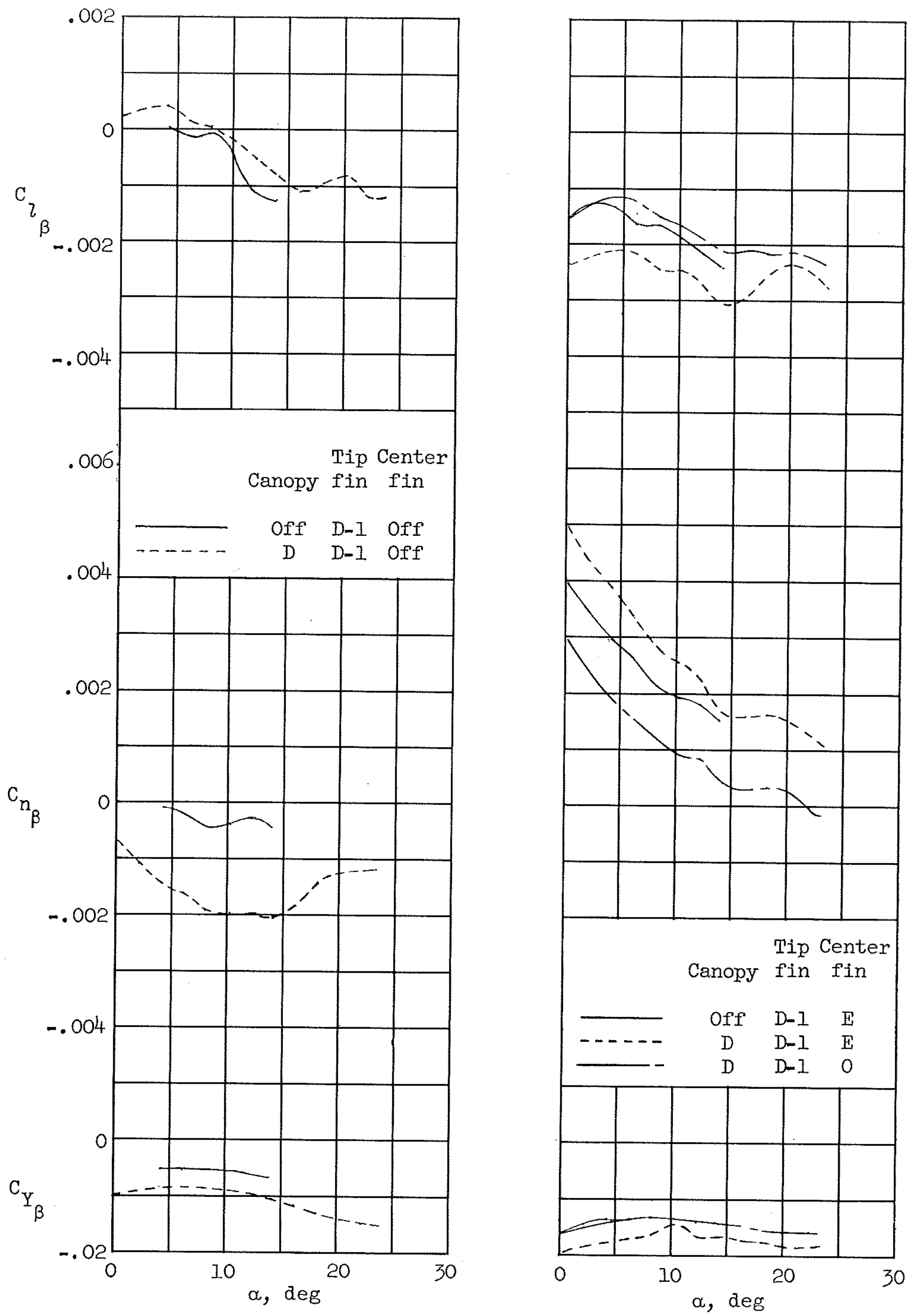

(f) M = 1.20; data from reference 5.

Figure 8.- Continued.

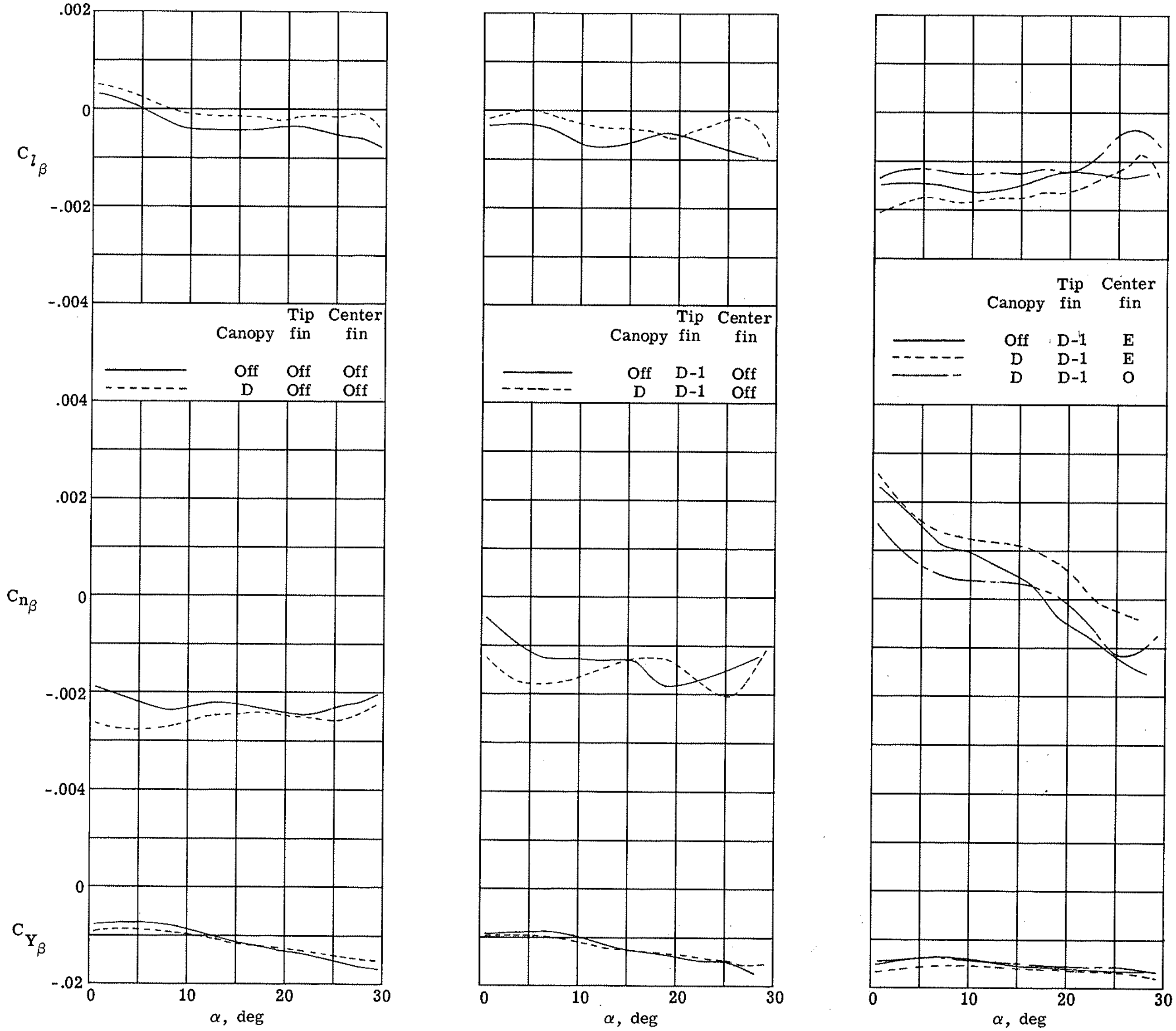

(g) M = 1.50; data from references 10 and 11.

Figure 8.- Continued.

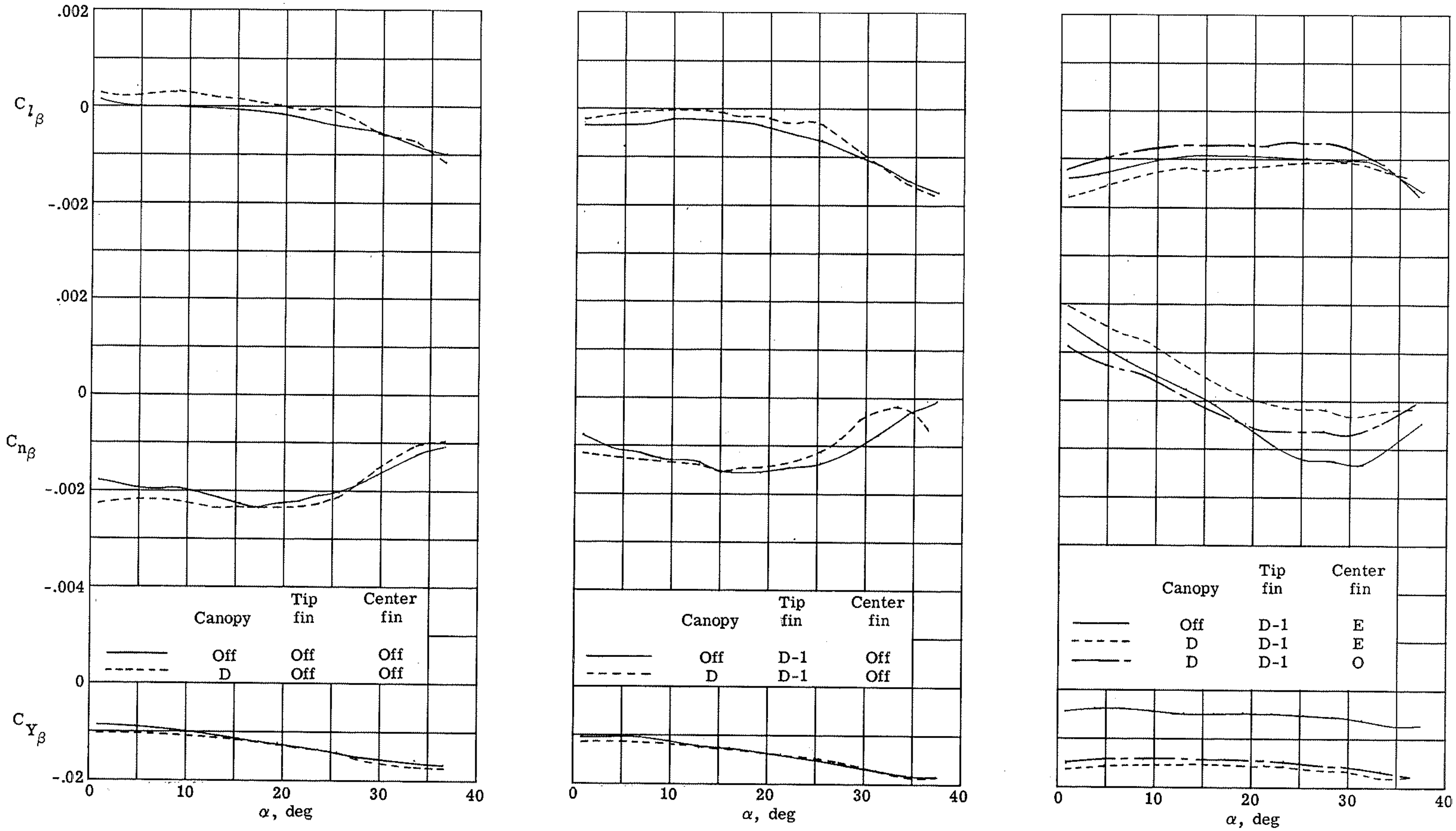

(h) M = 1.80; data from references 10 and 11.

Figure 8.- Continued.

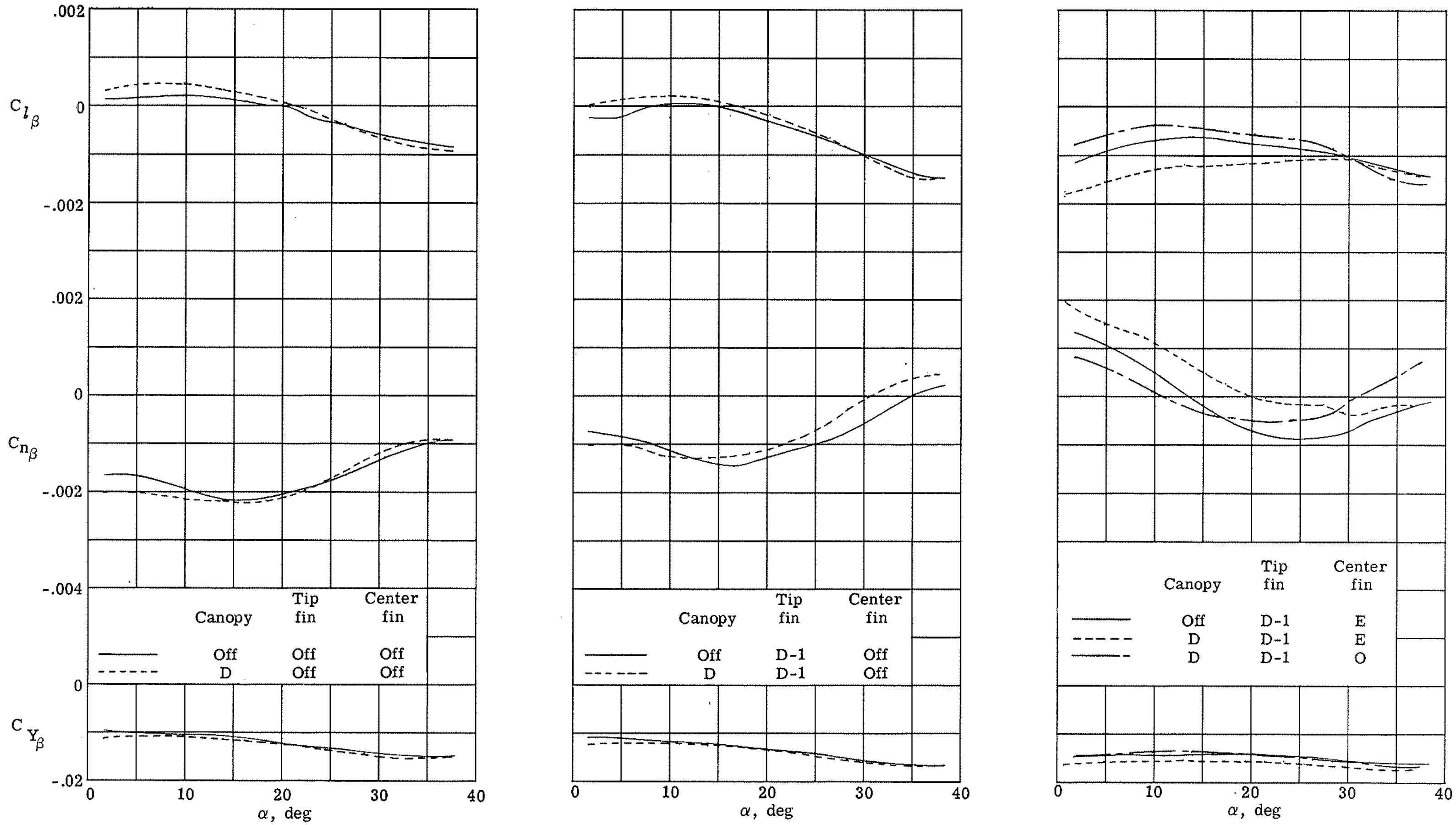

(i) M = 2.16; data from references 10 and 11.

Figure 8.- Continued.

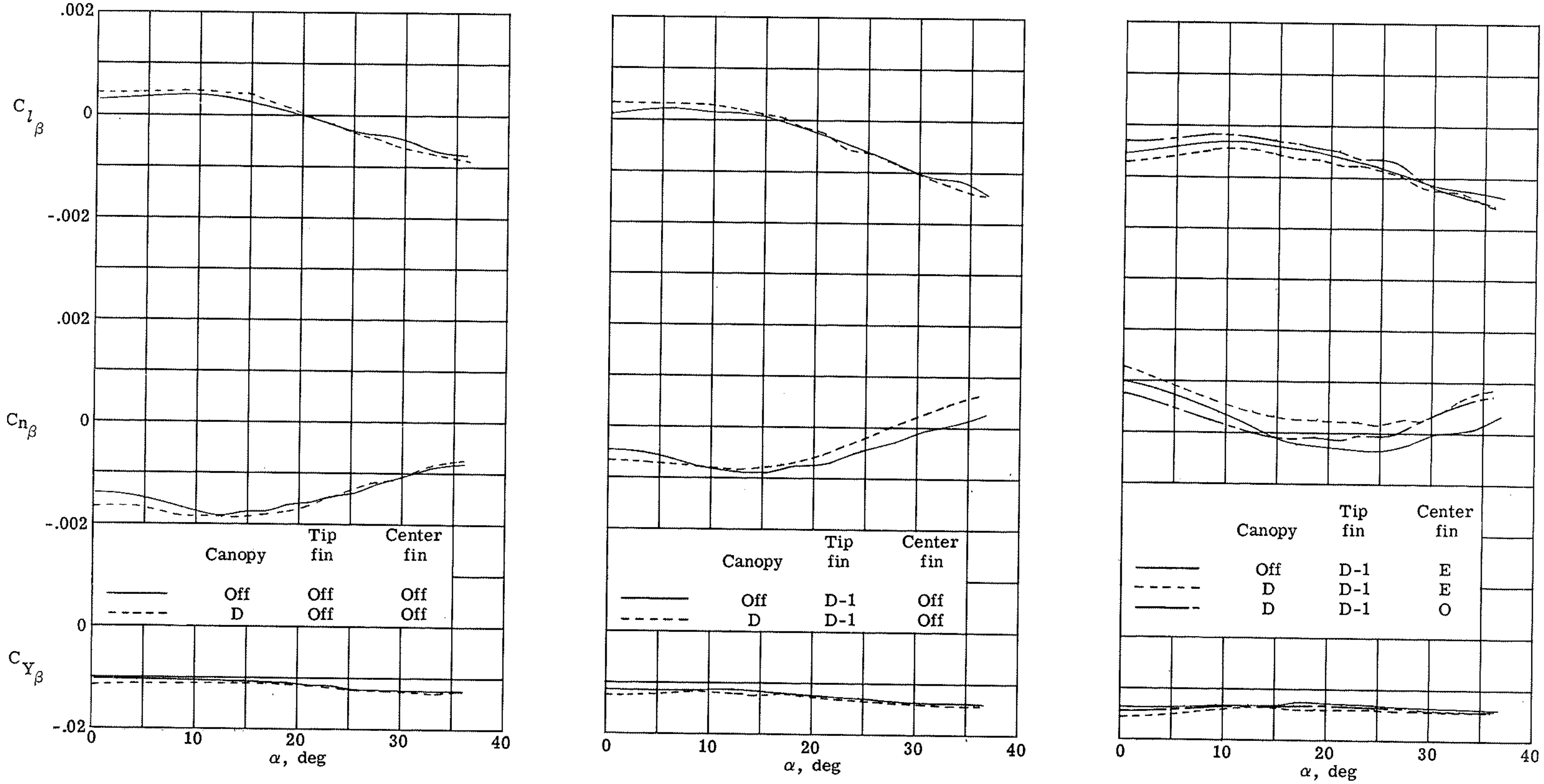

(j) M = 2.86; data from references 10 and 11.

Figure 8.- Continued.

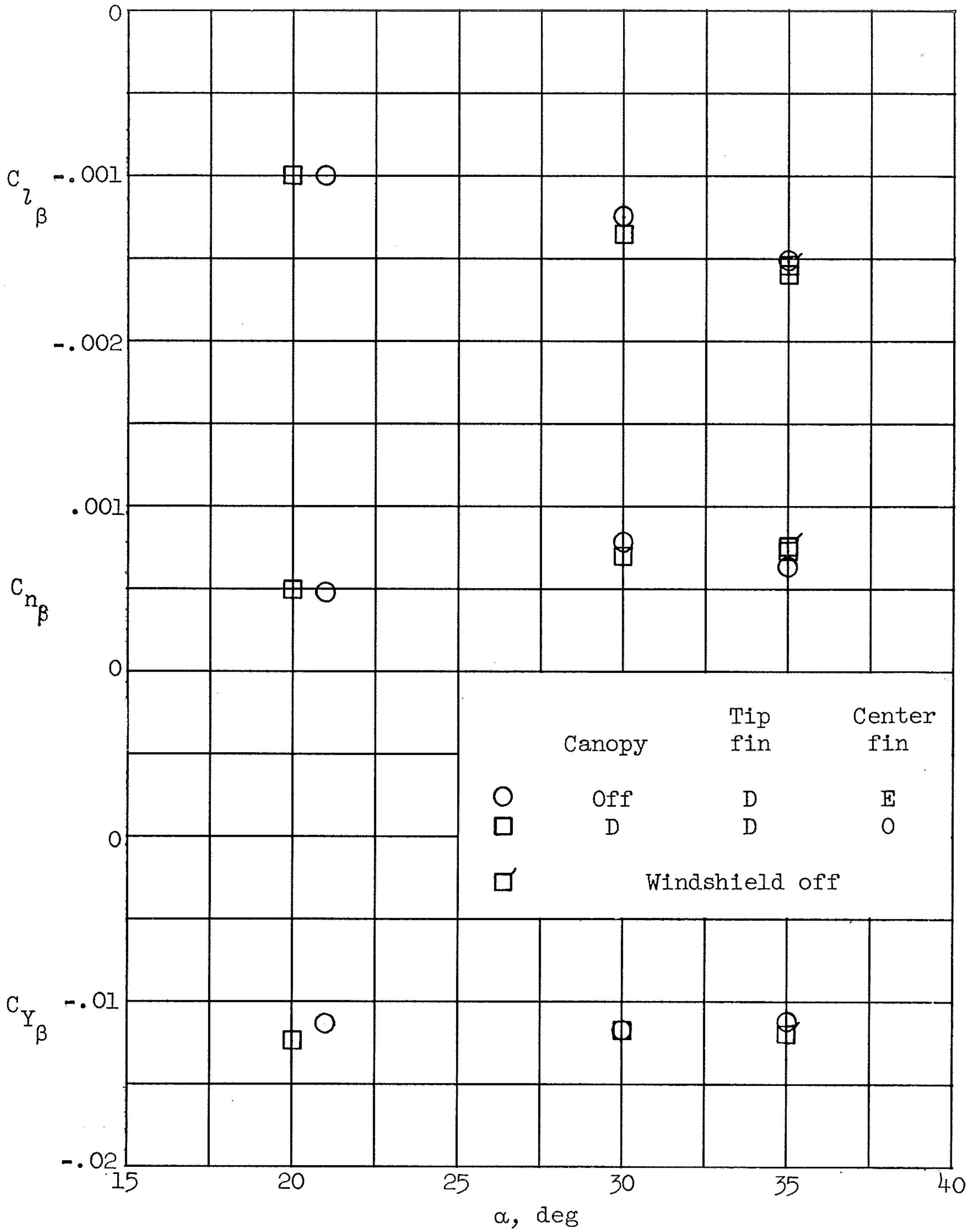

(k) M = 6.8; data from reference 3 and unpublished results.

Figure 8.- Concluded.

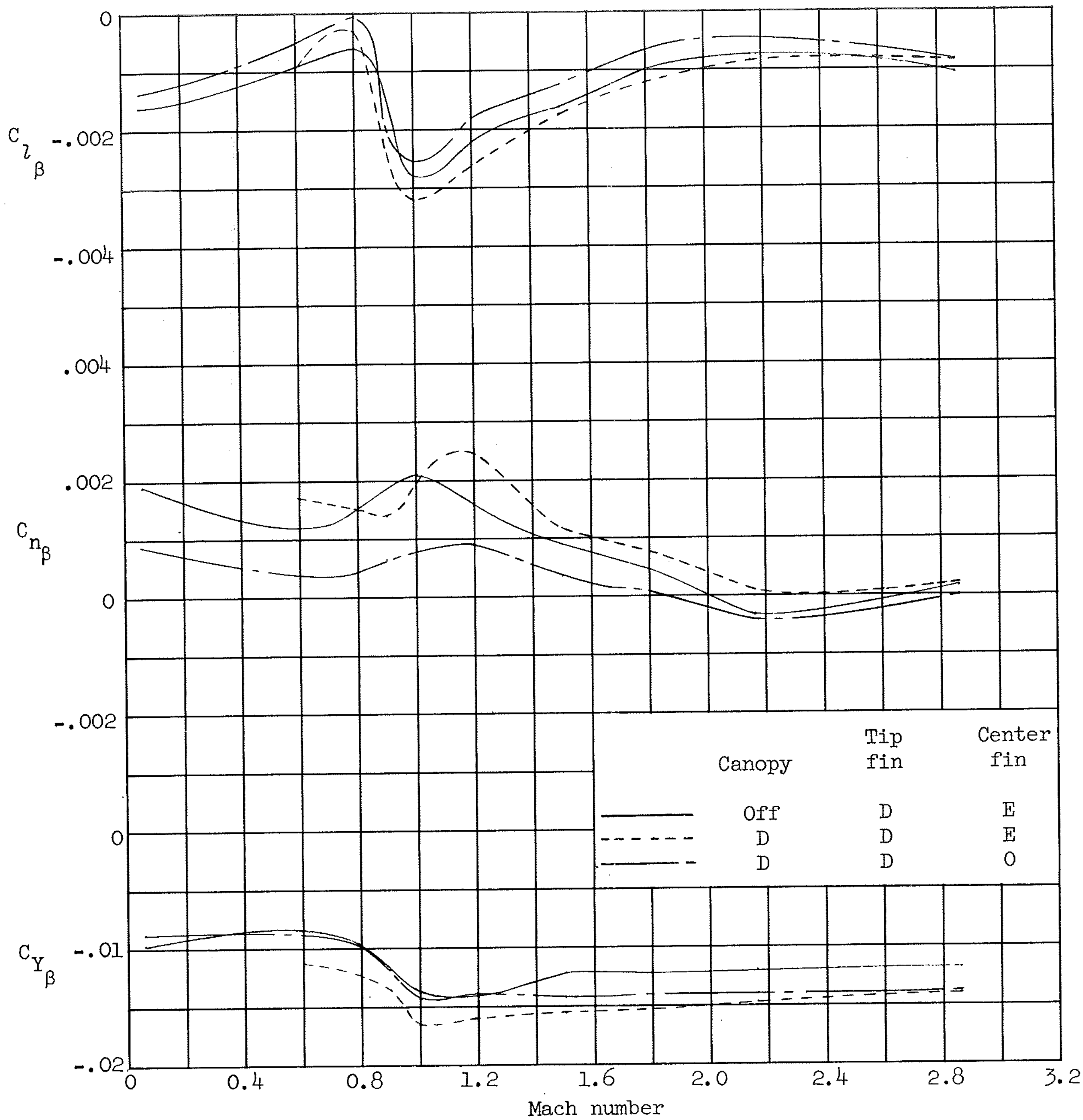

Figure 9.- Effects of canopy D on the directional and lateral stability characteristics at trim for $\delta_e = 0^0$.

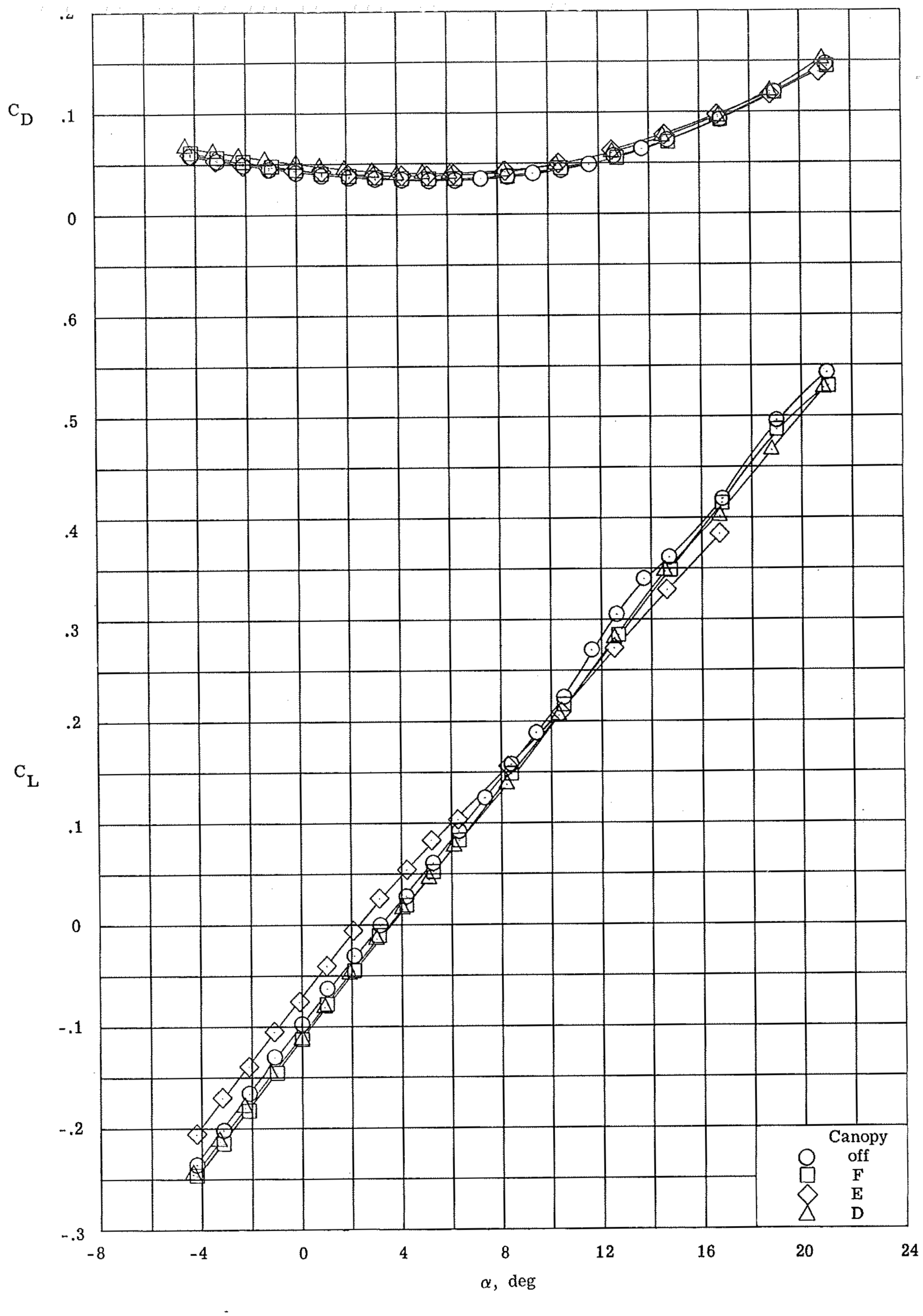

(a) $\delta_e = 0^0$.

Figure 10.- Effects of various canopies and elevon deflection angles on the longitudinal characteristics at $M = 0.35$. Tip fin I_4; center fin E_2; tip-fin and elevon flaps in subsonic mode.

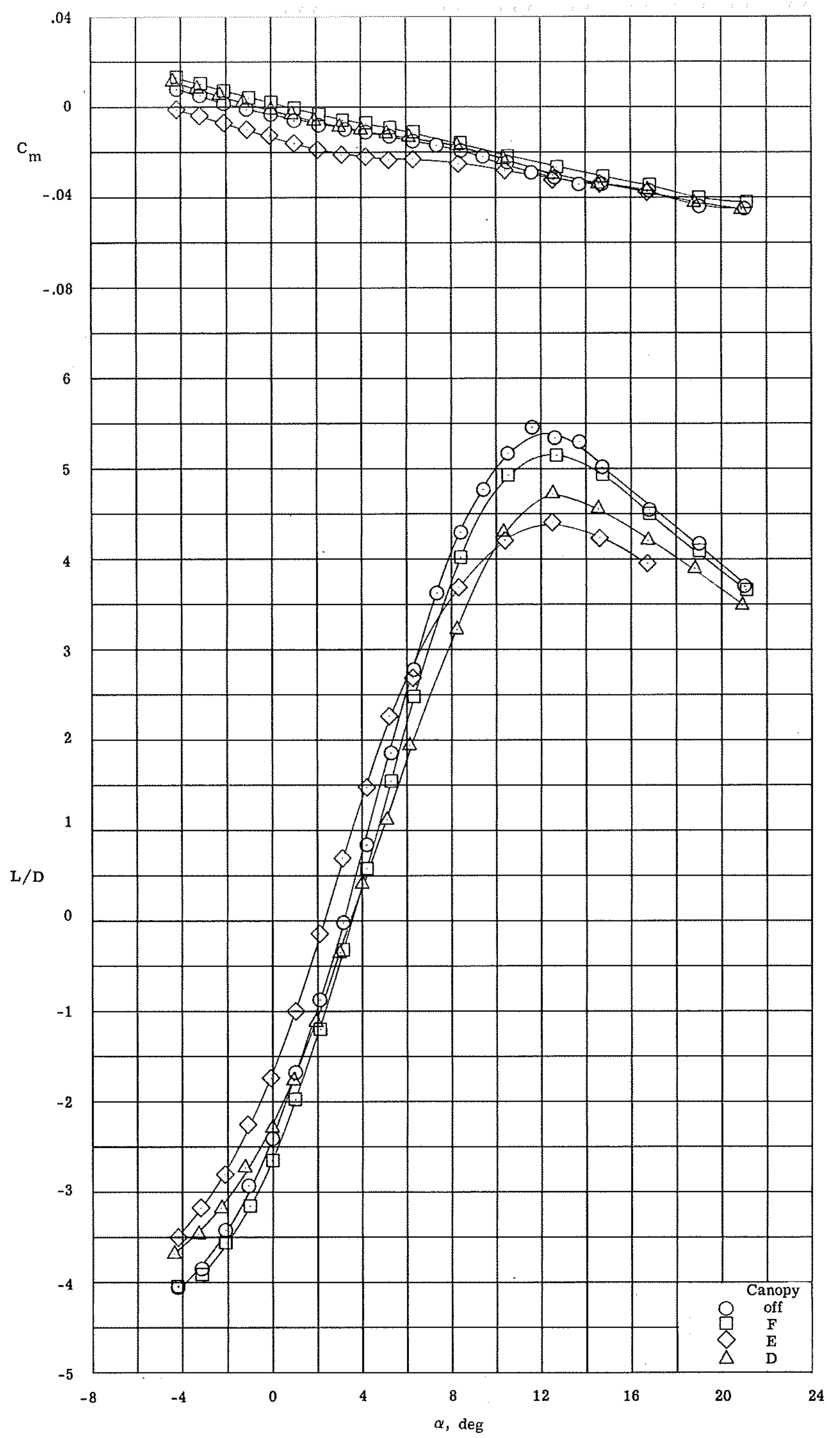

(a) Concluded.

Figure 10.- Continued.

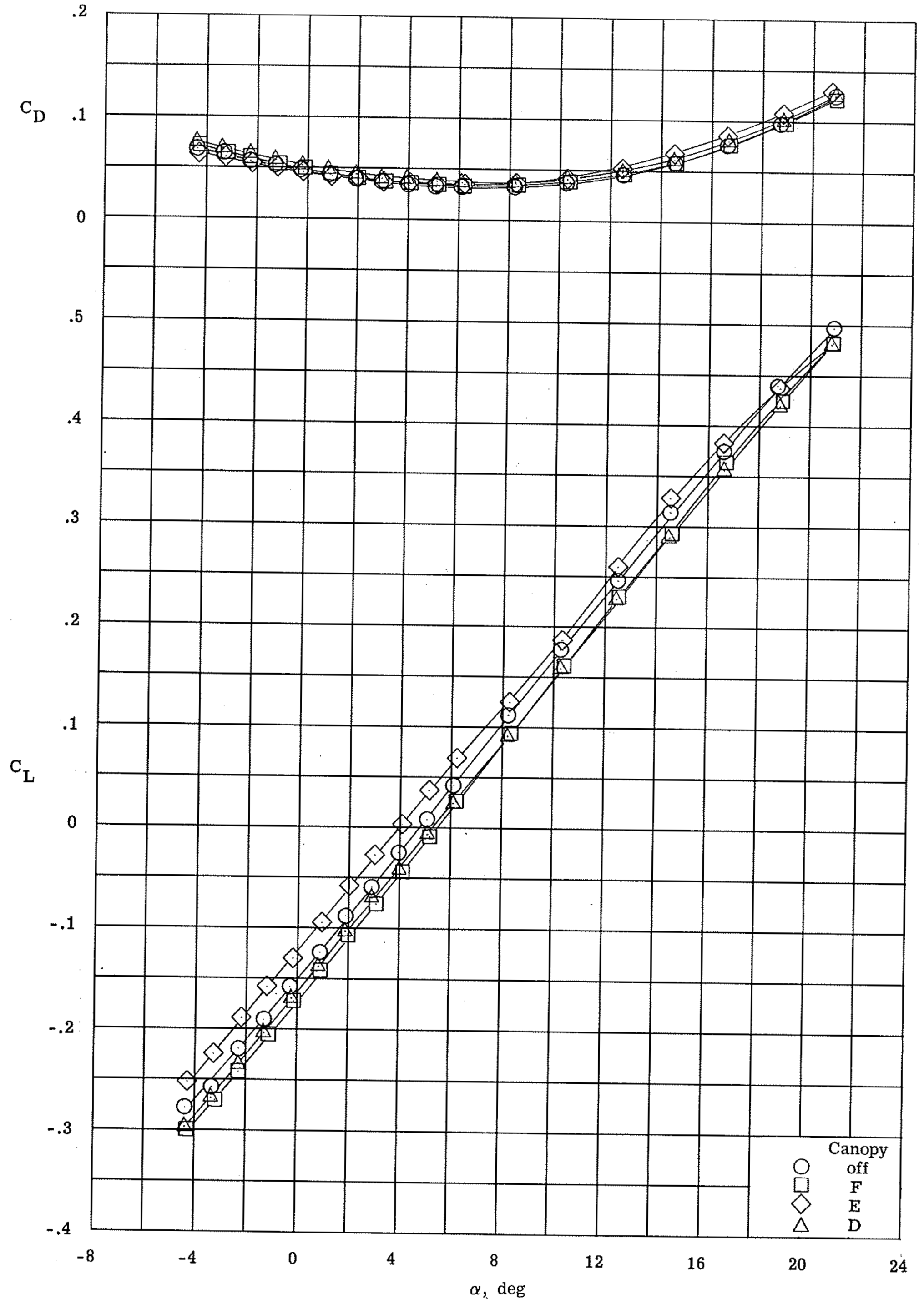

(b) $\delta_e = -5^{\circ}$.

Figure 10.- Continued.

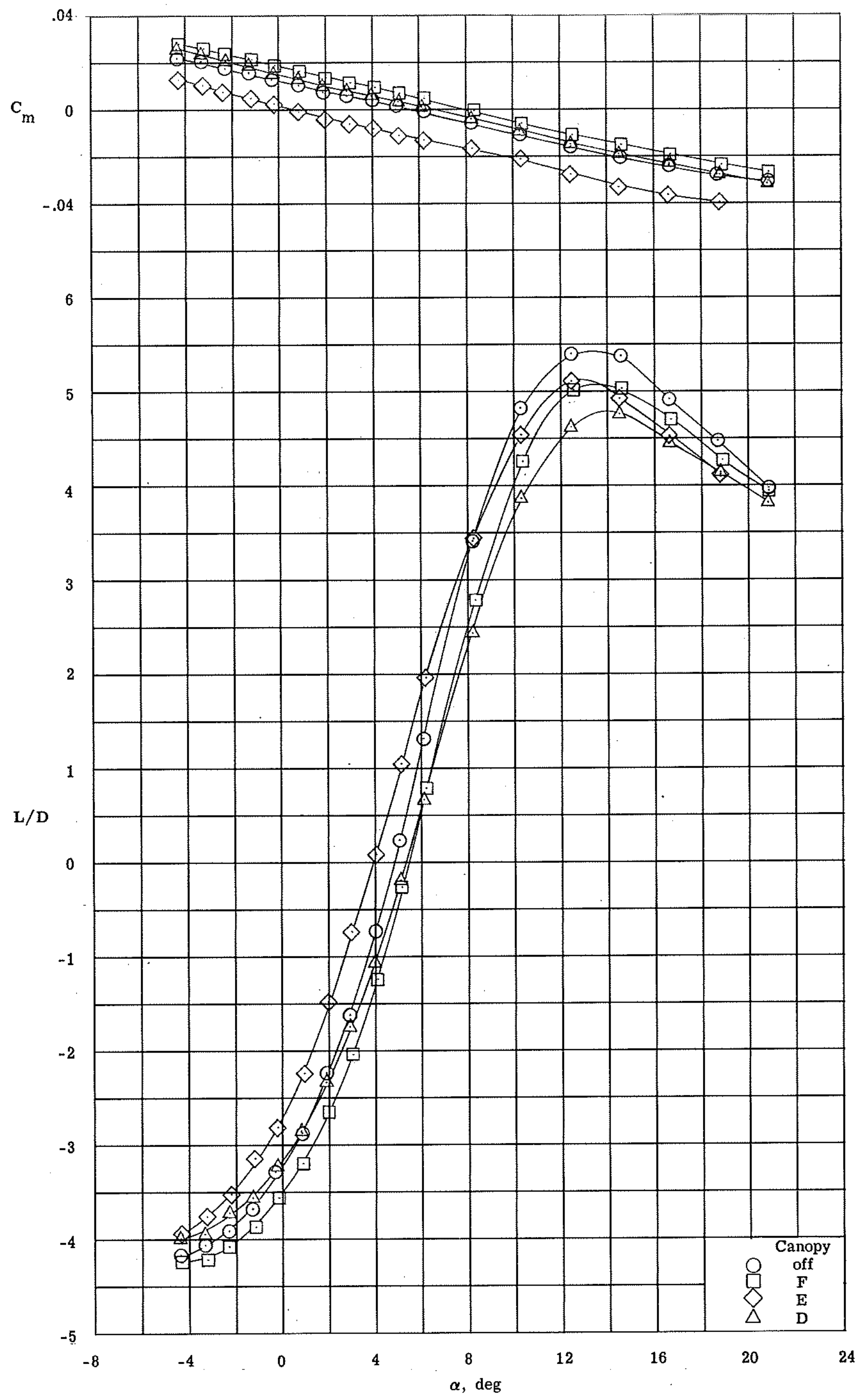

(b) Concluded.

Figure 10.- Continued.

[redacted]

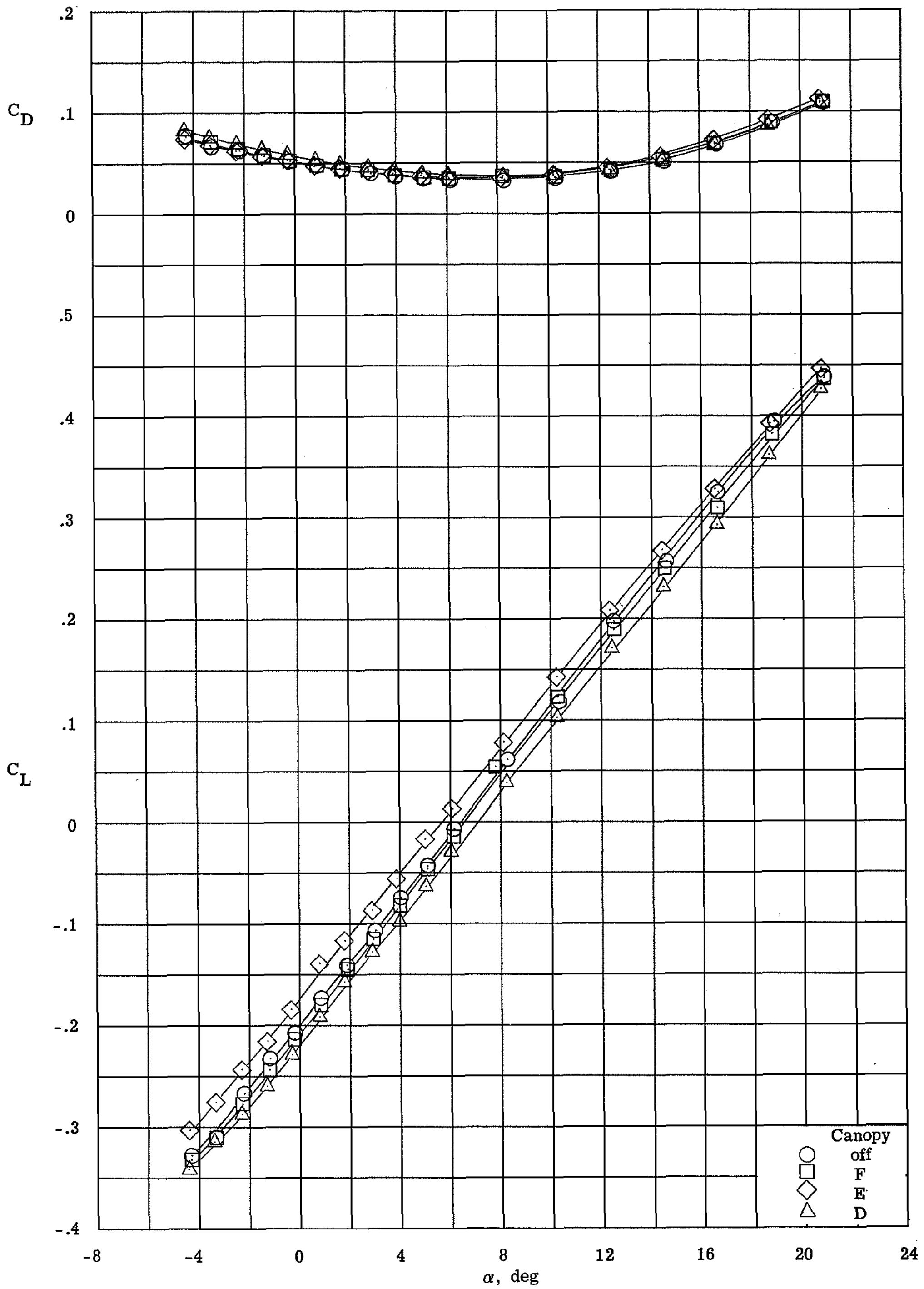

(c) $\delta_e = -10^\circ$.

Figure 10.- Continued.

[redacted]

[redacted]

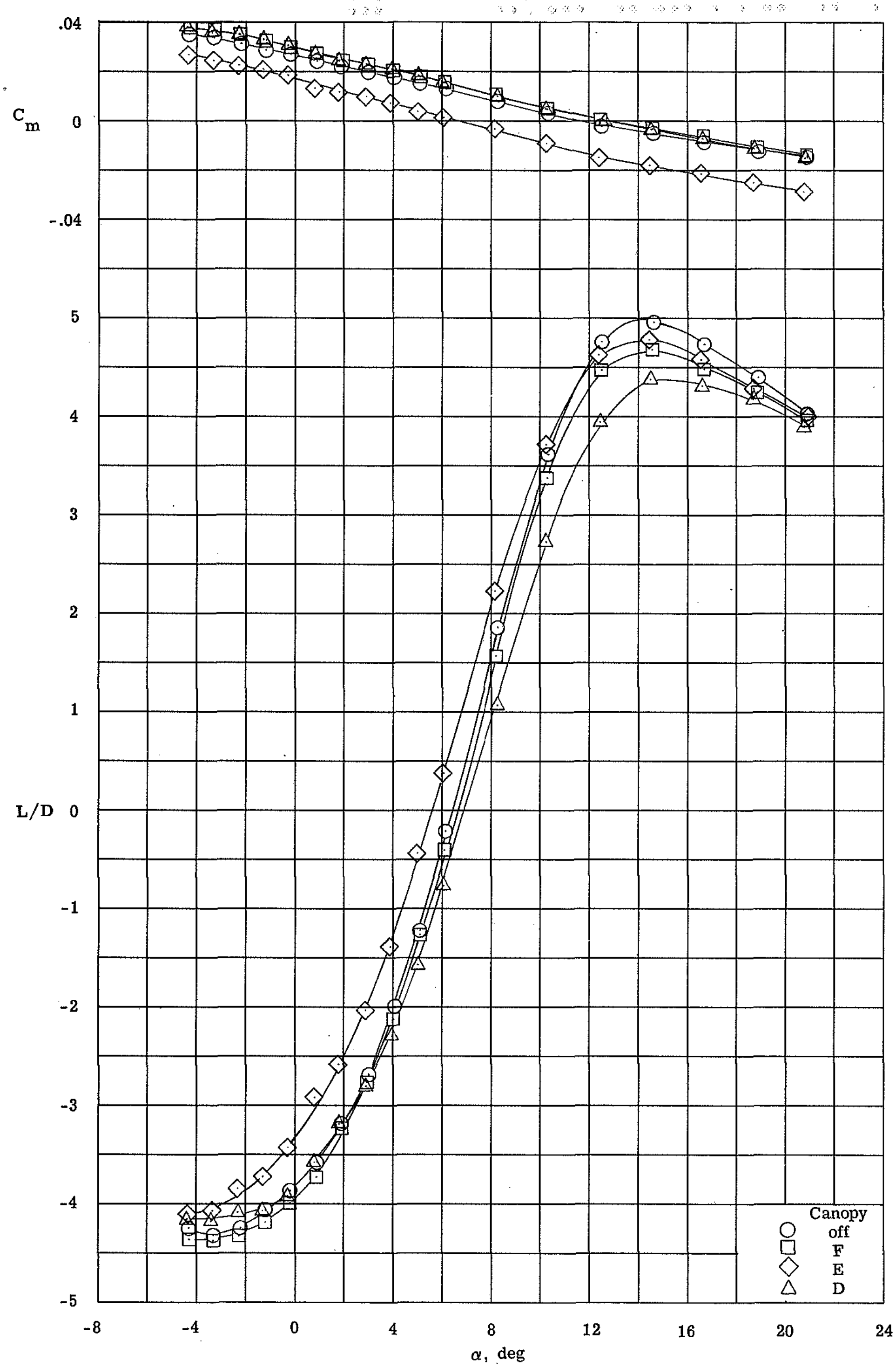

(c) Concluded.

Figure 10.- Continued.

[redacted]

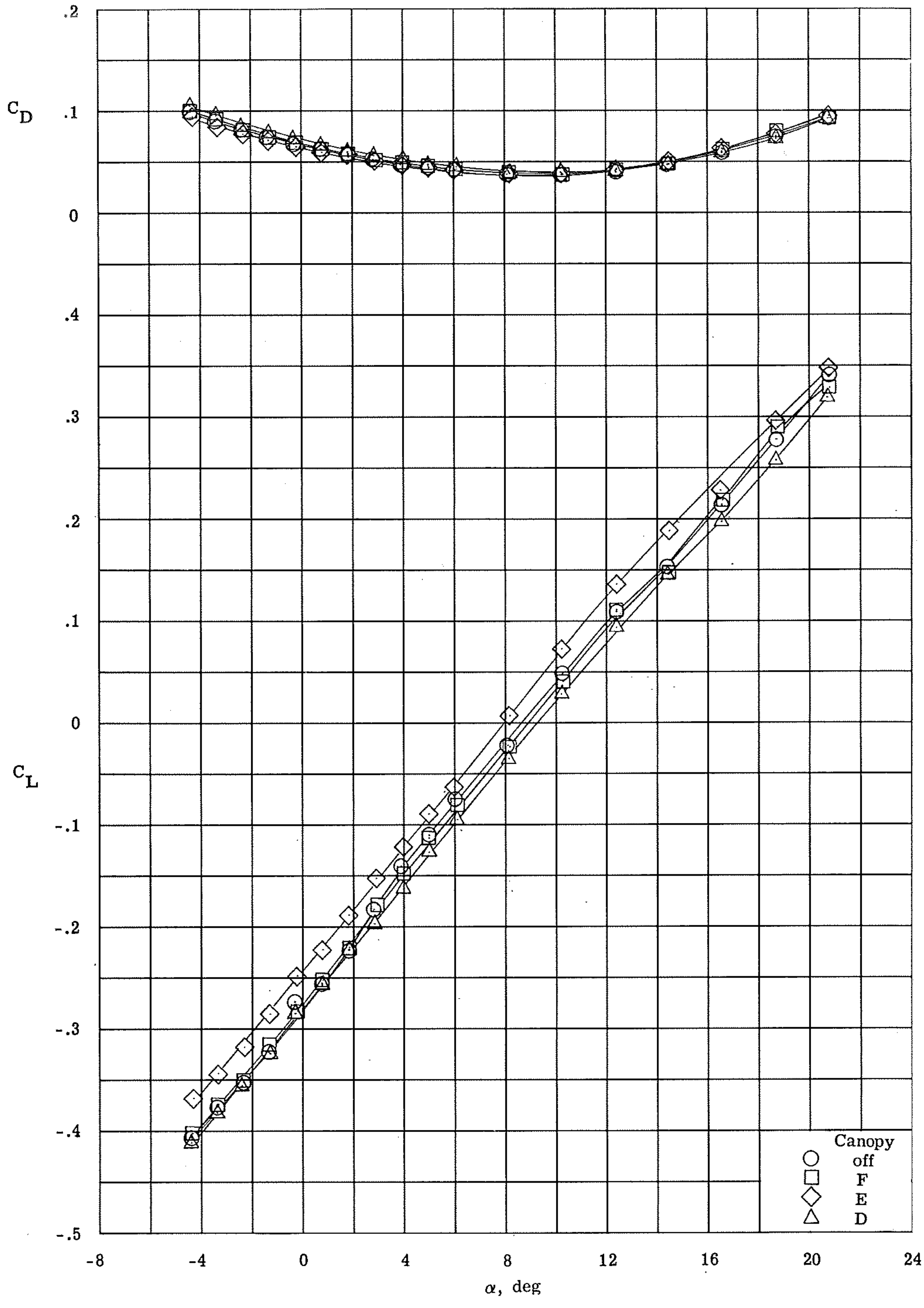

(d) $\delta_e = -15^0$.

Figure 10.- Continued.

CONFIDENTIAL

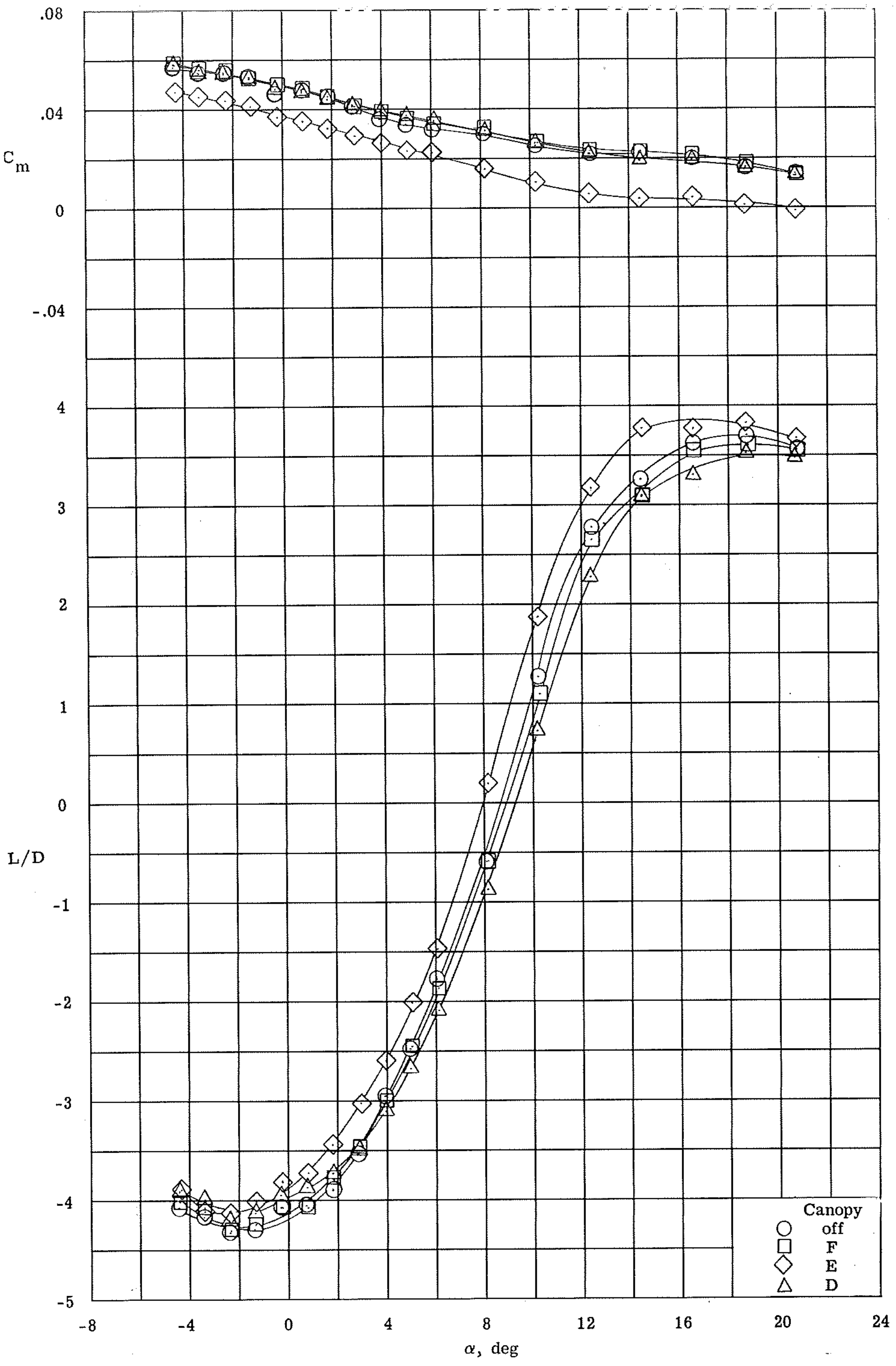

(d) Concluded.

Figure 10.- Concluded.

CONFIDENTIAL

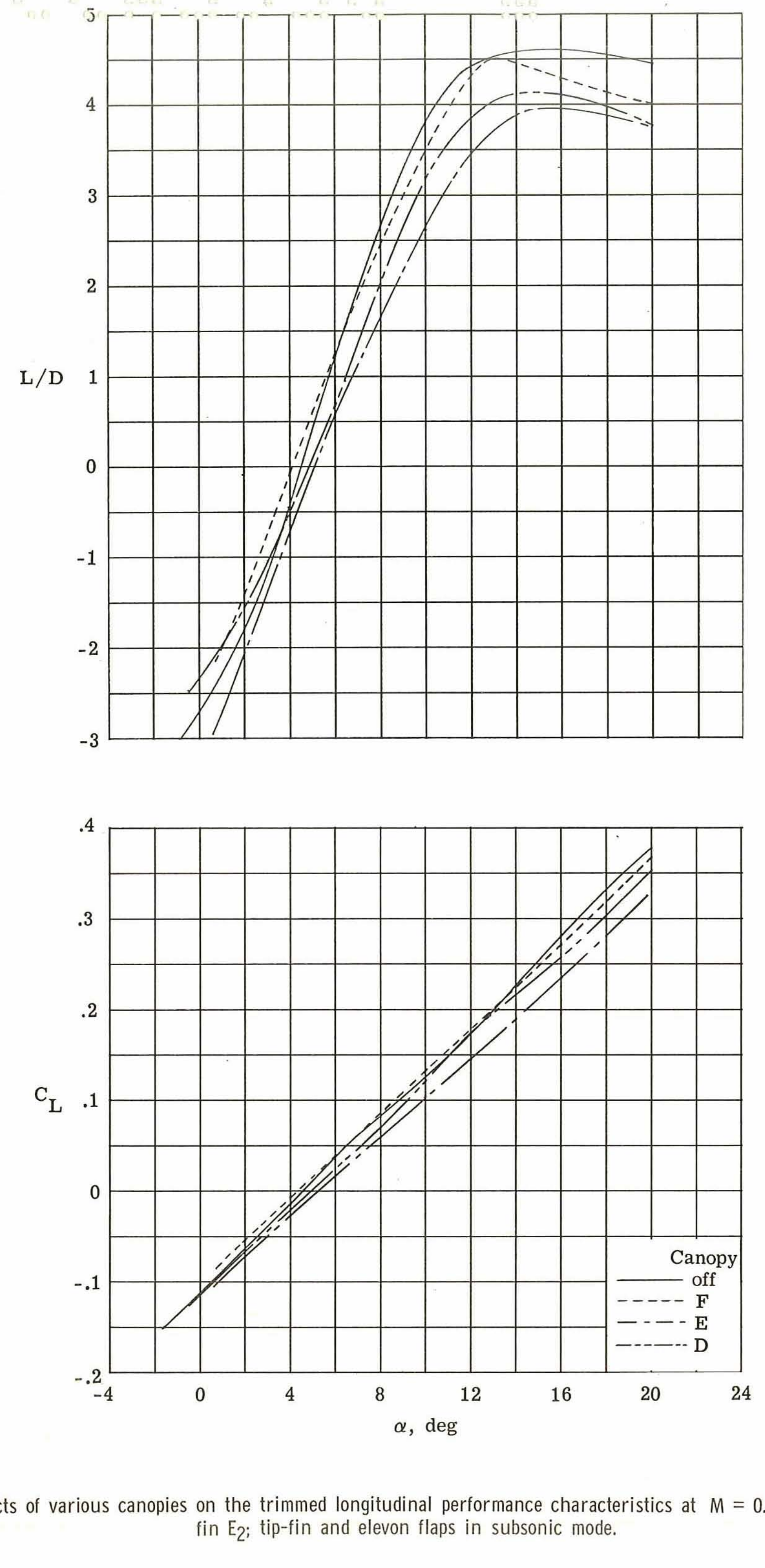

Figure 11.- Effects of various canopies on the trimmed longitudinal performance characteristics at M = 0.35. Tip fin I_4; center fin E_2; tip-fin and elevon flaps in subsonic mode.

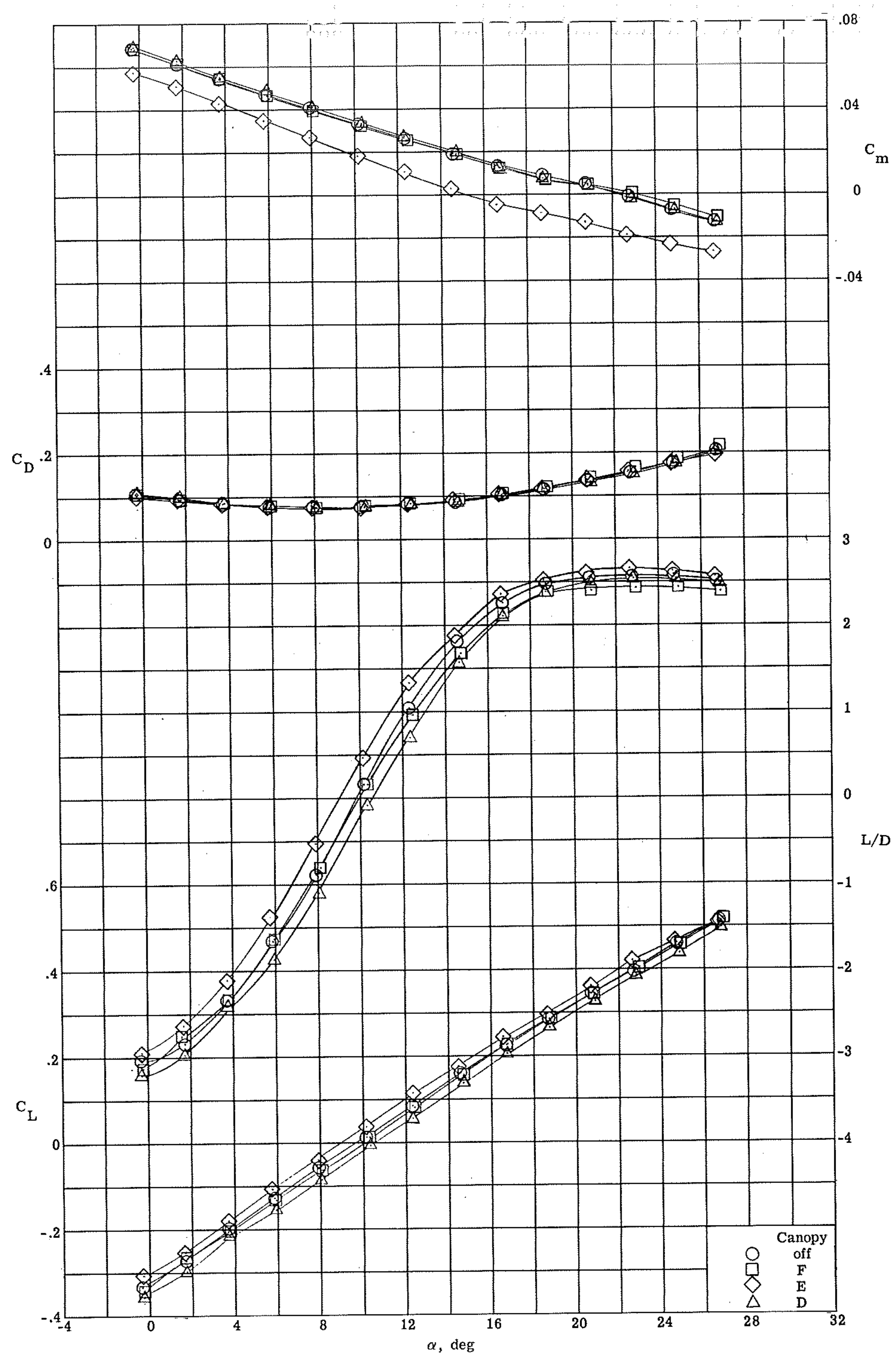

(a) M = 0.40.

Figure 12.- Effects of canopies D, E, and F on the longitudinal characteristics at various Mach numbers for $\delta_e = 0^o$. Tip fin I_4; center fin E_2; tip-fin and elevon flaps in transonic mode.

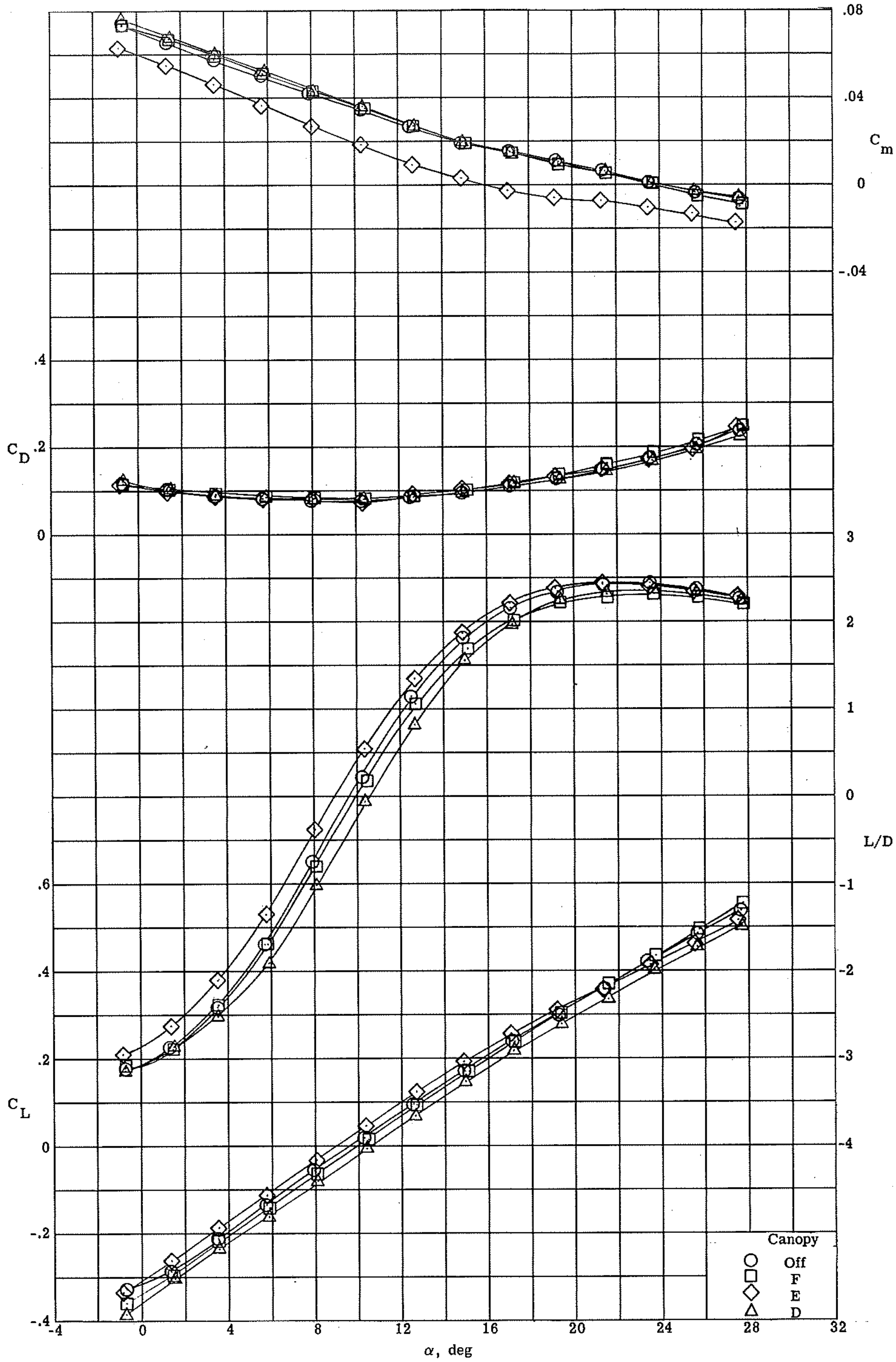

(b) M = 0.60.

Figure 12.- Continued.

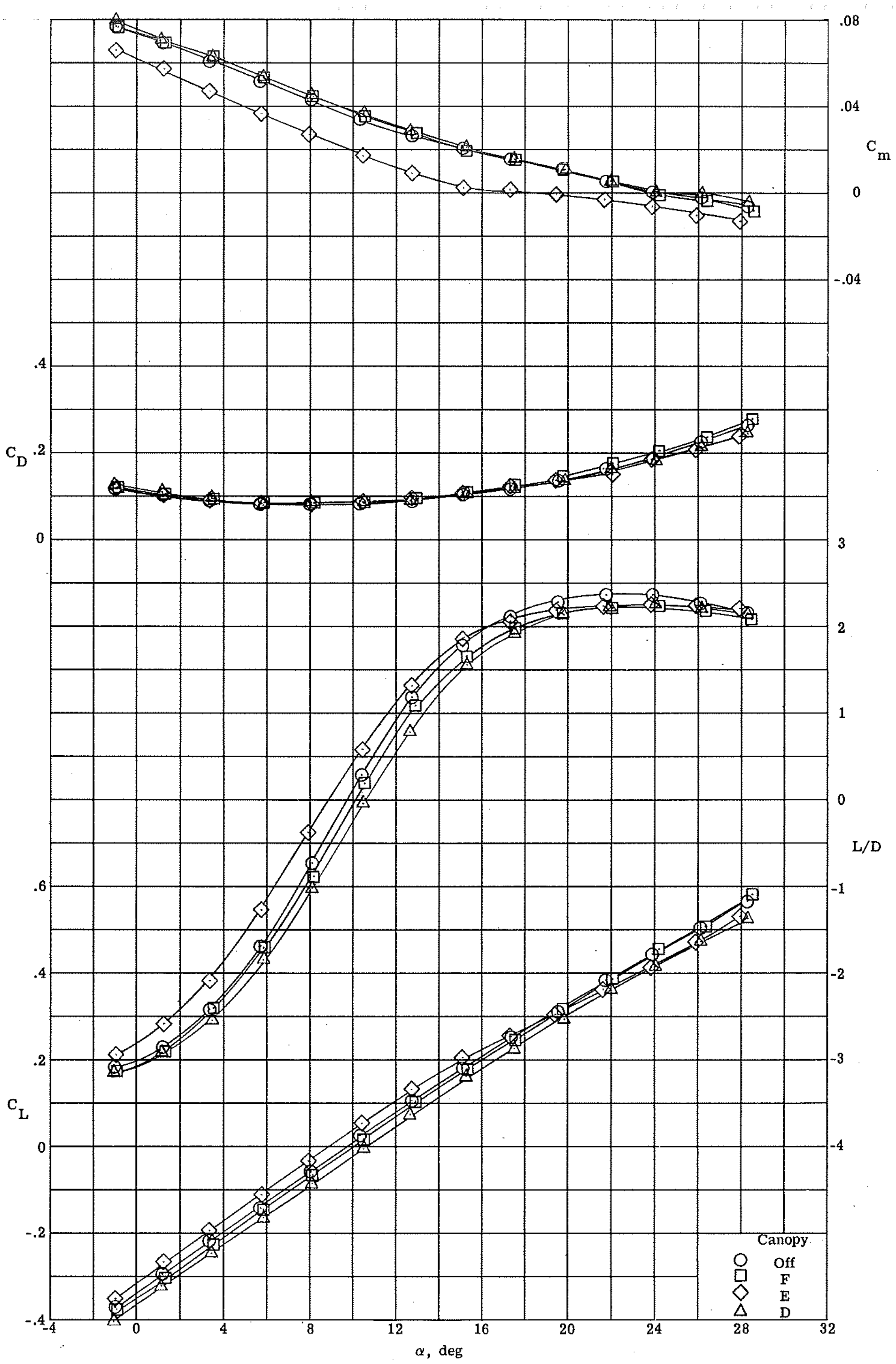

(c) M = 0.70

Figure 12.- Continued.

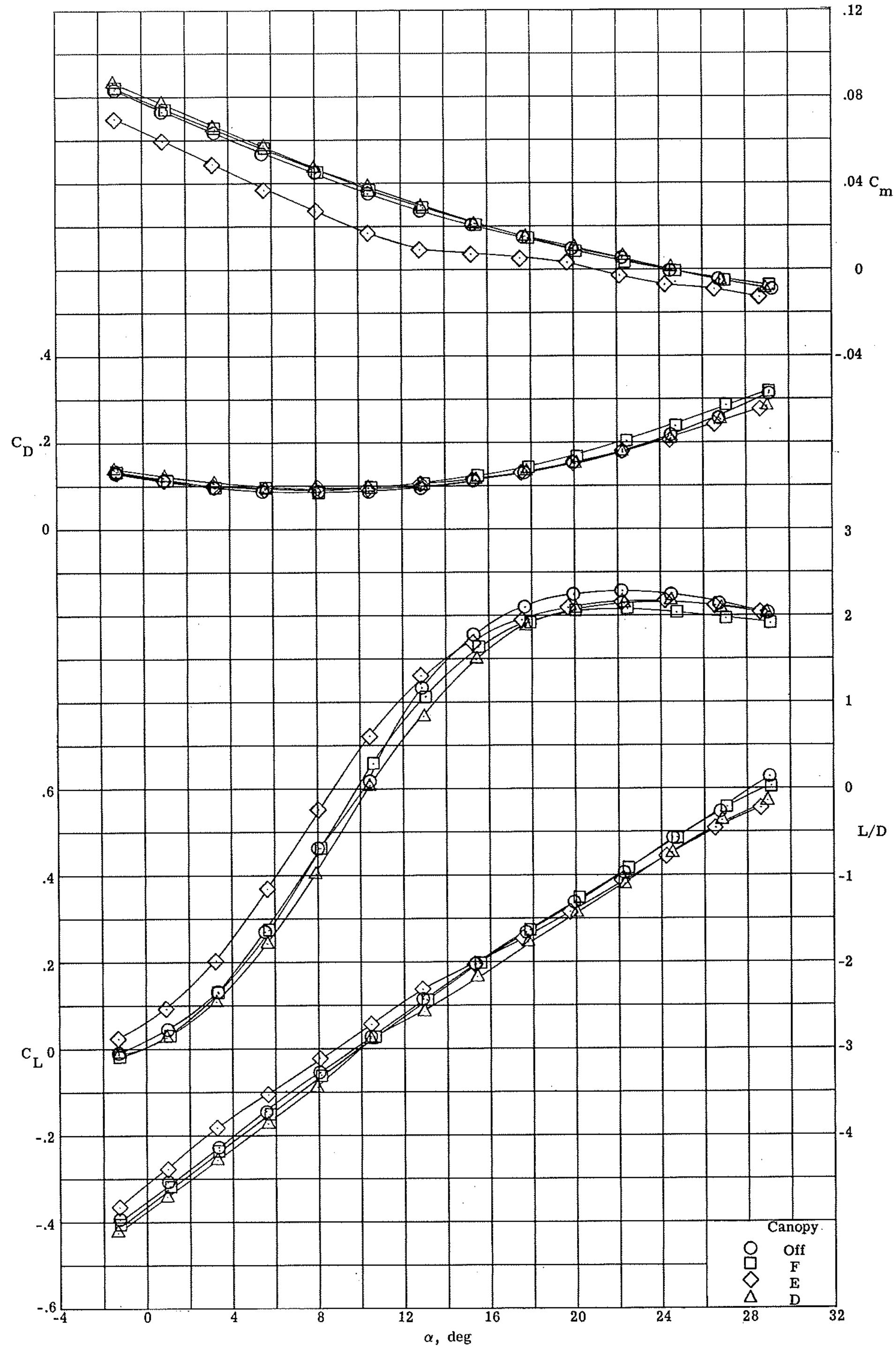

(d) M = 0.80.

Figure 12.- Continued.

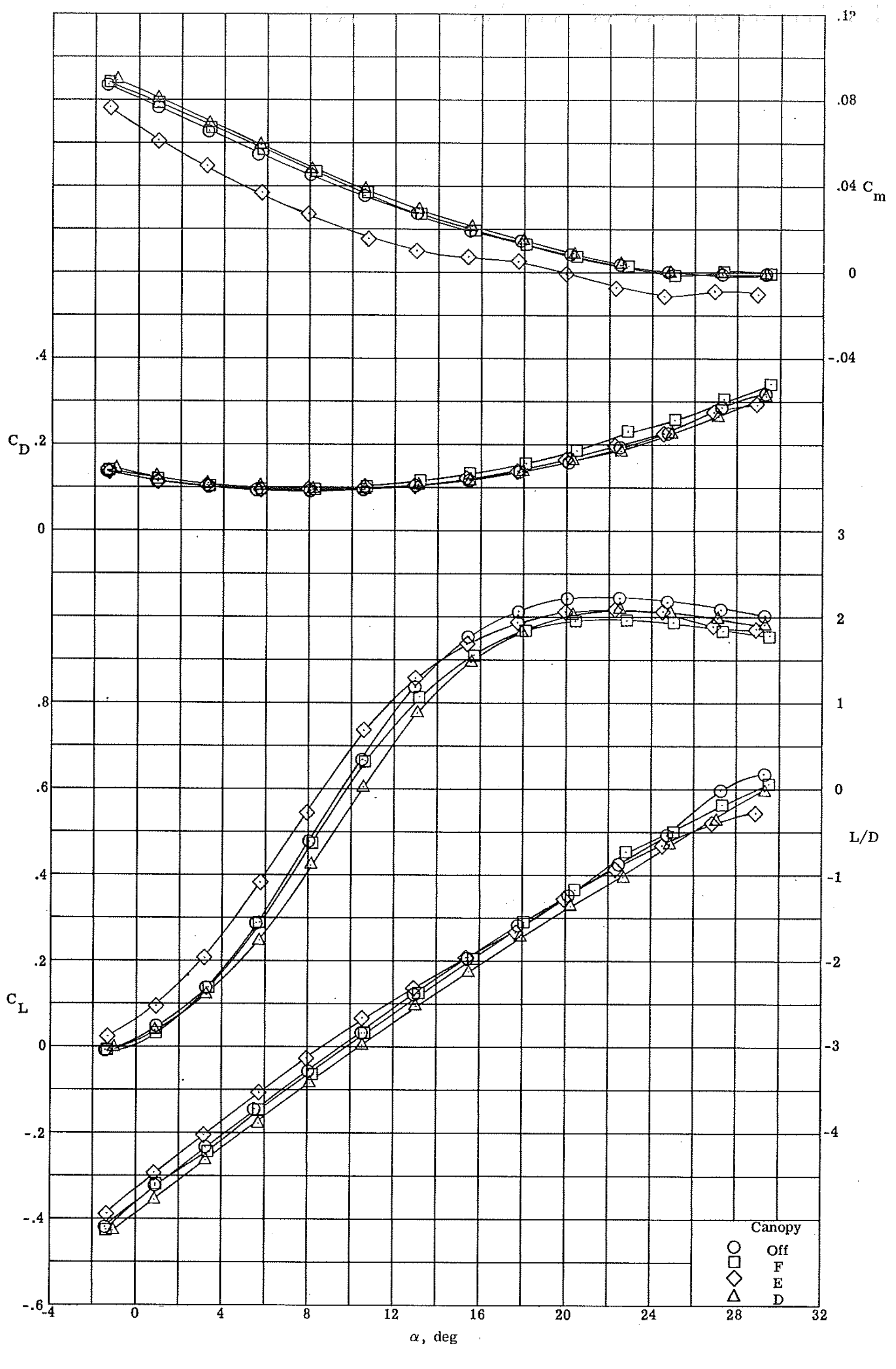

(e) M = 0.86.

Figure 12.- Continued.

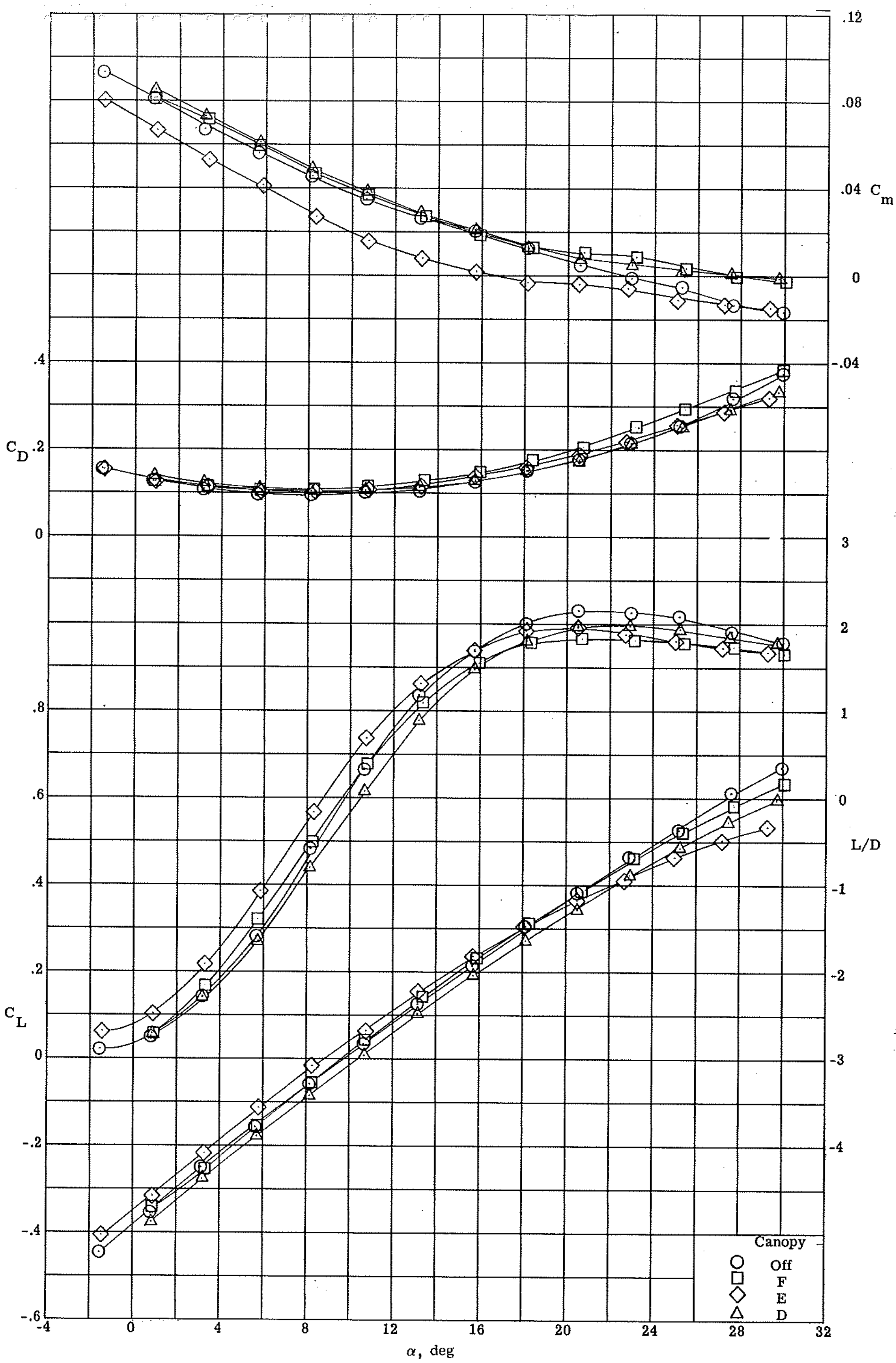

(f) M = 0.92.

Figure 12.- Continued.

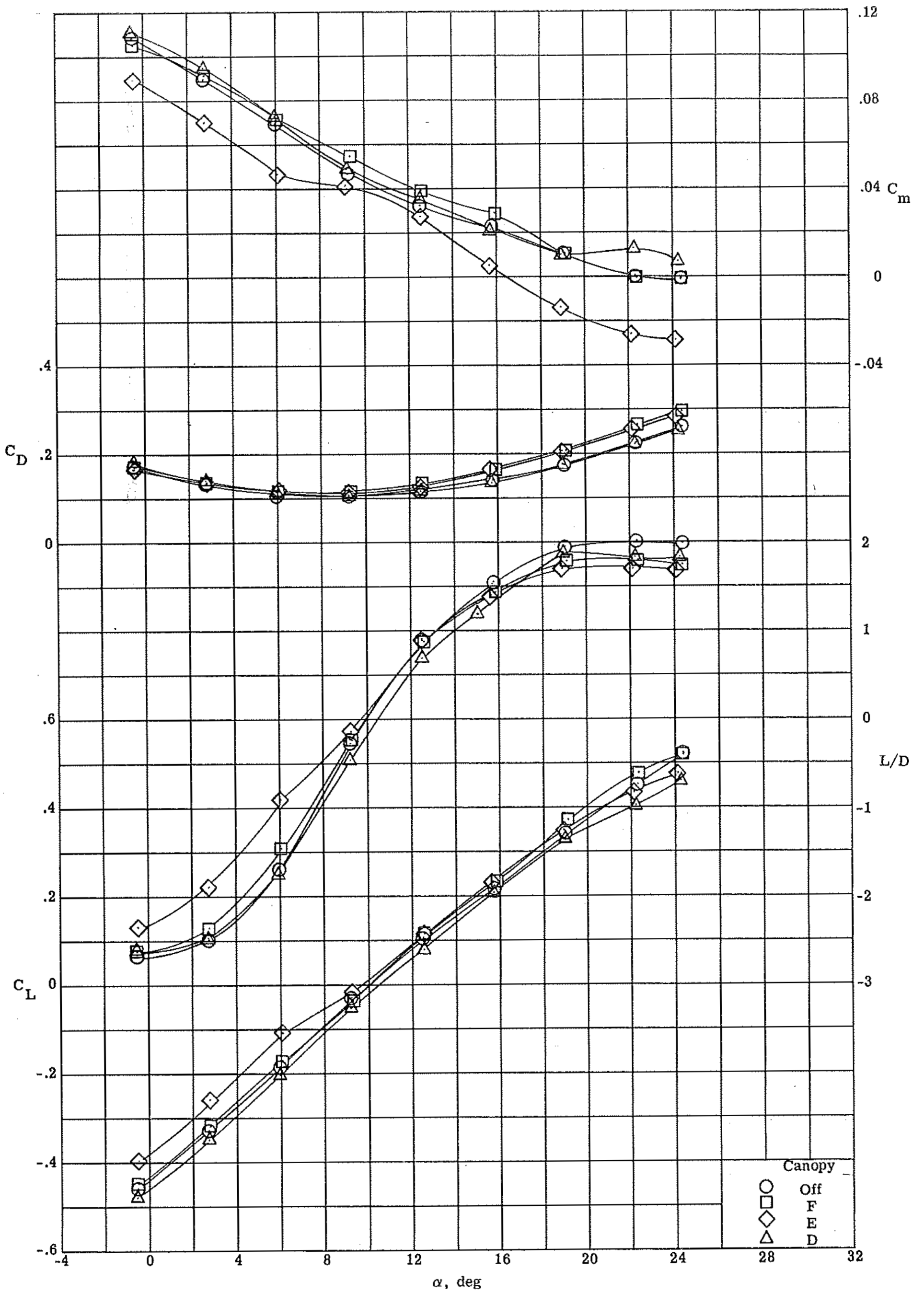

(g) M = 0.95.

Figure 12.- Continued.

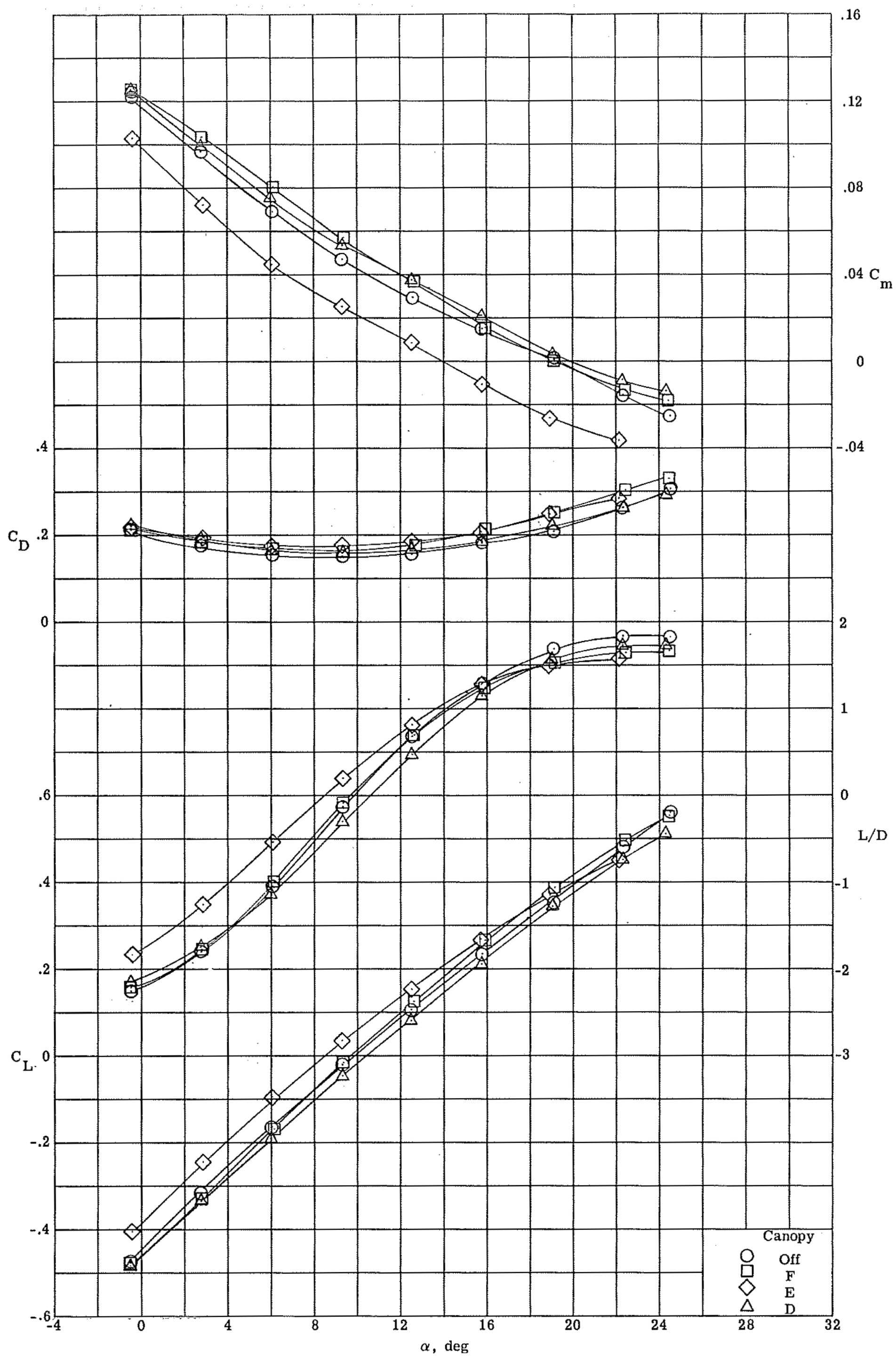

(h) M = 1.00.

Figure 12.- Continued.

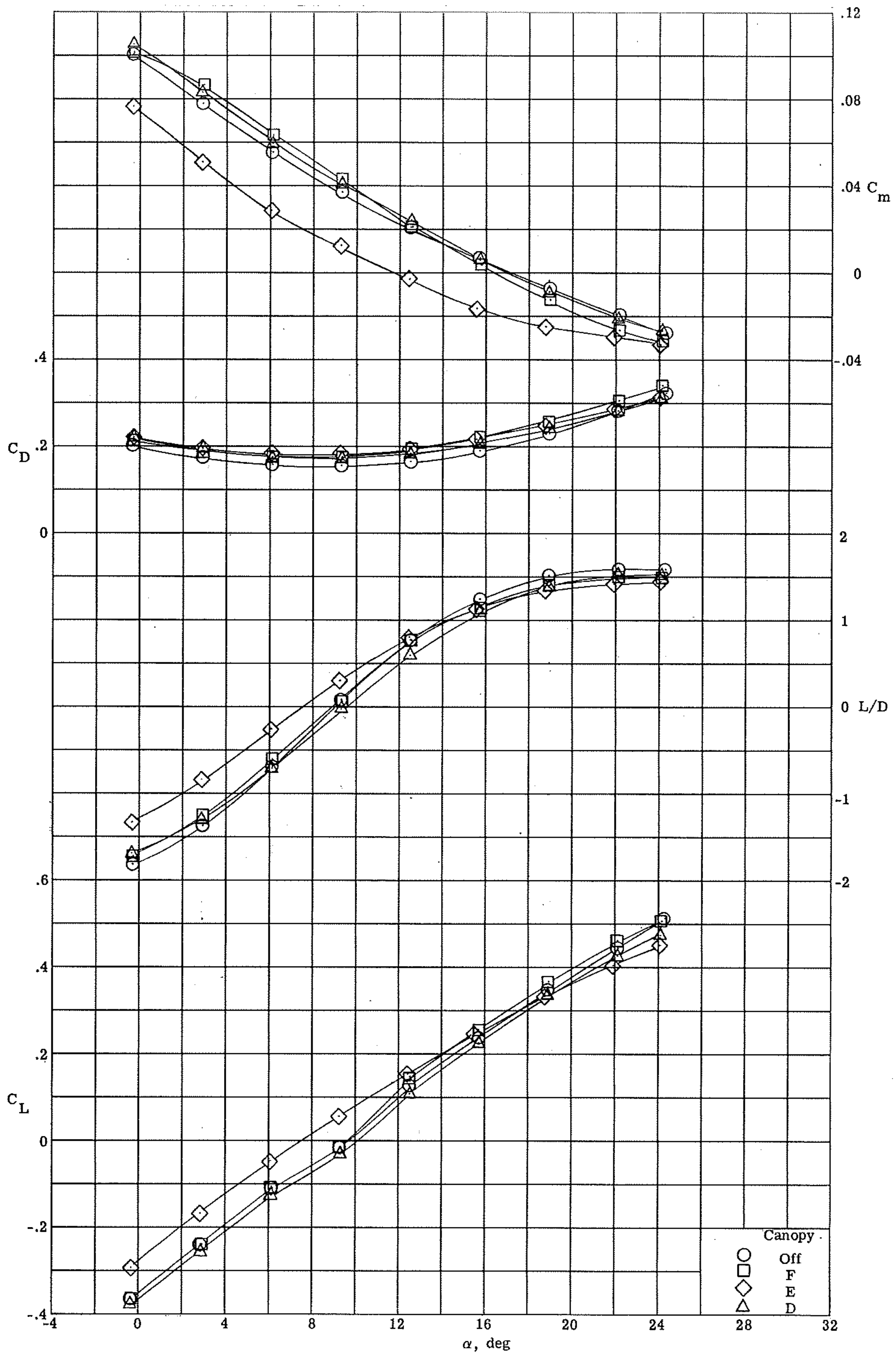

(i) M = 1.20.

Figure 12.- Continued.

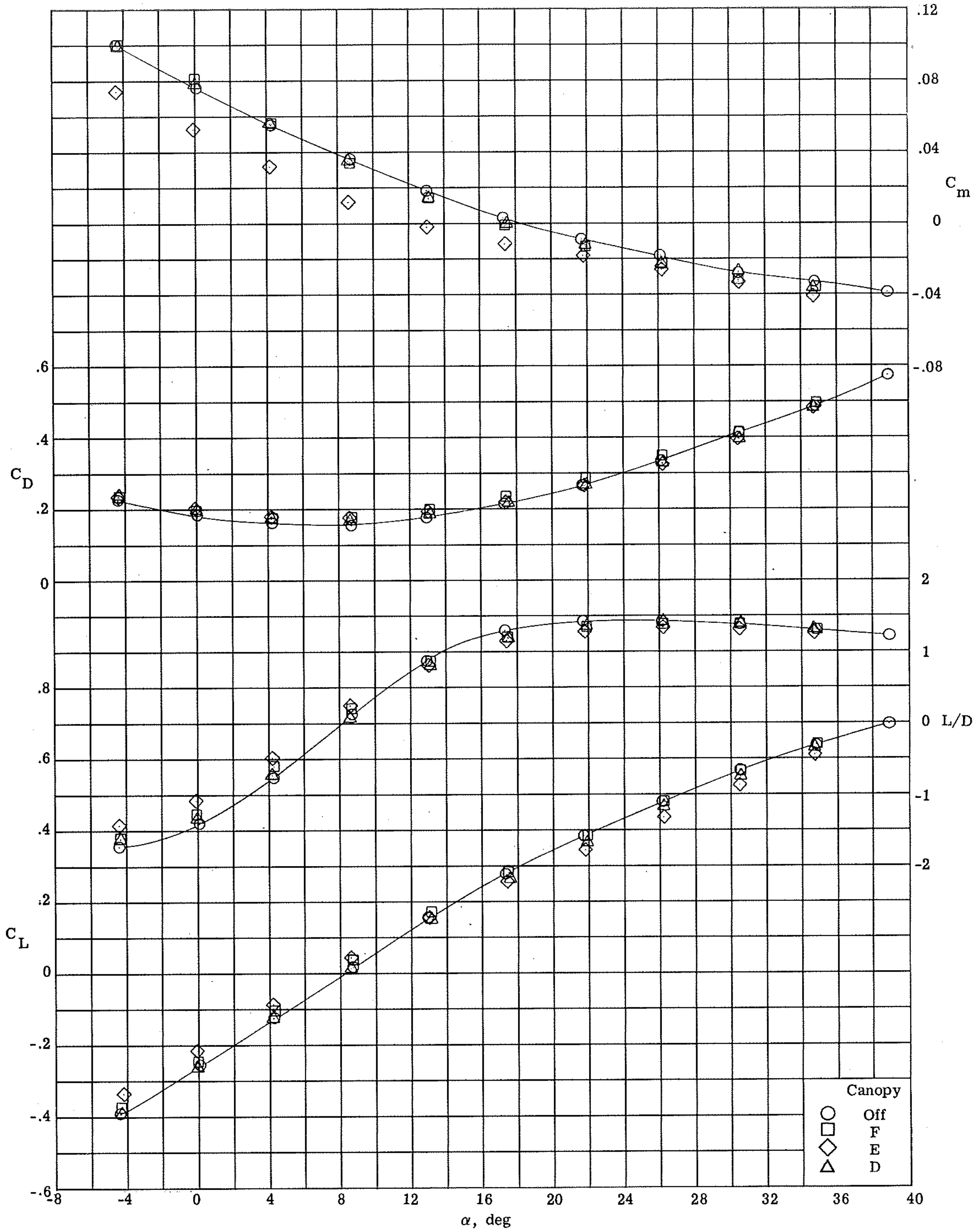

(j) M = 1.50.

Figure 12.- Continued.

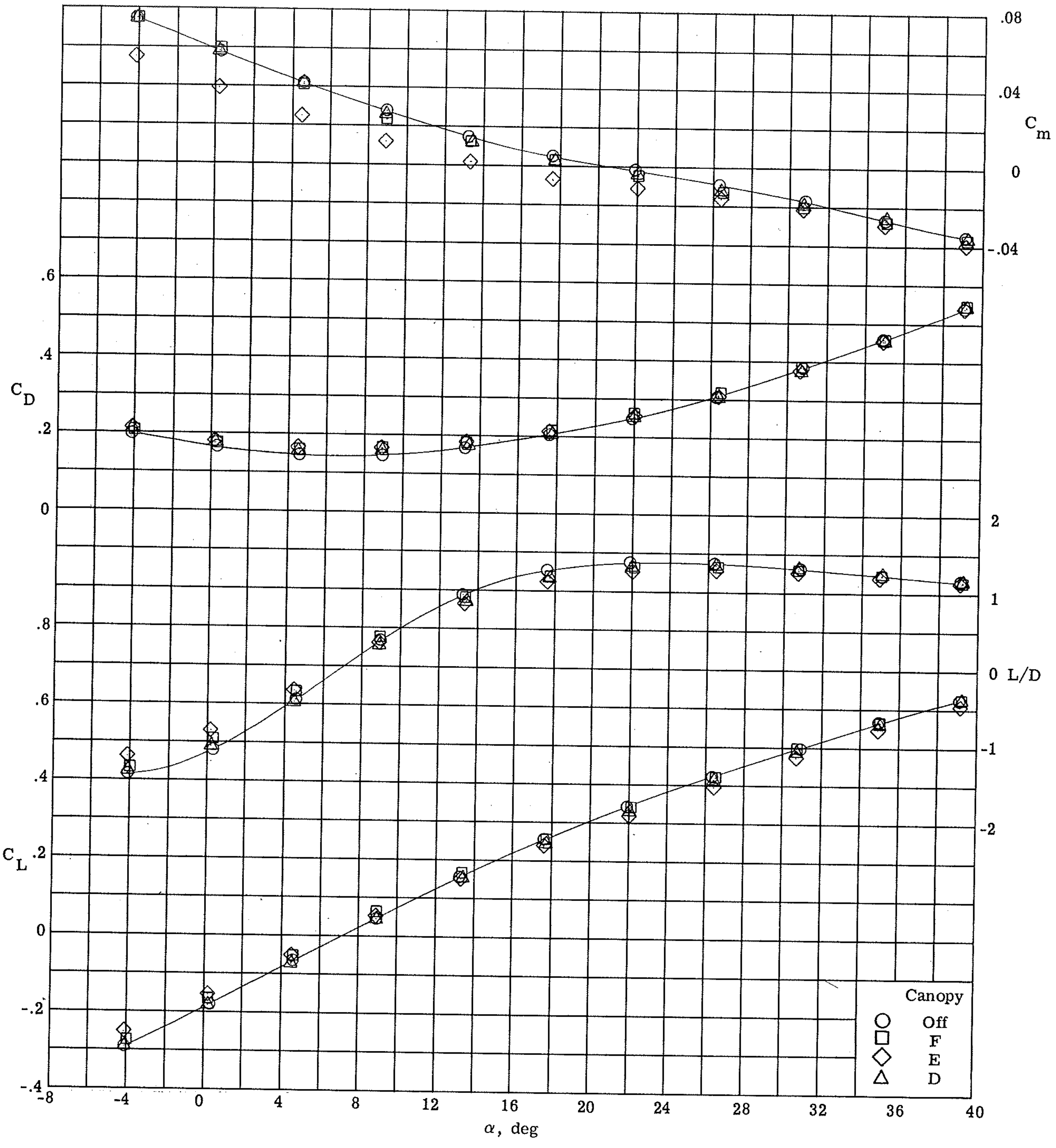

(k) M = 1.80.

Figure 12.- Continued.

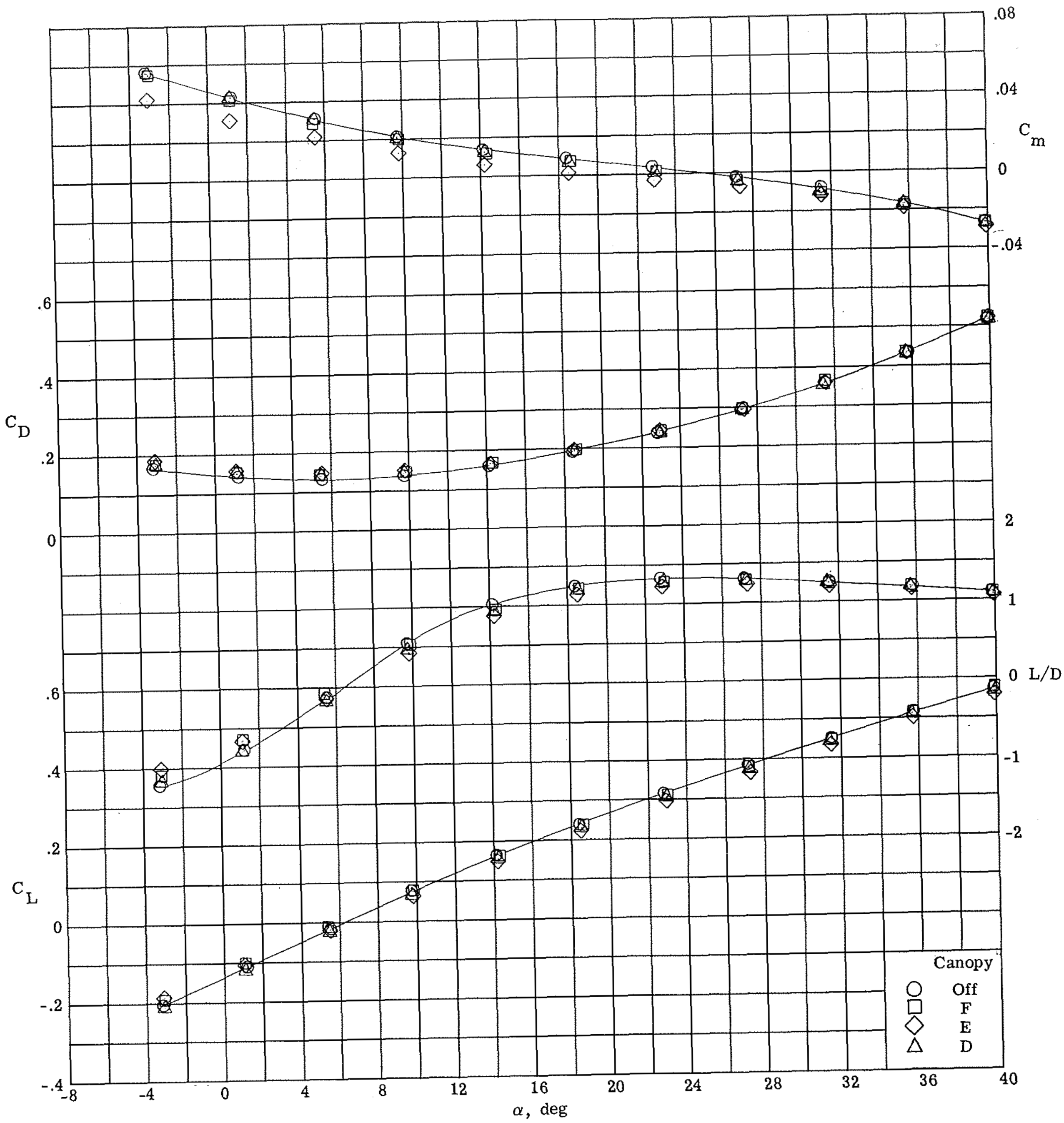

(l) M = 2.16.

Figure 12.- Concluded.

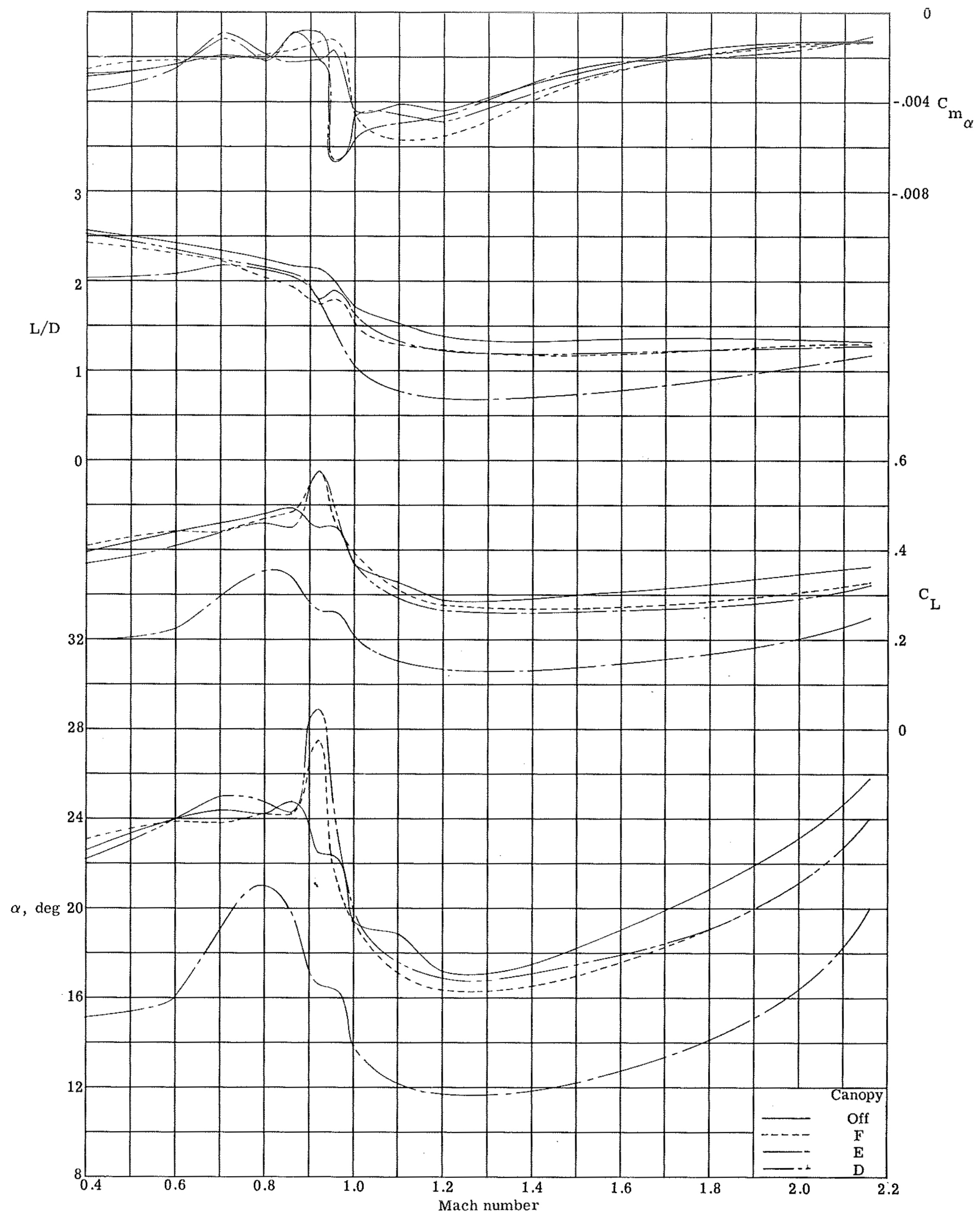

(a) Trim conditions for $\delta_e = 0^0$.

Figure 13.- Summary of effects of canopies D, E, and F and Mach number variation on the longitudinal characteristics. Tip fin I_4; center fin E_2; tip-fin and elevon flaps in transonic mode.

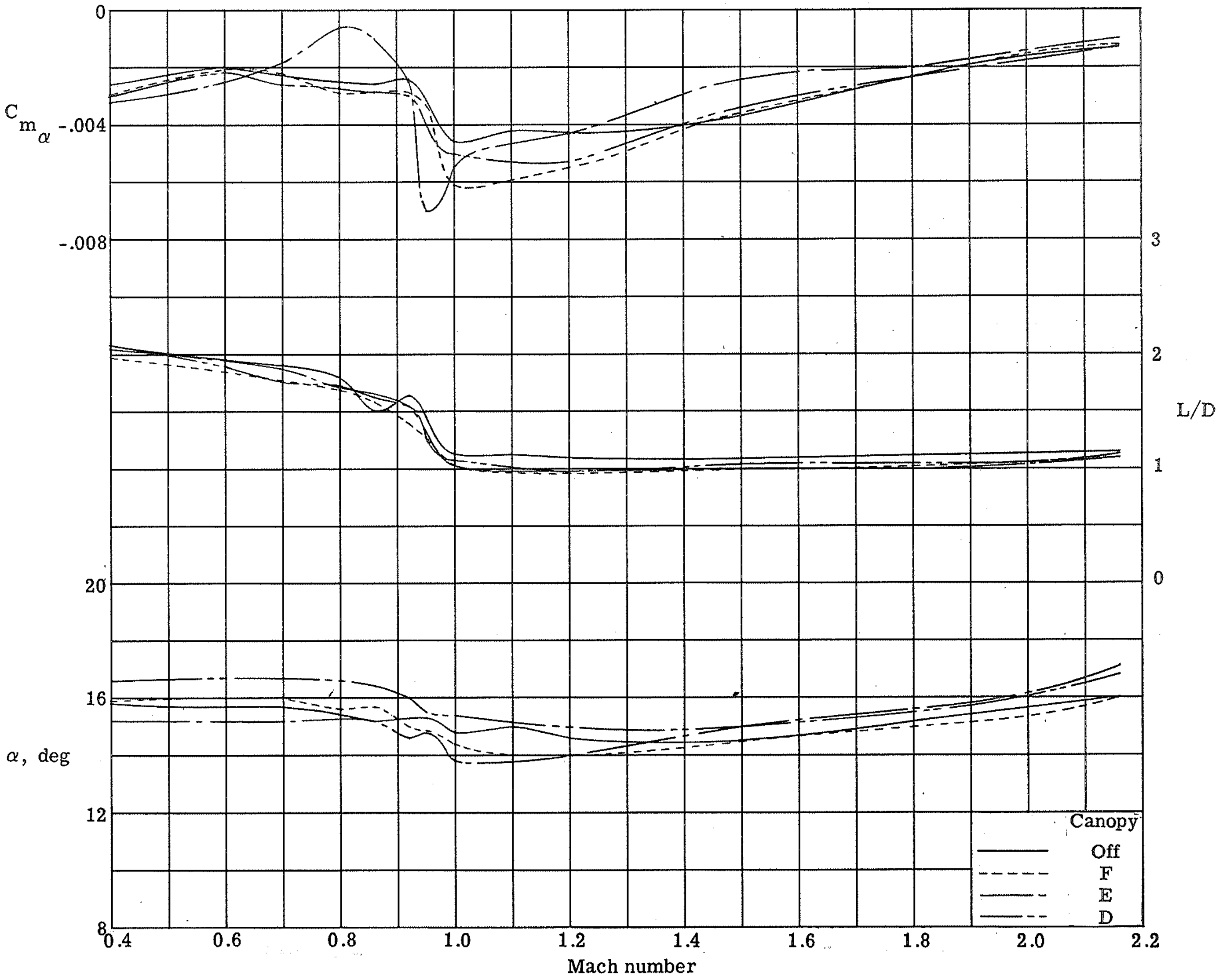

(b) $C_L = 0.20.$

Figure 13.- Continued.

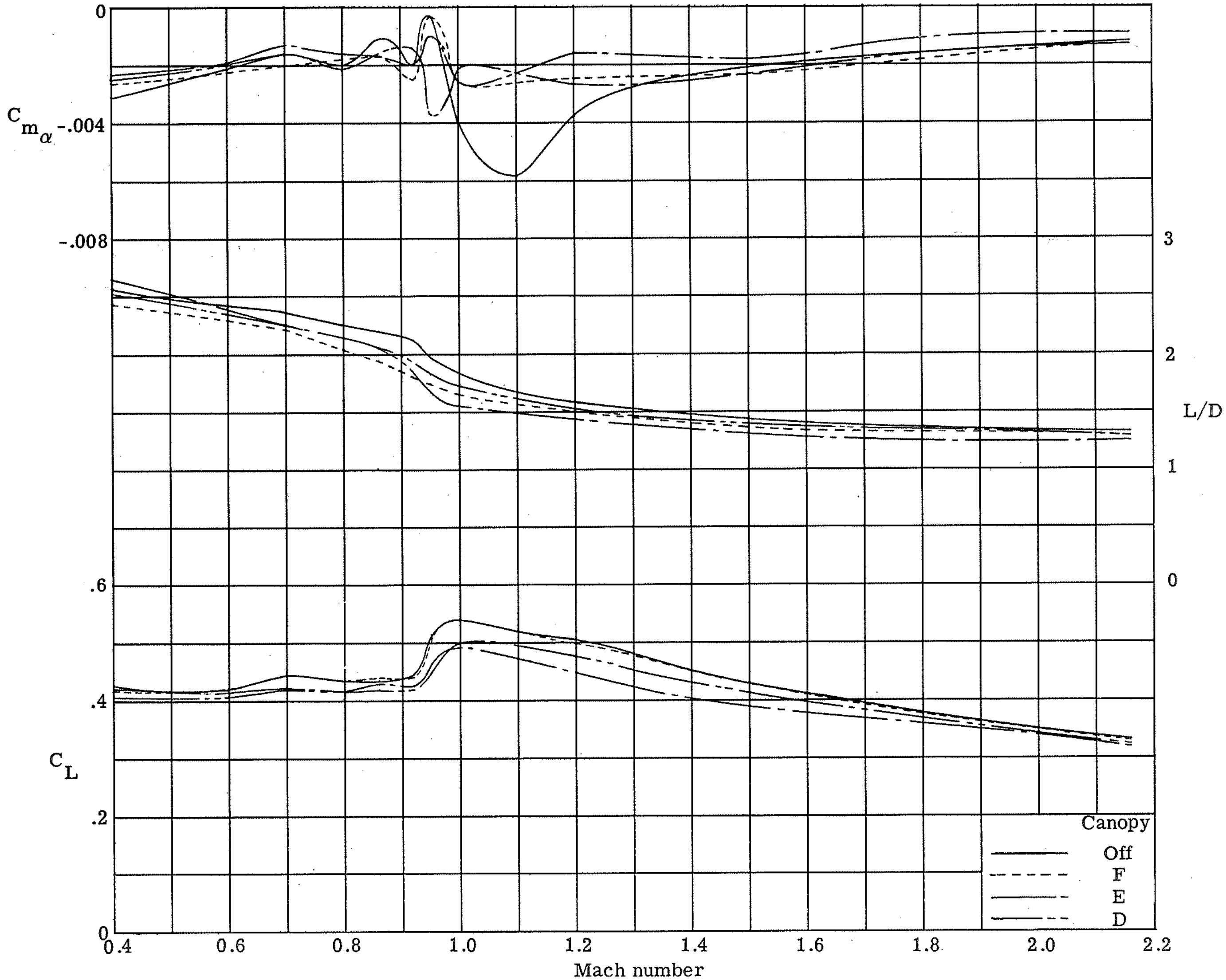

(c) $\alpha = 24^{0}$.

Figure 13.- Concluded.

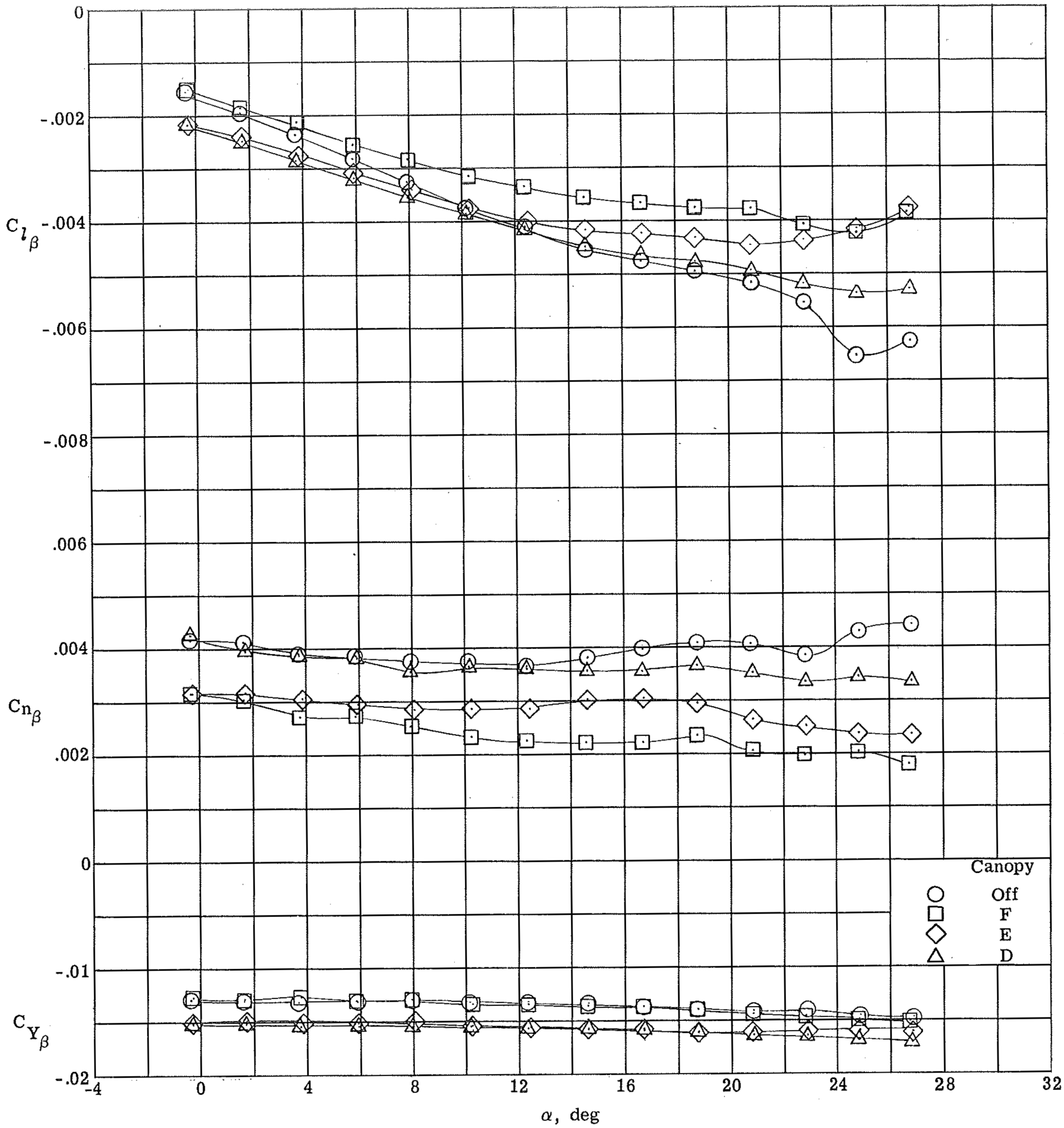

(a) M = 0.40.

Figure 14.- Effects of canopies D, E, and F on the directional and lateral stability characteristics at various Mach numbers for $\delta_e = 0^o$. Tip fin I_4; center fin E_2; tip-fin and elevon flaps in transonic mode.

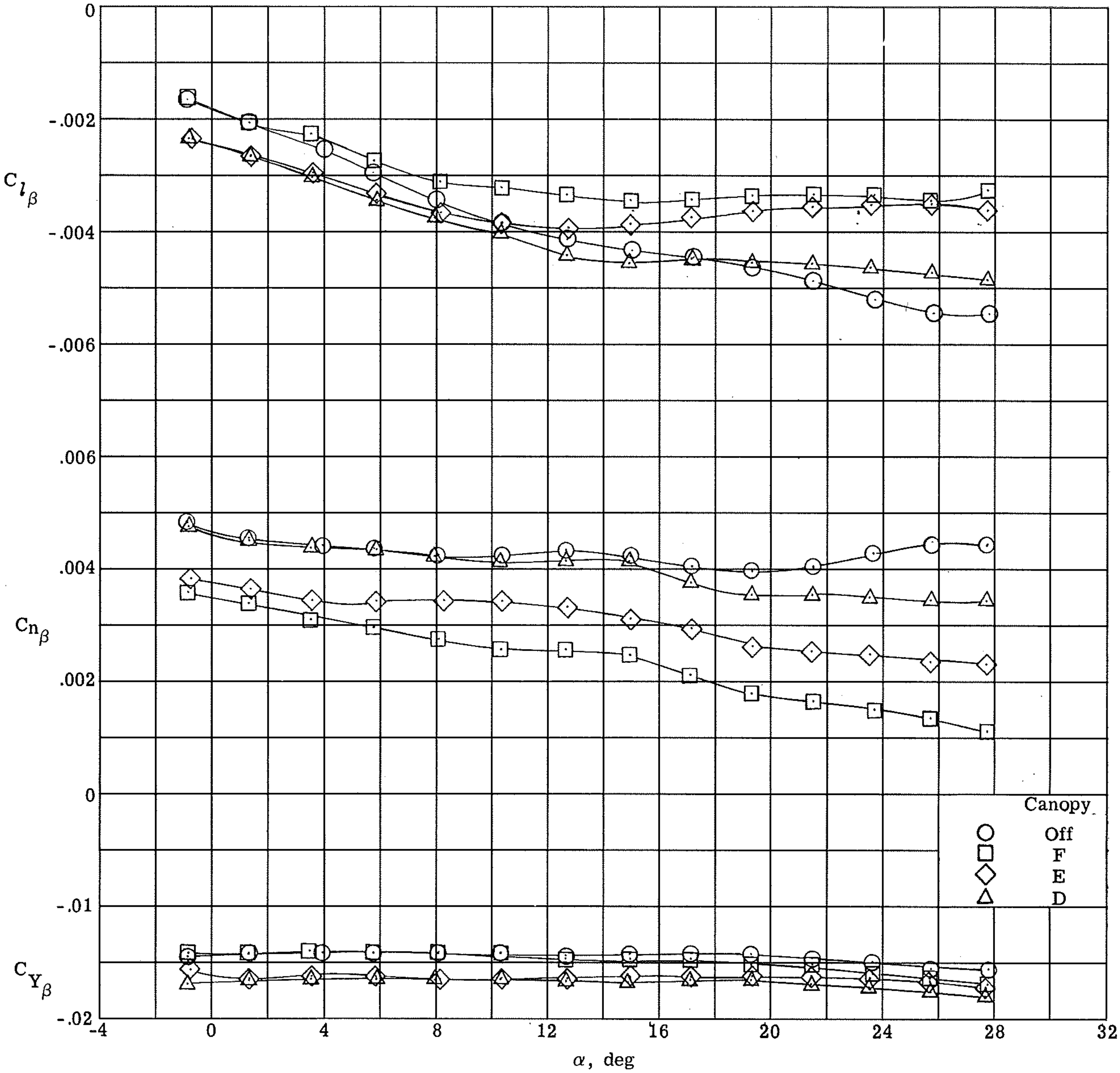

(b) M = 0.60.

Figure 14.- Continued.

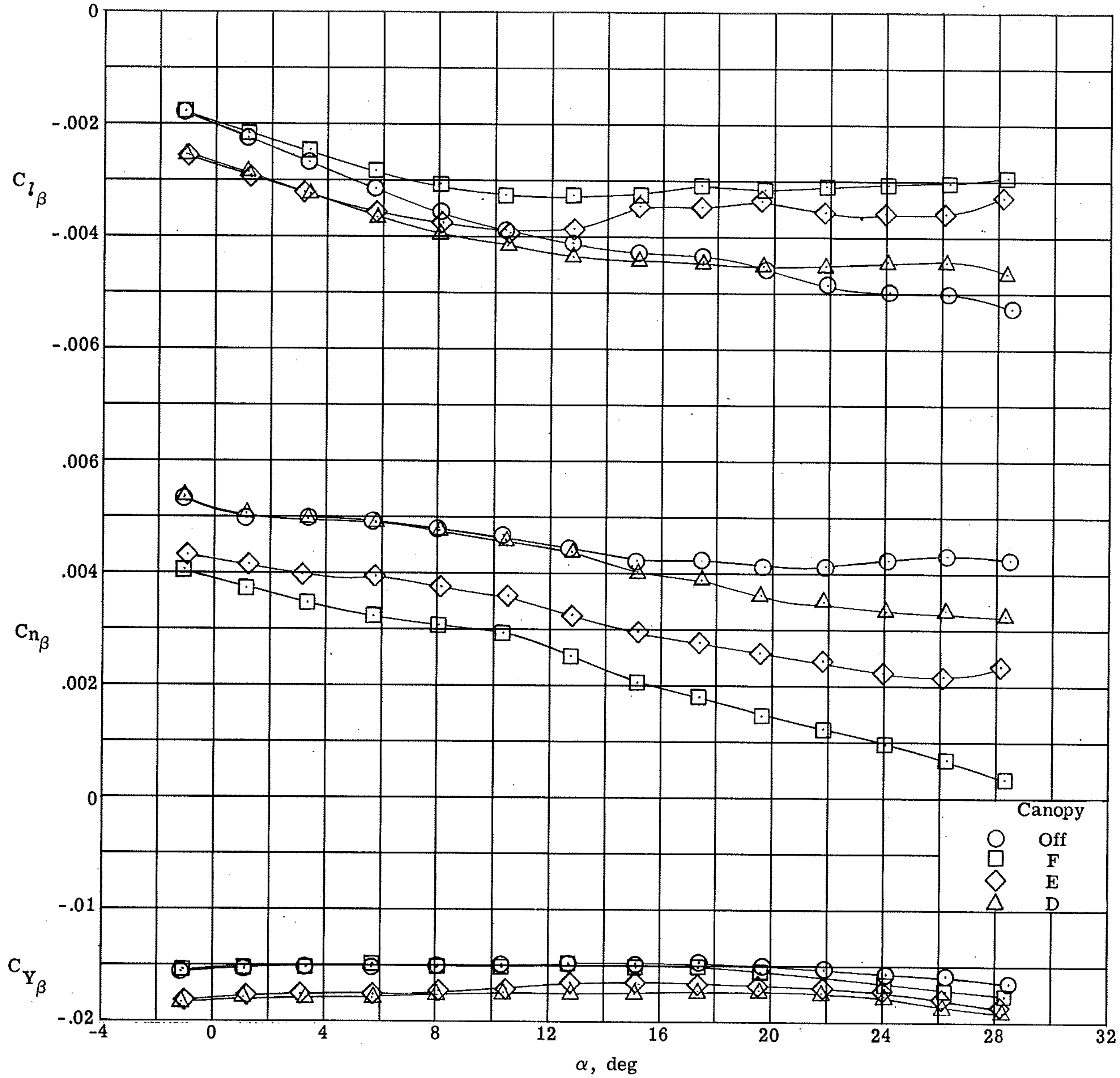

(c) M = 0.70.

Figure 14.- Continued.

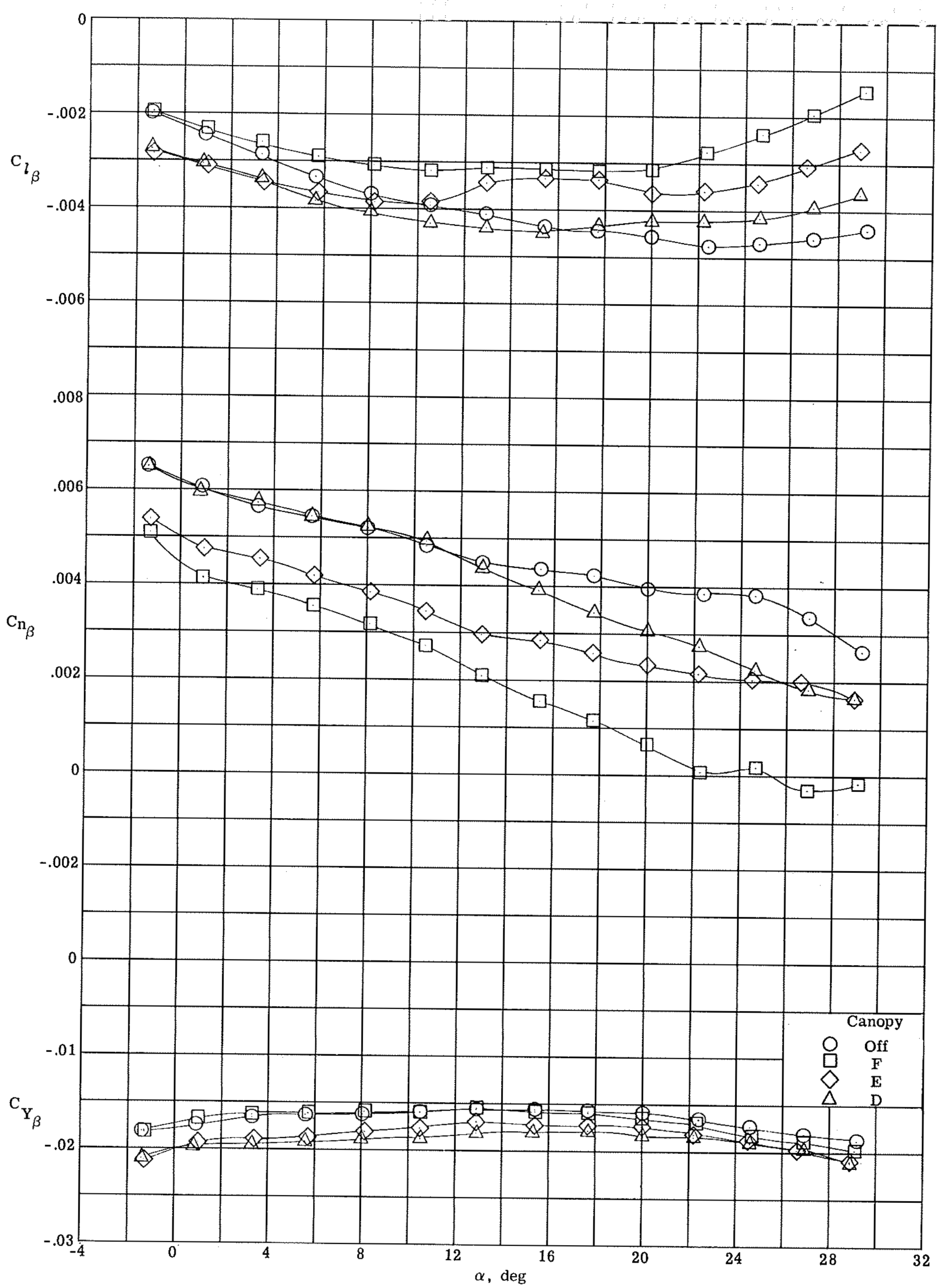

(d) M = 0.80.

Figure 14.- Continued.

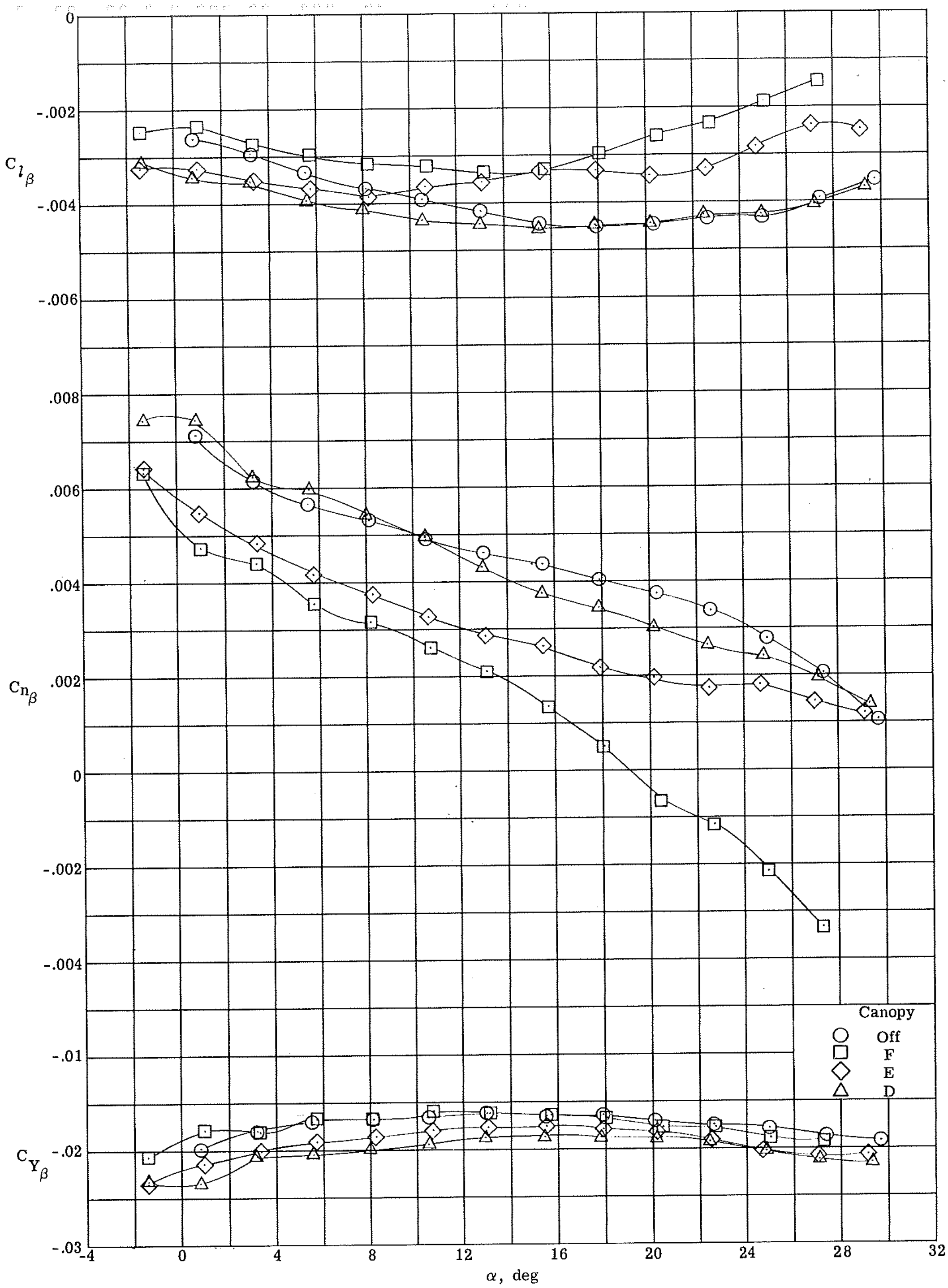

(e) M = 0.86.

Figure 14.- Continued.

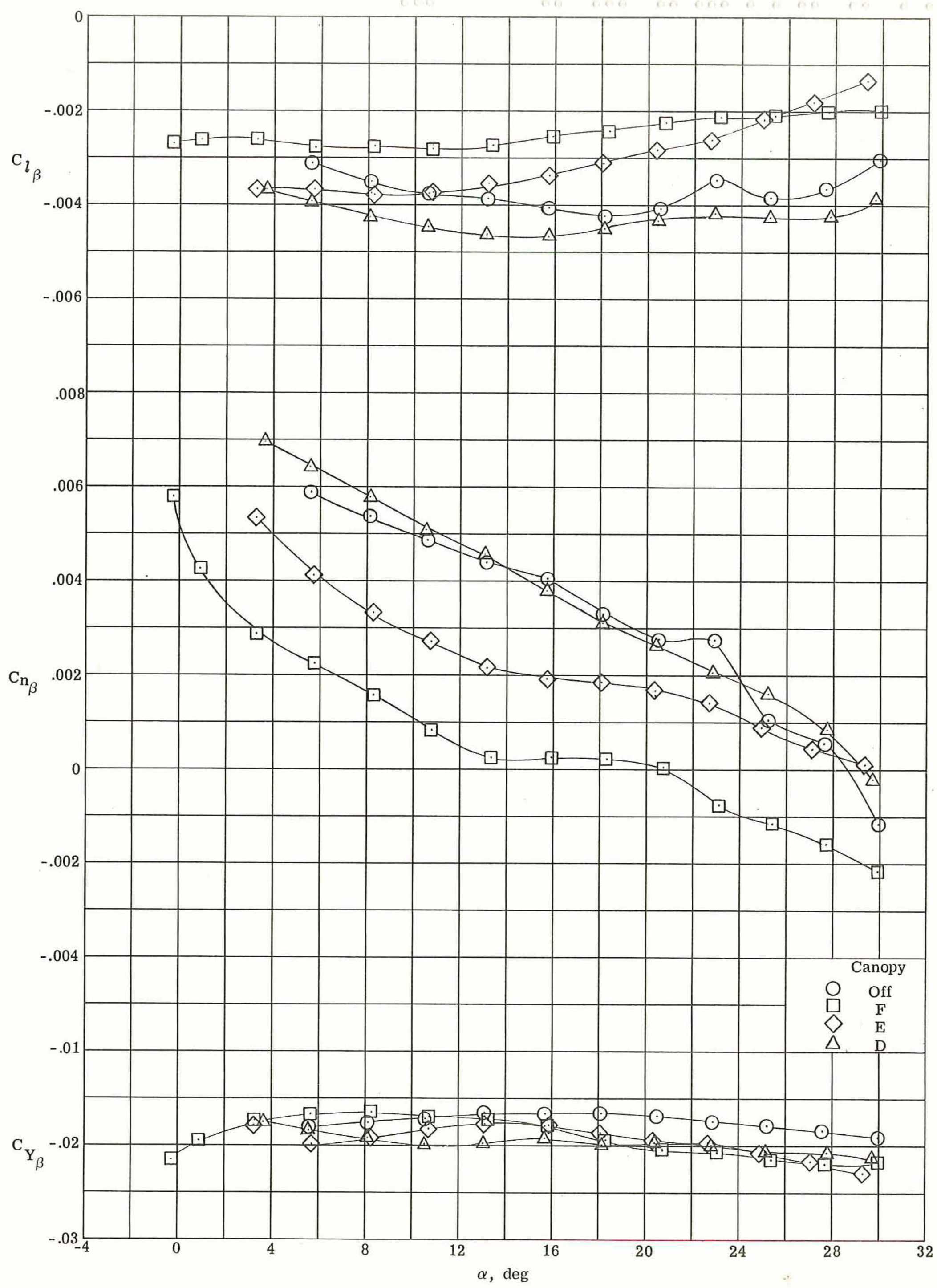

(f) M = 0.92.

Figure 14.- Continued.

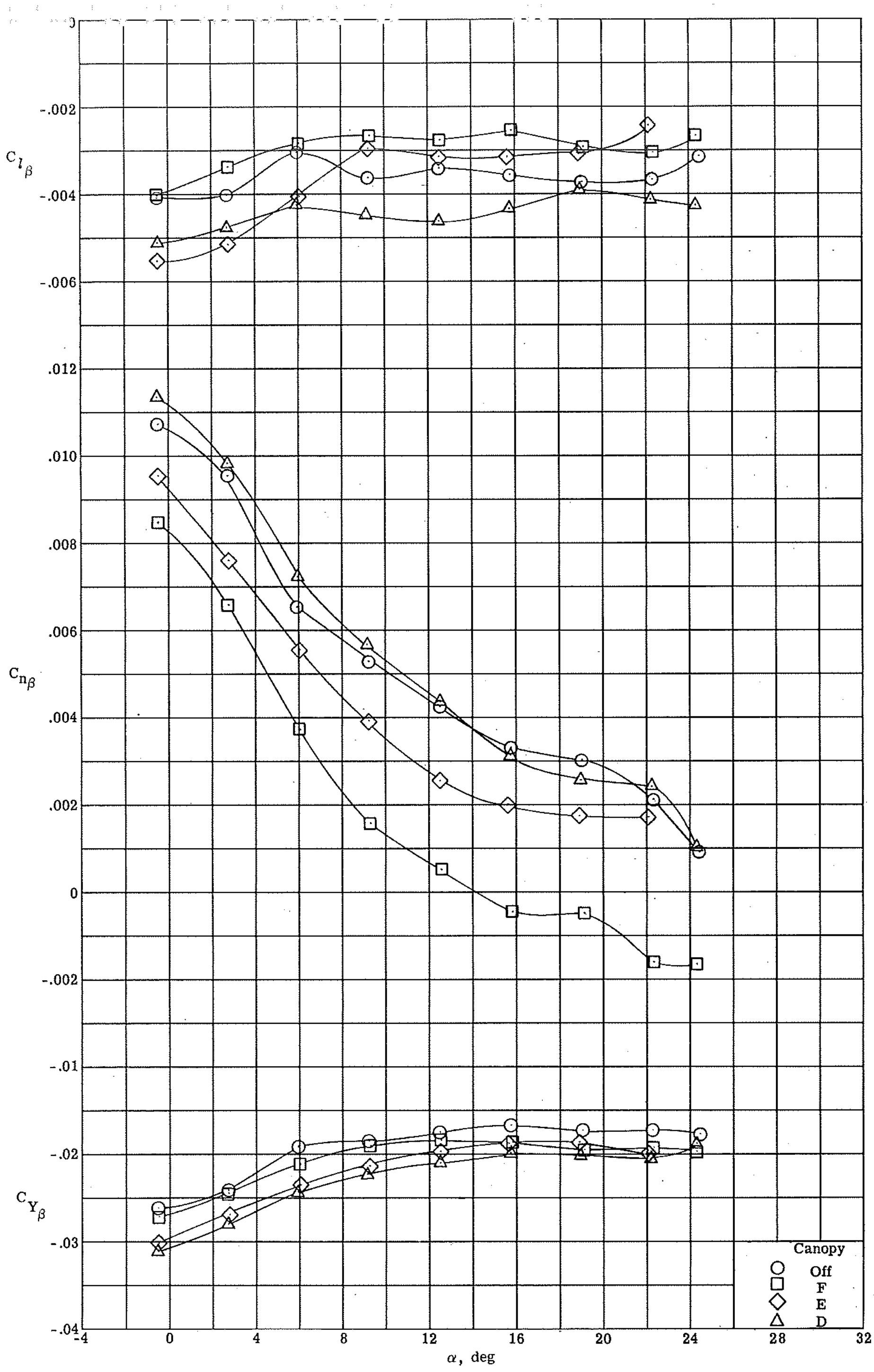

(g) M = 0.95.

Figure 14.- Continued.

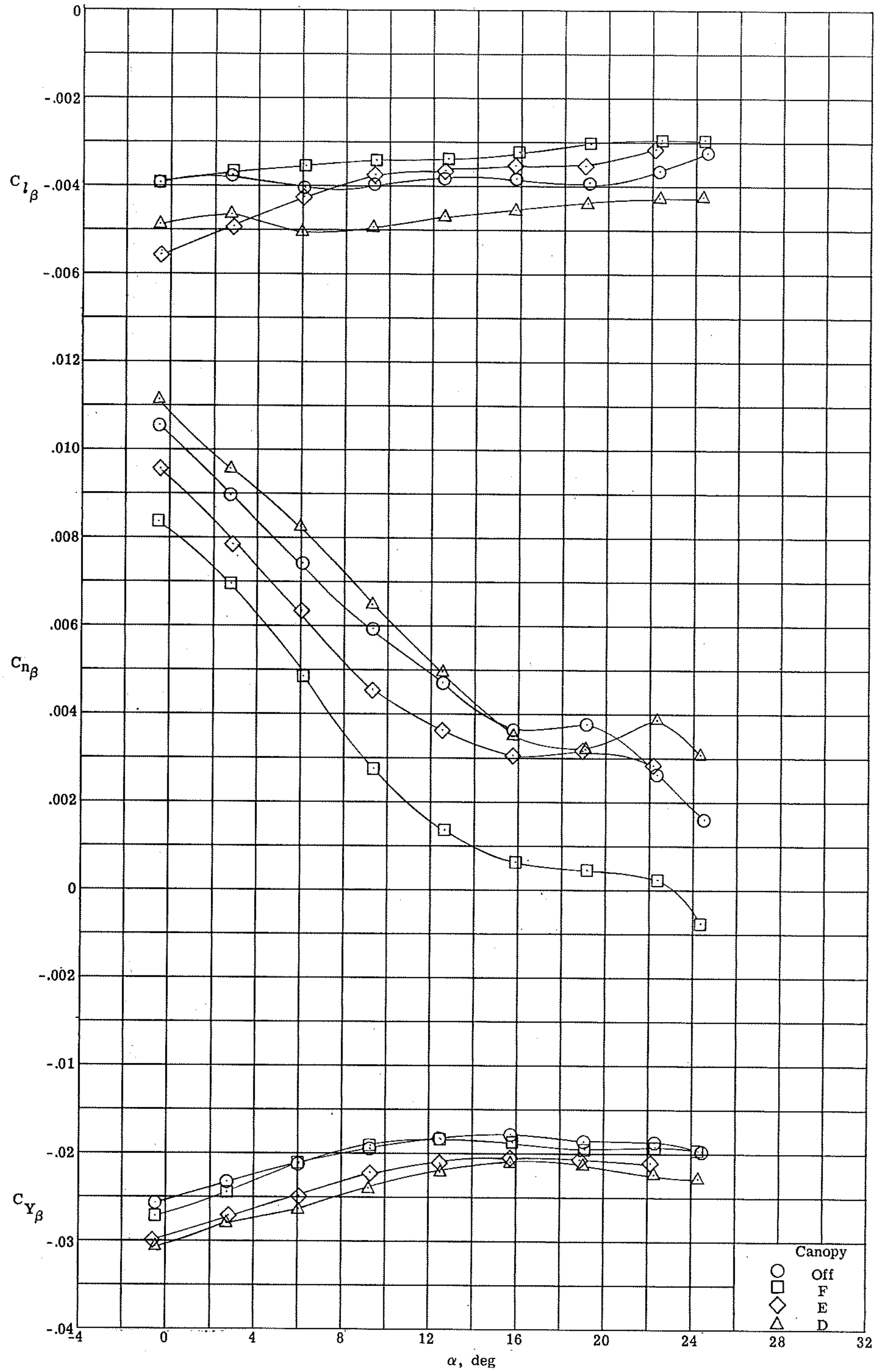

(h) M = 1.00.

Figure 14.- Continued.

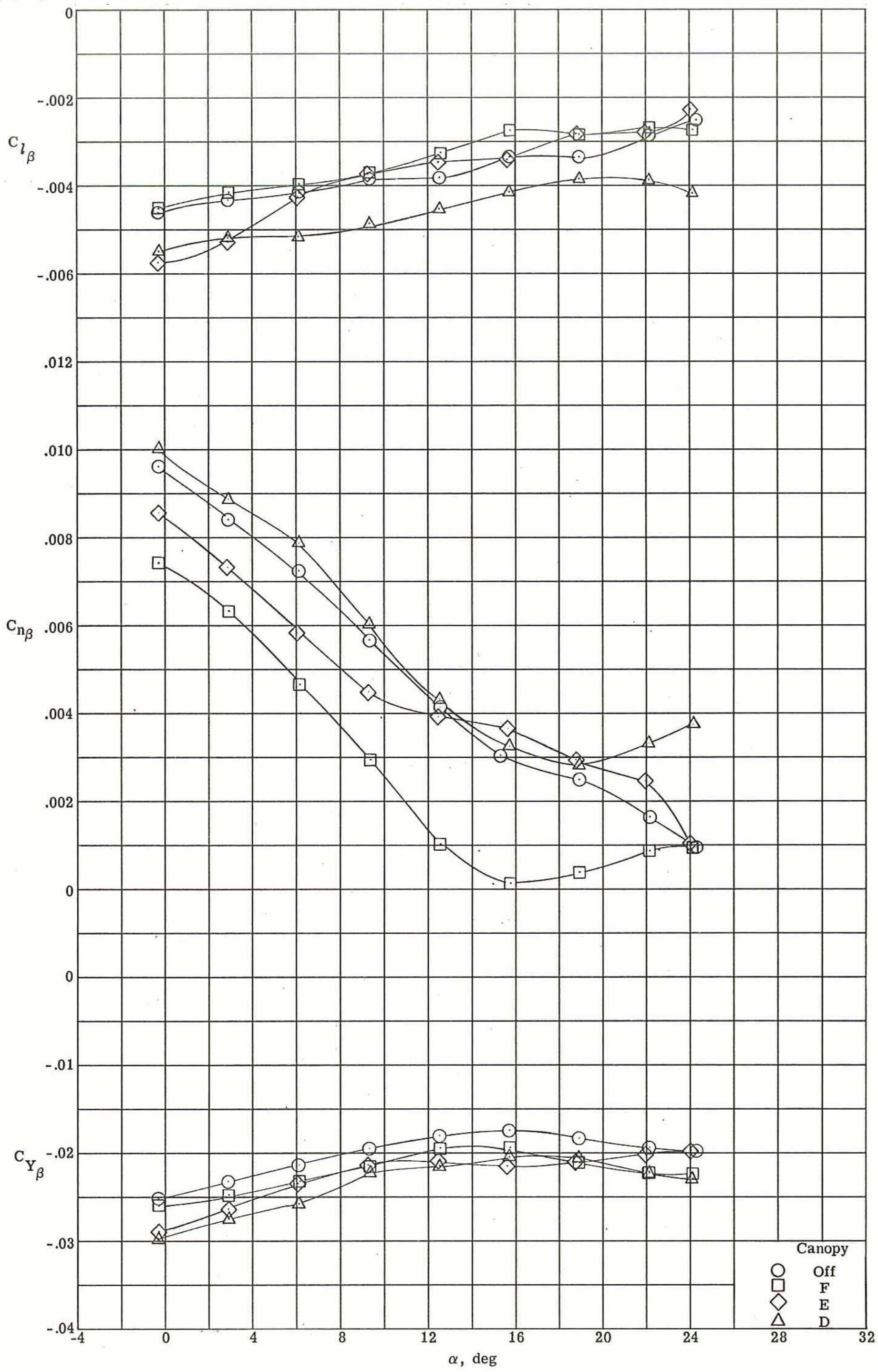

(i) M = 1.20.

Figure 14.- Continued.

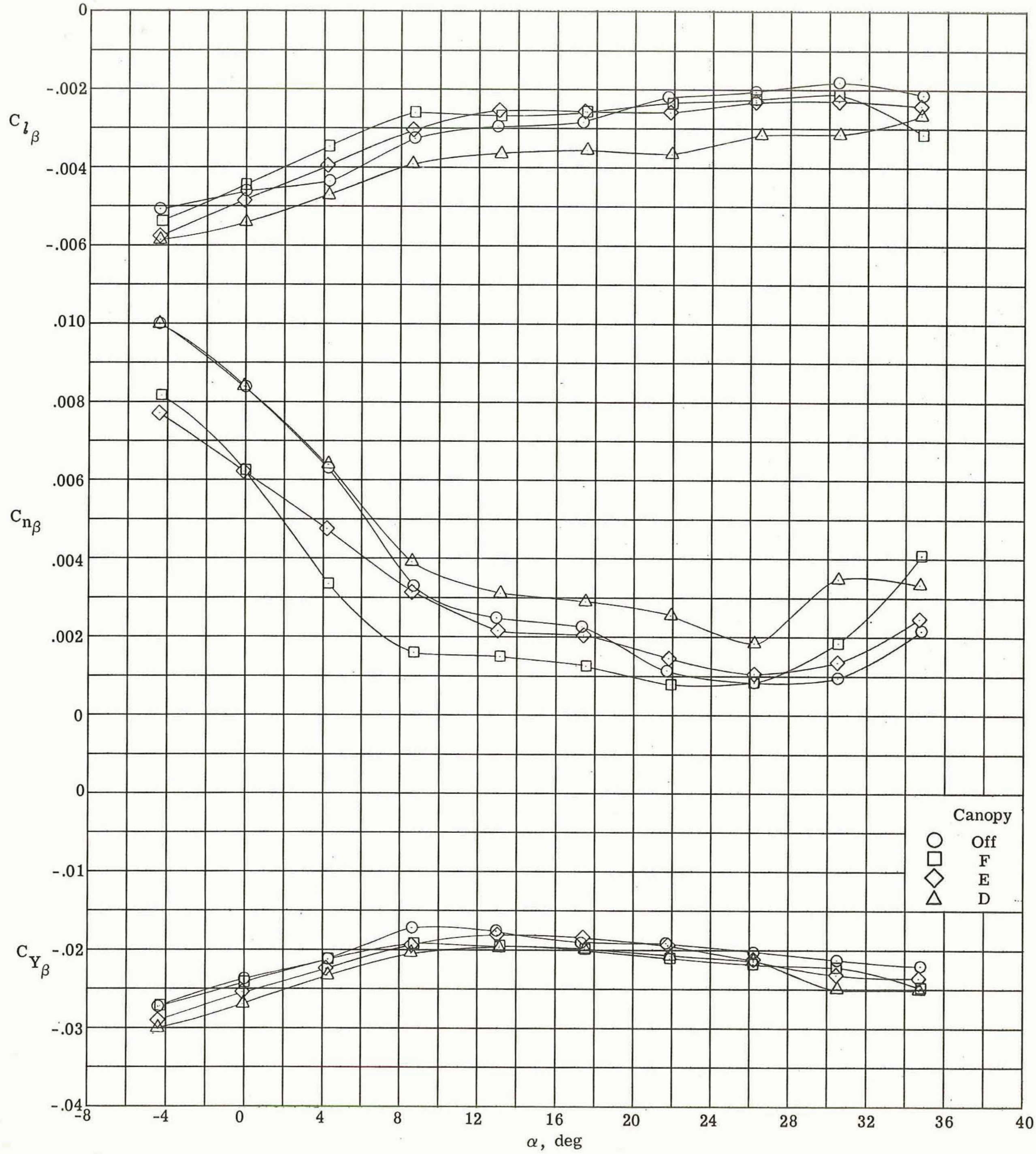

(j) M = 1.50.

Figure 14.- Continued.

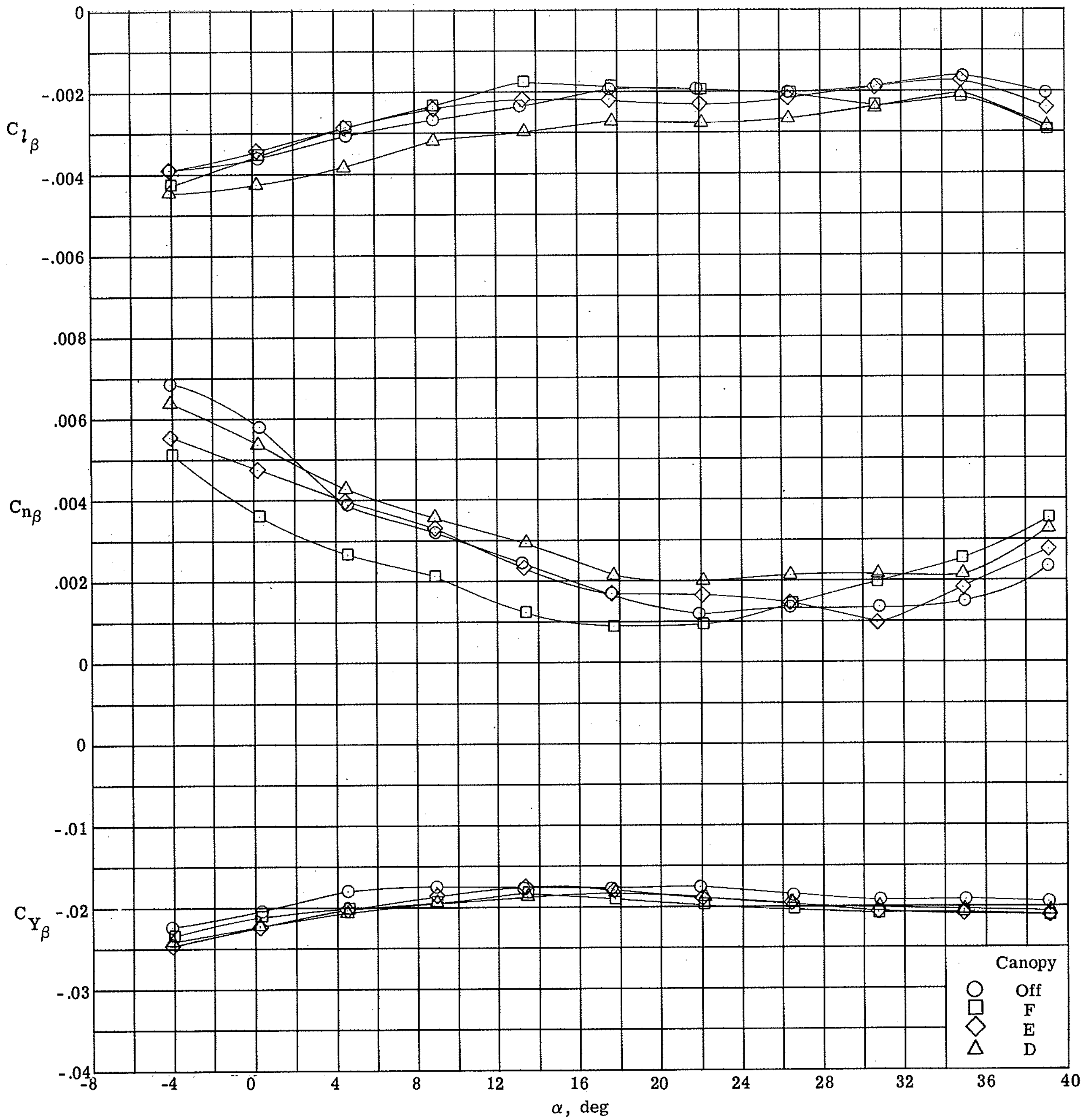

(k) M = 1.80.

Figure 14.- Continued.

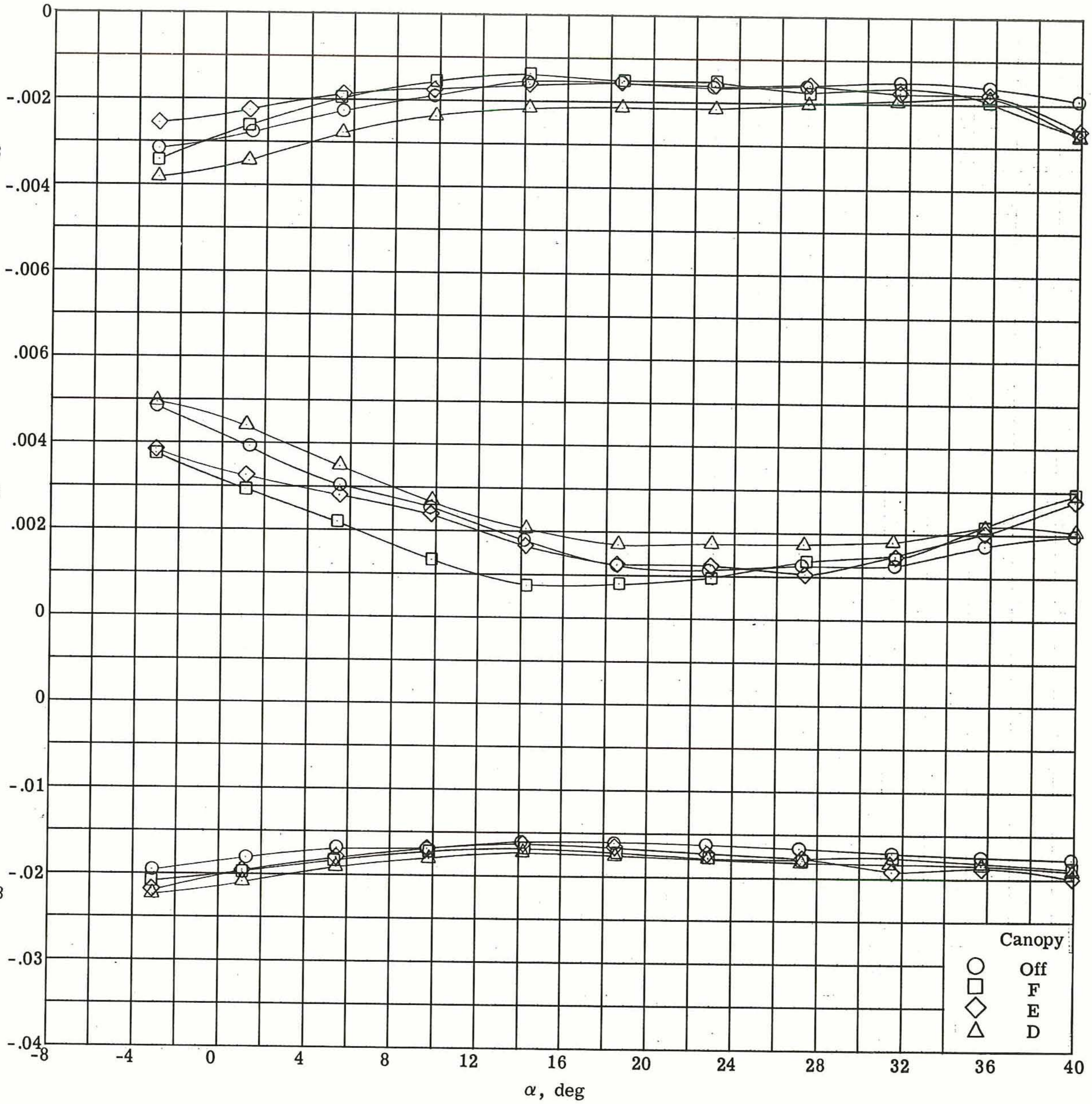

(l) M = 2.16.

Figure 14.- Concluded.

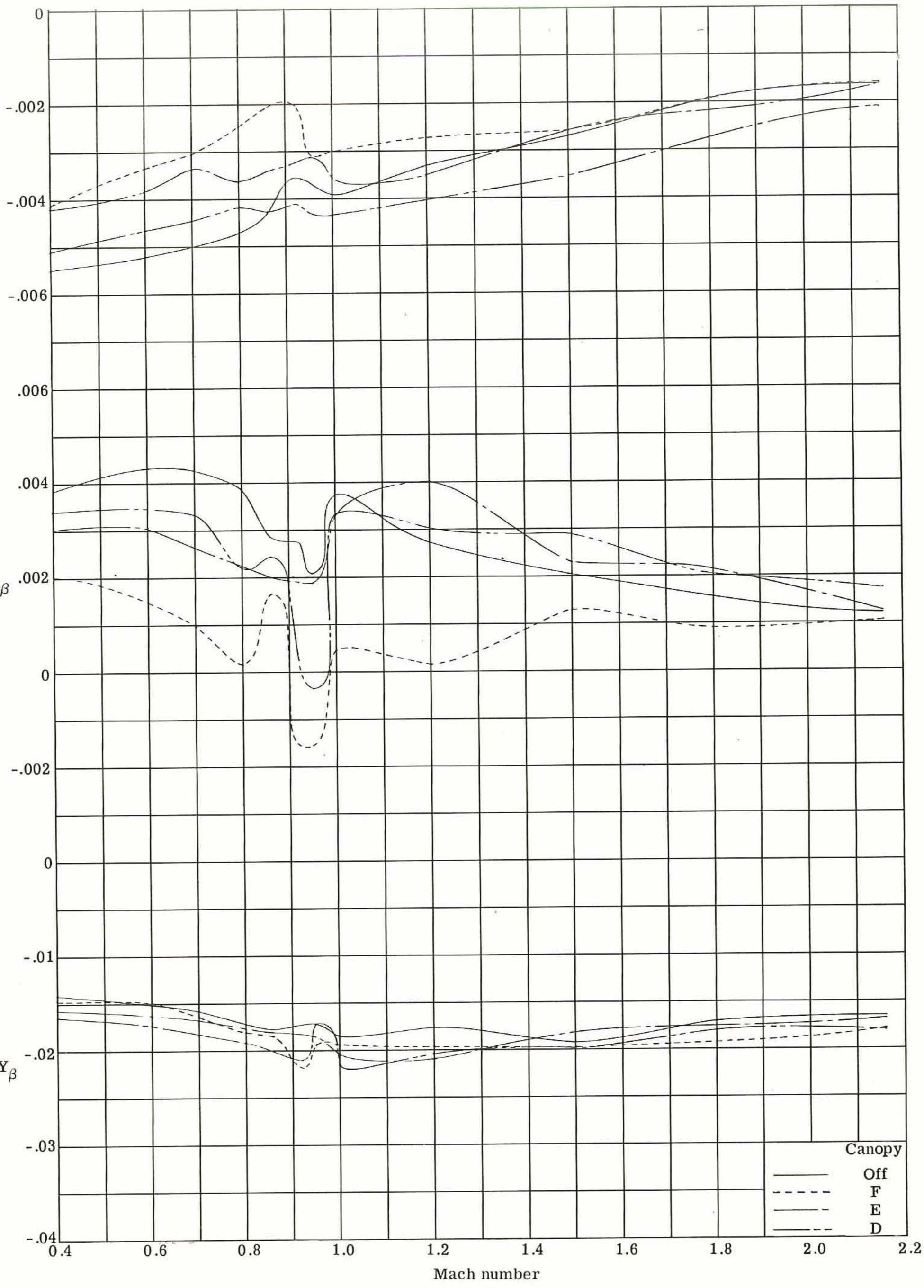

(a) Trim conditions for $\delta_e = 0^0$.

Figure 15.- Summary of effects of canopies D, E, and F and Mach number variation on the directional and lateral stability characteristics. Tip fin I_4; center fin E_2; tip-fin and elevon flaps in transonic mode.

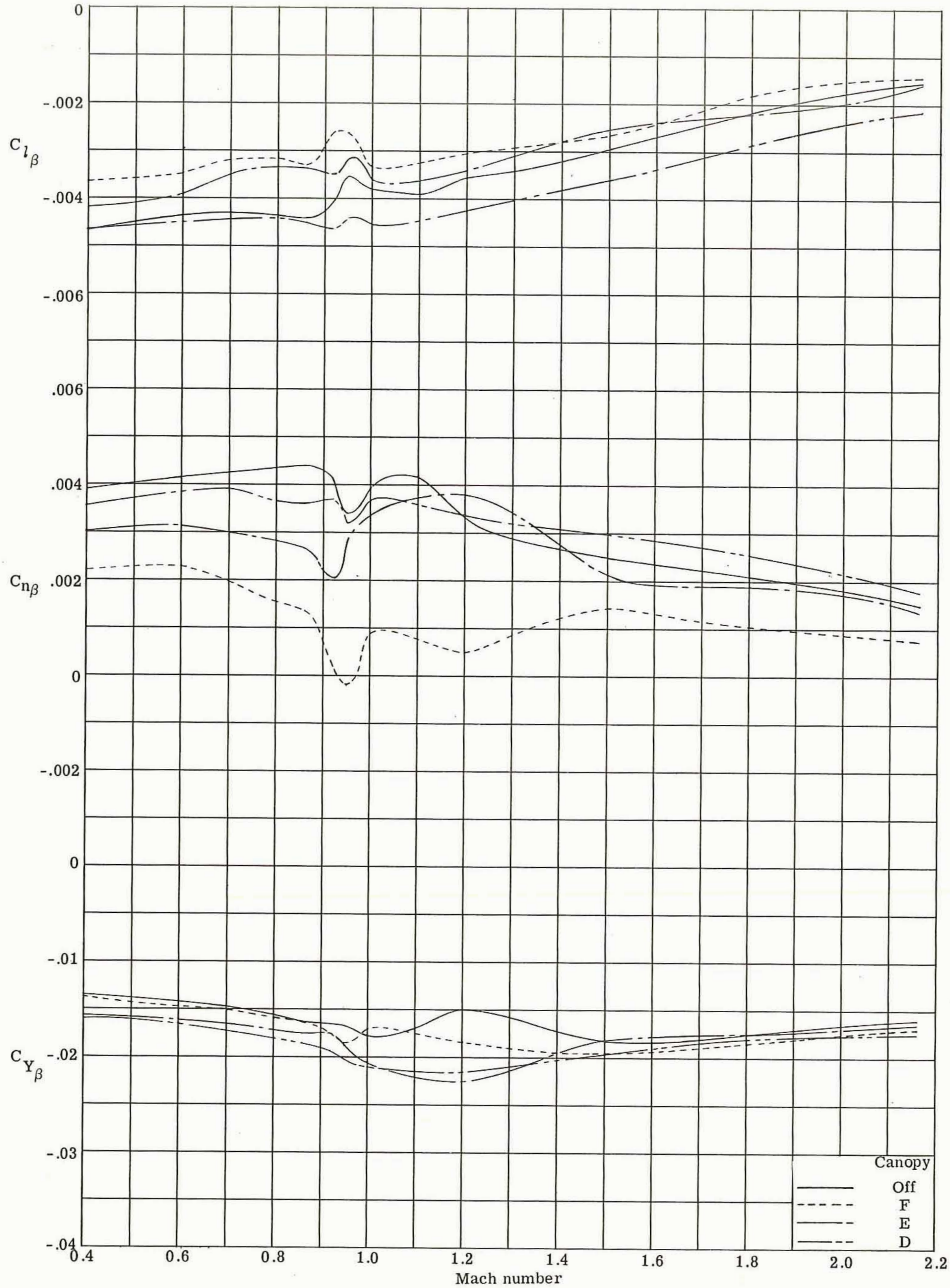

(b) $C_L = 0.20.$

Figure 15.- Continued.

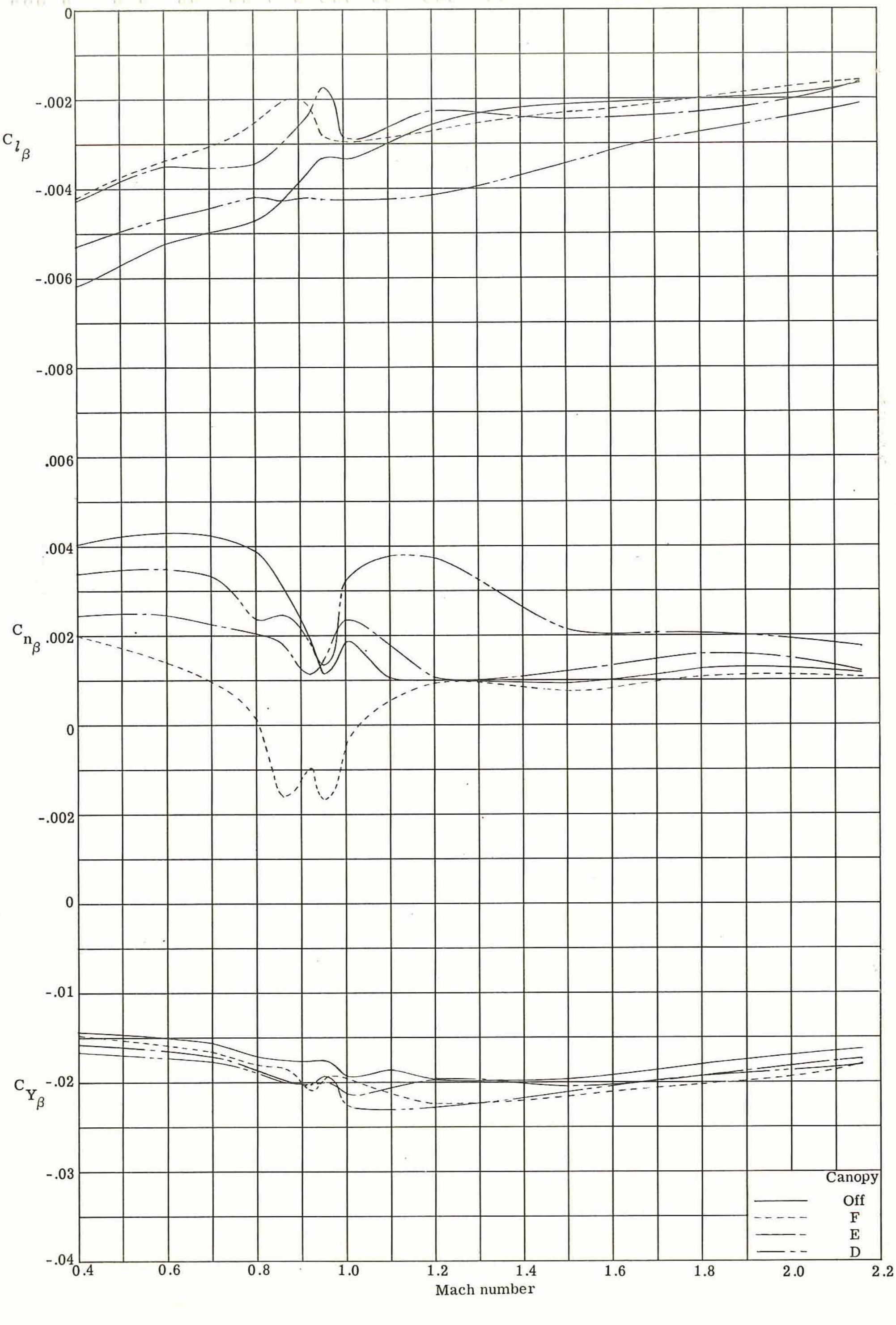

(c) $\alpha = 24^{\circ}$.

Figure 15.- Concluded.

[redacted]

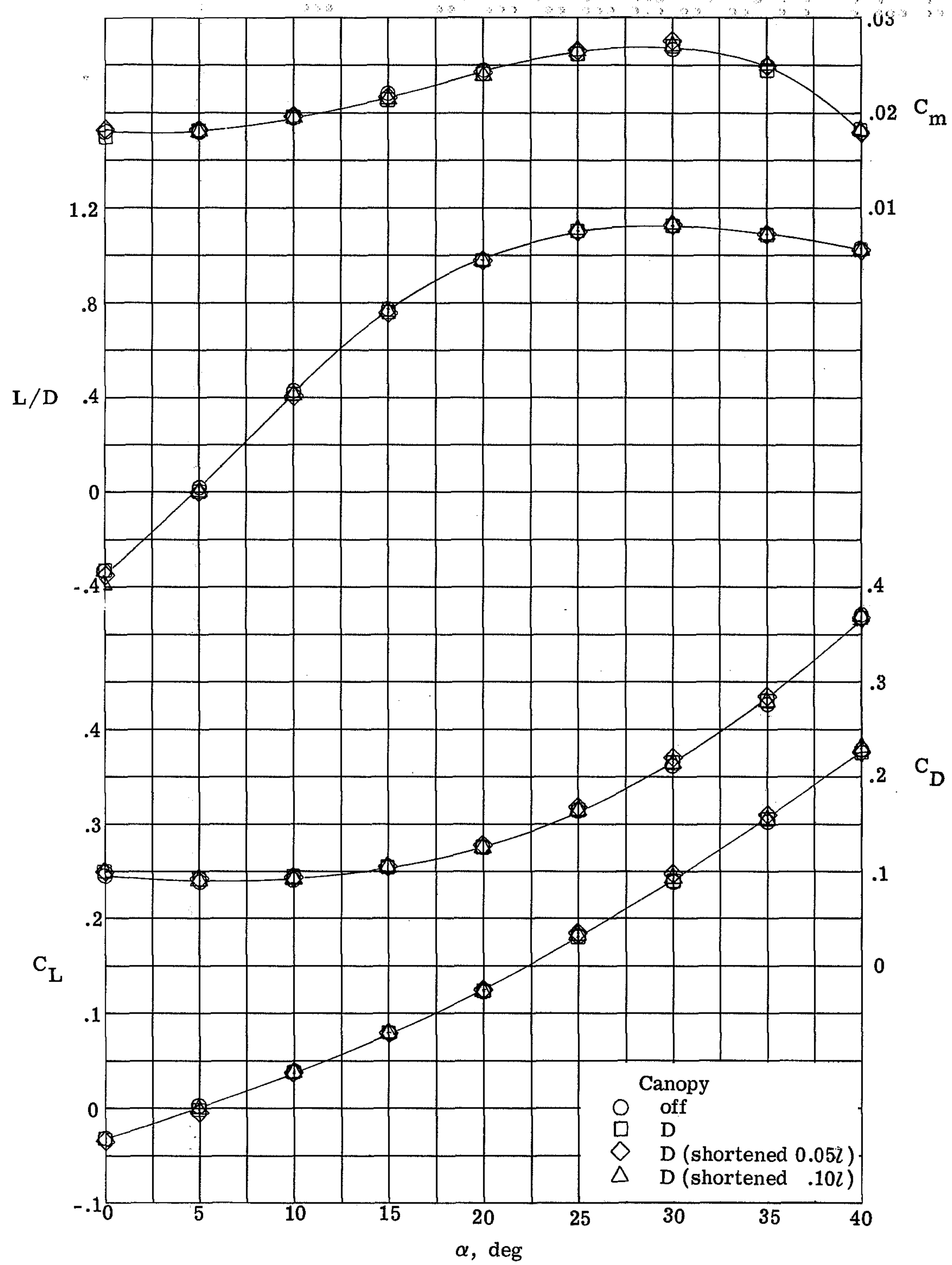

Figure 16.- Effects of length of canopy D with windshield cover on longitudinal characteristics at $M = 6.8$. $\delta_e = 0^0$; tip fin I_4; center fin E_2.

[redacted]

[redacted]

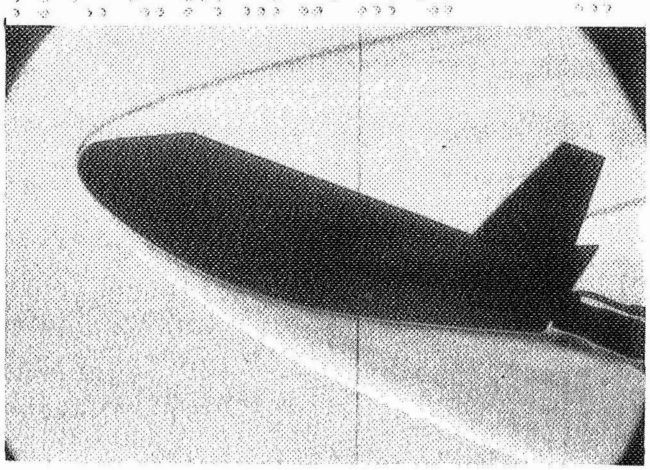

Full-length canopy

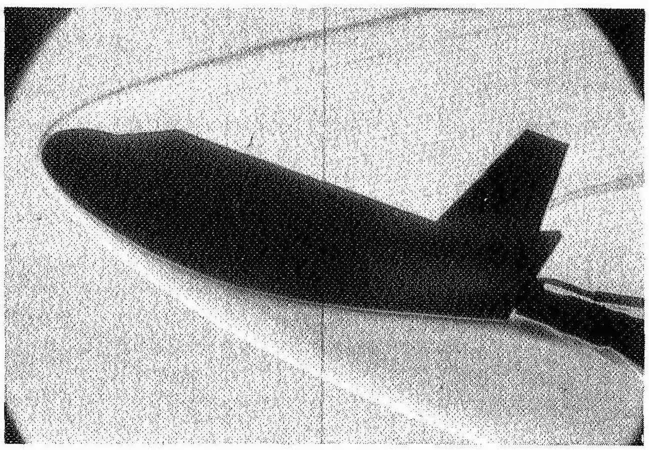

Canopy shortened 0.05l

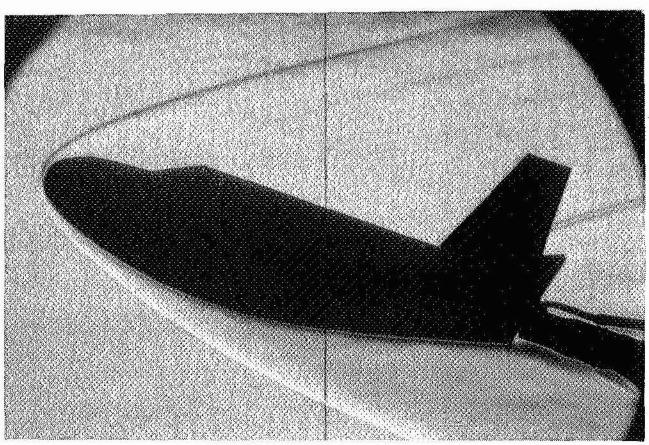

Canopy shortened 0.10l

(a) $\alpha = 20^{\circ}$.

L-66-4551

Figure 17.- Schlieren flow photographs for various lengths of canopy D with windshield cover. $M = 6.8$.

[redacted]

[redacted]

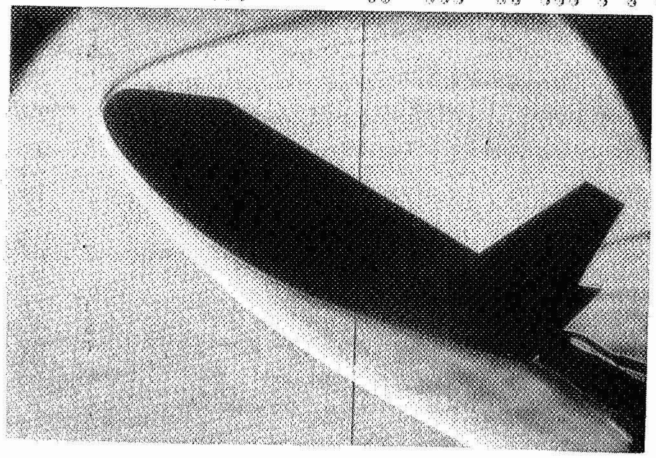

Full-length canopy

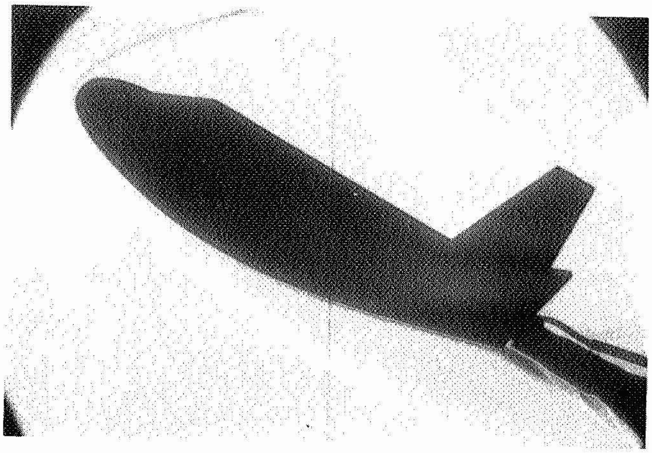

Canopy shortened 0.05l

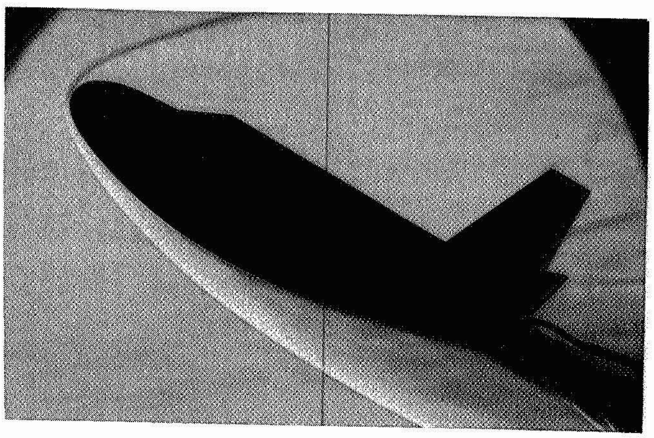

Canopy shortened 0.10l

(b) $\alpha = 30^{\circ}$.

L-66-4552

Figure 17.- Concluded.

[redacted]

[redacted]

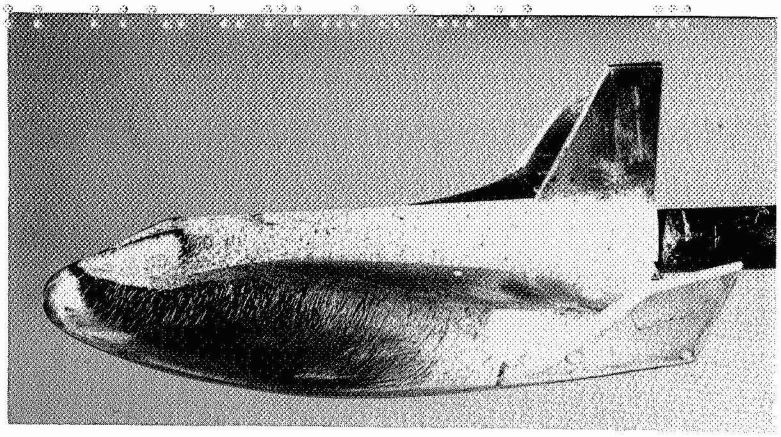

Full-length canopy

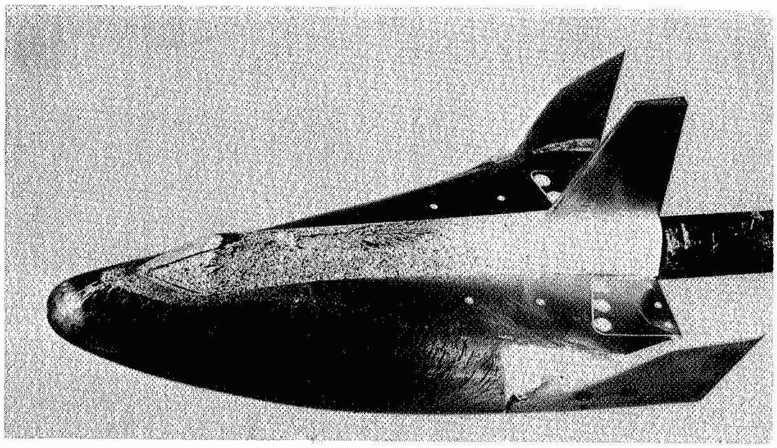

Canopy shortened $0.05l$

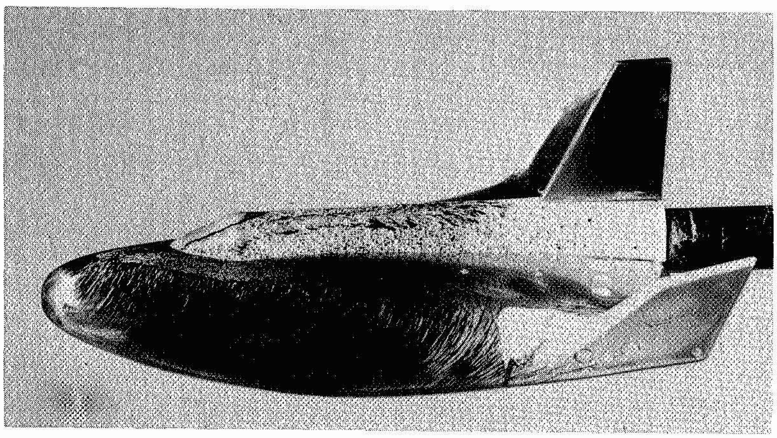

Canopy shortened $0.10l$

L-66-4553

Figure 18.- Surface oil-flow patterns for various lengths of canopy D with windshield cover. $M = 6.8$; $\alpha = 30^{\circ}$; $\delta_e = 0^{\circ}$; tip fin I_4; center fin E_2.

[redacted]

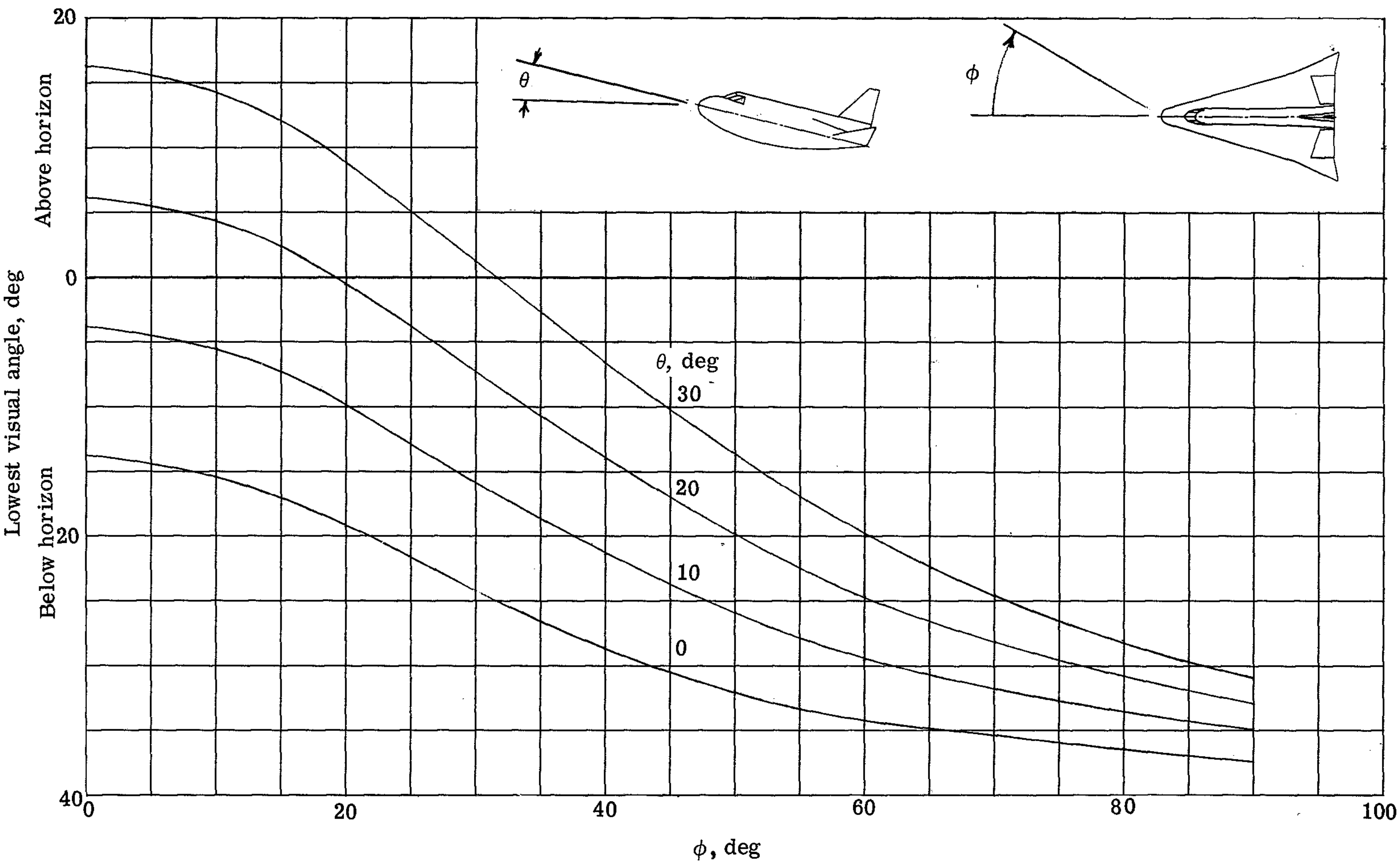

Figure 19.- Visual angles for HL-10 with canopy D. Pilot's eye at 20 percent of vehicle length.

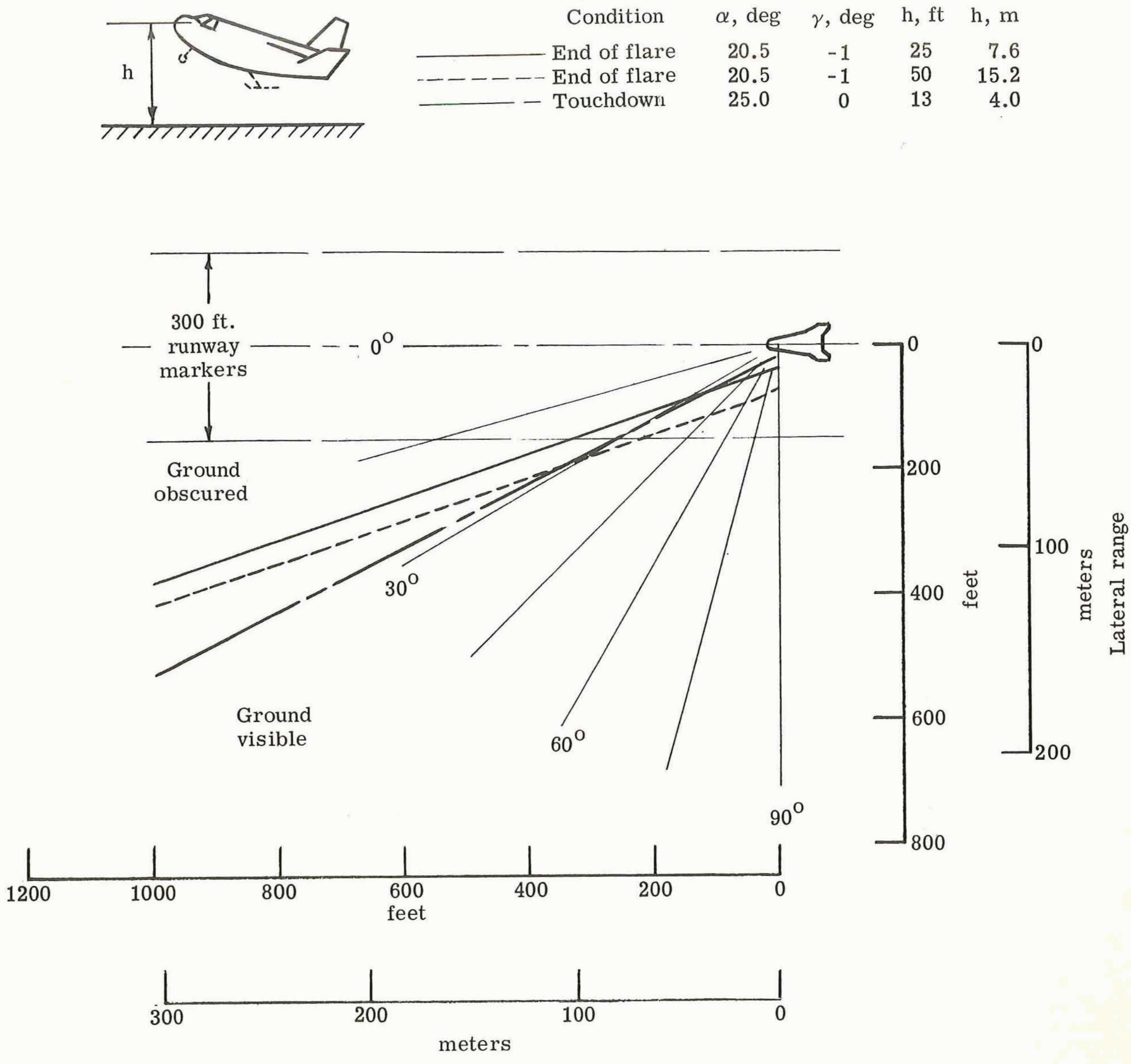

Figure 20.- HL-10 visibility at landing with canopy D.

CONFIDENTIAL

CONFIDENTIAL

~~CONFIDENTIAL~~

"The aeronautical and space activities of the United States shall be conducted so as to contribute . . . to the expansion of human knowledge of phenomena in the atmosphere and space. The Administration shall provide for the widest practicable and appropriate dissemination of information concerning its activities and the results thereof."

—National Aeronautics and Space Act of 1958

NASA SCIENTIFIC AND TECHNICAL PUBLICATIONS

TECHNICAL REPORTS: Scientific and technical information considered important, complete, and a lasting contribution to existing knowledge.

TECHNICAL NOTES: Information less broad in scope but nevertheless of importance as a contribution to existing knowledge.

TECHNICAL MEMORANDUMS: Information receiving limited distribution because of preliminary data, security classification, or other reasons.

CONTRACTOR REPORTS: Technical information generated in connection with a NASA contract or grant and released under NASA auspices.

TECHNICAL TRANSLATIONS: Information published in a foreign language considered to merit NASA distribution in English.

TECHNICAL REPRINTS: Information derived from NASA activities and initially published in the form of journal articles.

SPECIAL PUBLICATIONS: Information derived from or of value to NASA activities but not necessarily reporting the results of individual NASA-programmed scientific efforts. Publications include conference proceedings, monographs, data compilations, handbooks, sourcebooks, and special bibliographies.

Details on the availability of these publications may be obtained from:

SCIENTIFIC AND TECHNICAL INFORMATION DIVISION

NATIONAL AERONAUTICS AND SPACE ADMINISTRATION

Washington, D.C. 20546

~~CONFIDENTIAL~~